REFLECTION PROPERTIES OF A GAUSSIAN LASER BEAM FROM MULTILAYER DIELECTRIC FILMS

Taner ŞEN

REFLECTION PROPERTIES OF A GAUSSIAN LASER BEAM FROM MULTILAYER DIELECTRIC FILMS

A Thesis Submitted to
the Graduate School of Engineering and Sciences of
İzmir Institute of Technology
in Particular Fulfillment of the Requirements for the Degree of

MASTER OF SCIENCE

in Electrical and Electronics Engineering

by
Taner ŞEN

December 2009

We approve the thesis of **Taner ŞEN**

_____

Assoc. Prof. Dr. M. Salih DİNLEYİCİ
Supervisor

_____

Assoc. Prof. Dr. Thomas BECHTELER
Committee Member

_____

Assist. Prof. Dr. Alp KUŞTEPELİ
Committee Member

14.12.2009

_____   _____

Prof. Dr. Ferit Acar SAVACI   **Assoc. Prof. Dr. Talat YALÇIN**
Head of Department of   Dean of the Graduate School of
Electrical and Electronics Engineering   Engineering and Sciences

ACKNOWLEDGEMENTS

ABSTRACT

REFLECTION PROPERTIES OF A GAUSSIAN LASER BEAM FROM MULTILAYER DIELECTRIC FILMS

A laser microphone is a surveillance device that uses a laser beam to detect sound vibrations in a distant object. The object is typically inside a room where a conversation is taking place, and can be anything that can vibrate (for example, picture or window) in response to the sound waves of the conversation. The object preferably has a smooth surface. The laser beam is directed into the room through a window, reflected off the object and returned to a receiver that converts the beam to audio signal. The beam is mostly bounced off the window itself. Usually these kinds of devices are used by surveillance intelligence in some parts of governments and these kinds of weapons analyze the laser beam which reflects from window.

In this thesis a countermeasure to the detection of laser beam is analyzed. In order to make this possible, the reflection from dielectric stratified surfaces of a Gaussian laser beam needs to be described.

The reflected beam profile of electromagnetic radiation exposes to various effects different from reflected plane waves. Gaussian beams which reflect from a dielectric slab experience in a shifting maximum point in one direction; lateral shift, focal shift and angular divergence are the shift and distortion of the beam profile.

The Gaussian beam propagates in z direction and broadens in transverse plane, in two dimensions and is decomposed into plane wave components. Upon analyzing the reflection coefficient and beam profile, reduction of beam power after reflection from stratified films is described.

ÖZET

GAUSS LAZER ISINLARININ ÇOK KATMANLI DİELEKTRİK FİLMLERDEN YANSIMA ÖZELLİKLERİ

Lazer mikrofon, belirli bir mesafede bulunan cisimdeki ses titreşimlerini lazer ışık huzmesiyle gizlice tespit ederek çalışan bir izleme cihazıdır. Cisim klasik olarak münazaranın yer aldığı bir odanın içindedir ve titreyen herhangi bir şey olabilir.(örneğin tablo veya cam). Lazer ışık huzmesi camdan geçirilerek odaya yönlendirilir, nesneden yansıtılır ve ışık huzmesini ses sinyaline çeviren bir alıcıya geri döndürülür. Çoğunlukla ışık huzmesi pencerenin kendisinden yansıtılır. Genelde bunun gibi cihazlar hükümetin gizli dinleme yapan istihbarat kısımlarında kullanılır ve bu çeşit silahlar pencereden yansıyan lazer ışık huzmesini inceler.

Bu tezde lazer ışık huzmesinin tespit edilmesine mukabil bir karşı tedbir incelenmiştir. Bunu mümkün kılmak için Gaussian ışık huzmeli lazerin bir yüzeyden nasıl yansıdığı tanımlanmıştır.

Elektromanyetik ışımalı yansımış ışık huzmesi profili, yansımış düzgün dalgaların karşılaştığı etkilerden farklı etkilere maruz kalır. Dielektrik bir tabakadan yansıyan Gaussian ışık huzmeleri maksimum noktalarında bir yöne kayma yapar; gecikerek kayma, odaksal kayma ve açısal kayma bu kaymayı ve ışık huzmesi görüntüsündeki bozulmayı temsil eder.

Gaussian ışık huzmesi z yönünde ilerler ve iki boyutlu yayılmaktadır ve düzgün dalga bileşenlerinden oluşmuştur. Yansıma katsayısını ve huzmenin şeklini tanımlamamızla birlikte katmanlar halindeki filmlerden yansımadan sonraki ışık huzmesinin gücündeki azalma tanımlanmıştır.

TABLE OF CONTENTS

LIST OF FIGURES

CHAPTER 1

INTRODUCTION

Laser beam structures are used in various fields. Usually there is a source from where the light source is composed of. From this source the light propagates and while spreads. The energy distribution of a laser beam is shown in Figure 1.1. The peak point is in the direction of propagation it travels. And the power it has is in the axis it propagates. The very usage of this representation is more common and can be analyzed by getting around with some examples.
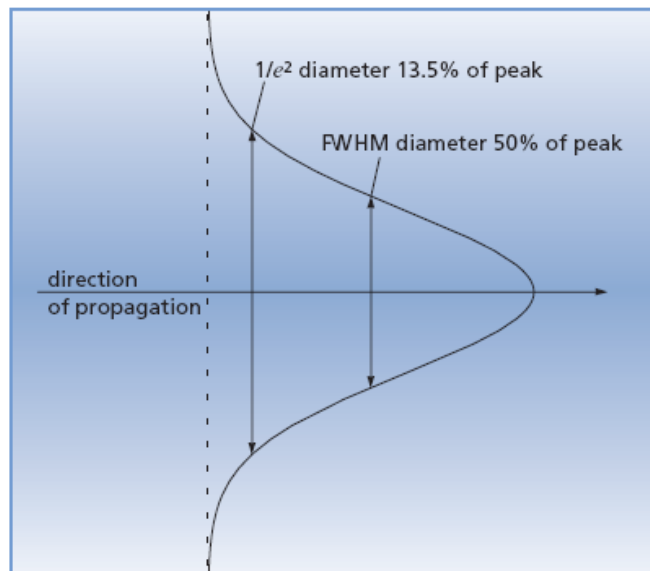
Figure 1.1. Energy Distribution of a Gaussian Beam Propagation Along One Direction

Usually the beam is reflected from a point and after reflection the beam has the information from which it is reflected. For example in the airborne ocean lidar system, laser beam is launched in the air and reflected and refracted on the water surface [1]. The wavy surface changes the energy distributions of reflective and refractive laser beams (Figure 1.2). Thus any different object on or under the sea level can be detected. It can be designed for oceanographic and coastal measurements, coastal topographic surveys, wave measurements, and coral reef research. Analyzing reflection form wavy surfaces is the base structure of these applications. According to the wave model on the

water surface, the returned laser power expression for the airborne laser bathymetry can be defined describing reflection.
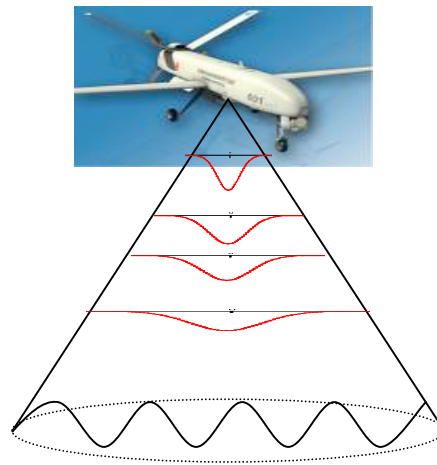
Figure 1.2. Gaussian Beam Reflection From A Wavy Surface

One such application of this technology is the designation of analyzing the beam reflected from blood vessels and detecting the blood pressure. By the help of this detection health organizations can understand what kind of illness the person has. And it is also used for detecting Land mines. Gaussian beam shape laser beams are backscattered from land mines and thus they are detected even if buried and nonmetallic materials. After analysis, backscattered photons from mines and soil or any other materials are differed by detection.

One usage fields of this technology is detecting vibrations on rotational targets [2]. Any kind of robotic material whose rotational stabilization needs to be analyzed smoothly detects by reflection of a Gaussian beam shape laser.
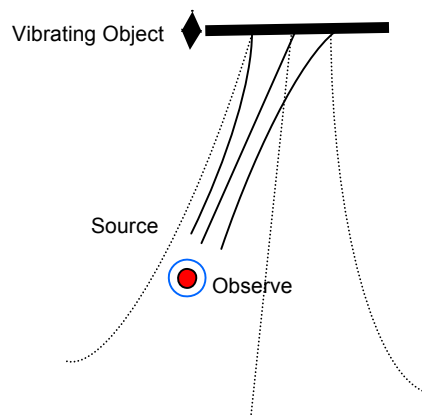
Figure 1.3. Gaussian Beam Reflection From A Surface

As it is known properly, laser beams are used for detecting the sound waves [3]. This device is called laser microphone (Figure 1.4). The people's sound waves talking in a room makes the window quiver. The sound vibrations cause the hard surface to act as a diaphragm and vibrate along with the sound. This vibration has the voice information and outside the window, a laser beam directed to the window is reflected and the reflected beam may be used for unauthorized listening by the help of the information it carries. In order to use the reflected laser beam, the source and the receiver must be on the same location or close to each other (Figure 1.3) [4-9]. Because the reflected beam profile must be matched with its original form and after voice recognition the pure voice can be listened. For the need of being in the same or near place, laser must be directed from exactly across the window because if, in the nature of reflection, the beam is directed to the window with 89º, the angle between reflected and transmitted wave is 2º. And if we increase the angle, for example about 45 º with the window, the beam reflects with nearly the same angle, then, the angle between reference beam and achieved beam is 90º.

Figure 1.4. Unauthorized Listening Using Laser Microphone

So, larger angles force the source and the receiver to be on different sides (an unwanted situation). But in order to eliminate just this, retro reflective tape applications are wide spread (Figure 1.5). A retro reflective tape in fact is being used for reflecting

3

the beam exactly backwards regardless of which angle it came from. Using the retro reflective tape, laser beam is reflected more purely than from any kind of place in the surface of building, mostly from window. It can be sticked to the car and by reflection, even if the engine is on and even if there is music inside, sound waves talking inside the car can be detected. But the nature of retro reflective tapes makes it necessary to stick it to the target. While you are doing such a job, trying to listen the target in an unauthorized manner, you don't want to be detected. And while you are not trying to be detected, you don't want to get closer to the target although you have to stick the retro reflective tape.
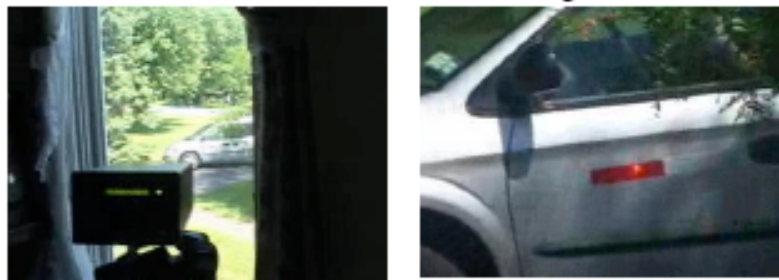
Figure 1.5. Retroreflective Tape Usage Fields

It can be understood that while listening within laser beams, using retro reflective tapes are nonsense. So the smoothest place that needs to be used to detect the laser beam profile is the most vibrating surface, window. And they do so.

In fact, the invisible laser beam is usually directed to a window within approximately maximum 50 meters. So light reflects backward and that means it travels round 100 meters. That means we will mostly study with far field divergence. More than 100m traveling may cause the beam profile diverge and would make it little possible to analyze. Assuming the wavelength 1000nm, W_0 0.1mm and after 100m traveling, the electric field distribution of Gaussian beam in transverse plane is nearly 3cm. As we know we can diverge or decrease the divergence of the beam using lenses. But maximum divergence must not be wider than window within 50m because these kind of systems work in this range. Our distance to the window is 50m and assuming the window not being wider than 1m, theoretically our beam will travel maximum 10 degree. Making our beam travel more than 10 degrees may decrease the beam power so much that after refection it can not be detected. That can be done by using lenses, and we can say that theoretically it is possible. As one might imagine, this has interesting

surveillance applications. This technology is currently being used by the CIA and many other surveillance-related organizations to eavesdrop. The infrared laser is used in real-world scenarios because of the fact that it is invisible; the ruby laser might cause the surveillance subject to realize that they are being watched.

In this thesis I will investigate a means of elimination for not being detected by this kind of unauthorized listening. There are various technical opportunities to apply this. For example the window surface can be designed as sinusoidal shape being the wavelength of this designation the same as the laser beams wavelength but it has some disadvantages by disrupting window function. We want the window to continue its functions properly. Doing so would cause the people talking inside the window unable to see the nature from inside.

Also the window can be vibrated using a buzzer onto the surface. That could be a solution for being undetected when the buzzing of window has a sinusoidal shape being the wavelength of this the same as the laser light. But this can also cause a buzzing sound and the vibration of window would cause the people unable to see the nature from inside. An unwanted buzzing and annoying sound spreads around the room. And these kind of structures must be mechanical and although the wavelength of buzzing sound has to be stable, it can not be. Because there is always distortion and this distortion causes the wavelength to be changed.

The most remarkable solution for not being detected by this kind of listening is using a material that could be sticked on the surface of the window. We need to design that kind of material which we know how it reacts to the light waves. The best structure is using multilayer films on the surface of the window, by the way we can alter the beam shape or reducing the beam power in the reflection more than 20db would give a hard time to be listened unauthorized.

CHAPTER 2

REFLECTION OF LIGHT WAVES FROM A DIELECTRIC SLAB USING MATRIX APPROACH

In this chapter the main properties of the electromagnetic field and the effect of matter on the propagation of the electromagnetic disturbance is described formally in terms of the usual material constants.

When a plane wave falls on to a boundary between two homogenous media of different optical properties, it is split into two waves: a transmitted wave proceeding into the second medium and a reflected wave propagated back into the first medium [5]. The existence of these two waves can be demonstrated from the boundary conditions, since it is easily seen that these conditions can not be satisfied without postulated both the transmitted and the reflected wave [10-11]. We shall tentatively in this chapter assume that these waves are also plane and derive expressions for their directions of propagation and their amplitudes. By the help of these descriptions I will study the reflection coefficient.

In this chapter a matrix approach will be described such that multilayer slab structures or cascaded films can be obtained by multiplication of characteristic matrices.

2.1. Reflection Law

A plane wave propagated in the direction specified by the unit vector $\mathbf{s}^{(i)}$ is determined when the time behaviour at one particular point in space is known [5]. For if $\mathbf{F(t)}$ represents the time behaviour at any one point, whose position vector relative to the first point is r, is given by $\mathbf{F}[t - (\mathbf{r} \bullet \mathbf{s})/v]$. At the boundary between the two media, the time variation of the secondary fields will be the same as that of the incident primary fields. Hence, if $\mathbf{s}^{(r)}$ and $\mathbf{s}^{(t)}$ denote unit vectors in the direction of propagation of the reflected and transmitted wave, one has, on equating the arguments of the three wave functions at a point r on the boundary plane z=0:

$$t - \frac{\mathbf{r} \bullet \mathbf{s}^{(i)}}{v_1} = t - \frac{\mathbf{r} \bullet \mathbf{s}^{(t)}}{v_1} = t - \frac{\mathbf{r} \bullet \mathbf{s}^{(r)}}{v_2} \qquad (2.1)$$

v_1 and v_2 being the velocities of propagation in the two media. Written out more explicitly, we have with $\mathbf{r} \equiv x, y, 0$:

$$\frac{xs_x^{(i)} + ys_y^{(i)}}{v_1} = \frac{xs_x^{(r)} + ys_y^{(r)}}{v_1} = \frac{xs_x^{(t)} + ys_y^{(t)}}{v_2} \qquad (2.2)$$

Since equation (2.2) must hold for all values x and y on the boundary,

$$\frac{s_x^{(i)}}{v_1} = \frac{s_x^{(r)}}{v_1} = \frac{s_x^{(t)}}{v_2} \qquad , \qquad \frac{s_y^{(i)}}{v_1} = \frac{s_y^{(r)}}{v_1} = \frac{s_y^{(t)}}{v_2} \qquad (2.3)$$

The plane specified by $\mathbf{s}^{(i)}$ and the normal to the boundary is called **the plane of incidence.** Equation (2.3) shows that $\mathbf{s}^{(t)}$ and $\mathbf{s}^{(r)}$ lie in this plane.

Taking the plane of incidence as the $x, z -$ plane and denoting by θ_i, θ_r and θ_t the angle which $\mathbf{s}^{(i)}, \mathbf{s}^{(r)}$ and $\mathbf{s}^{(t)}$ make with 0z, one has

$$\left. \begin{array}{lll} s_x^{(i)} = \sin \theta_i , & s_y^{(i)} = 0 , & s_z^{(i)} = \cos \theta_i , \\[2mm] s_x^{(r)} = \sin \theta_r , & s_y^{(r)} = 0 , & s_z^{(r)} = \cos \theta_r , \\[2mm] s_x^{(t)} = \sin \theta_t , & s_y^{(t)} = 0 , & s_z^{(t)} = \cos \theta_t . \end{array} \right\} \qquad (2.4)$$

For waves propagated from the first into the second medium, the z components of the s vectors are positive; for those propagated in the opposite sense, they are negative:

$$s_z^{(i)} = \cos \theta_i \geq 0 , \qquad s_z^{(r)} = \cos \theta_r \leq 0 , \qquad s_z^{(t)} = \cos \theta_t \geq 0 \qquad (2.5)$$
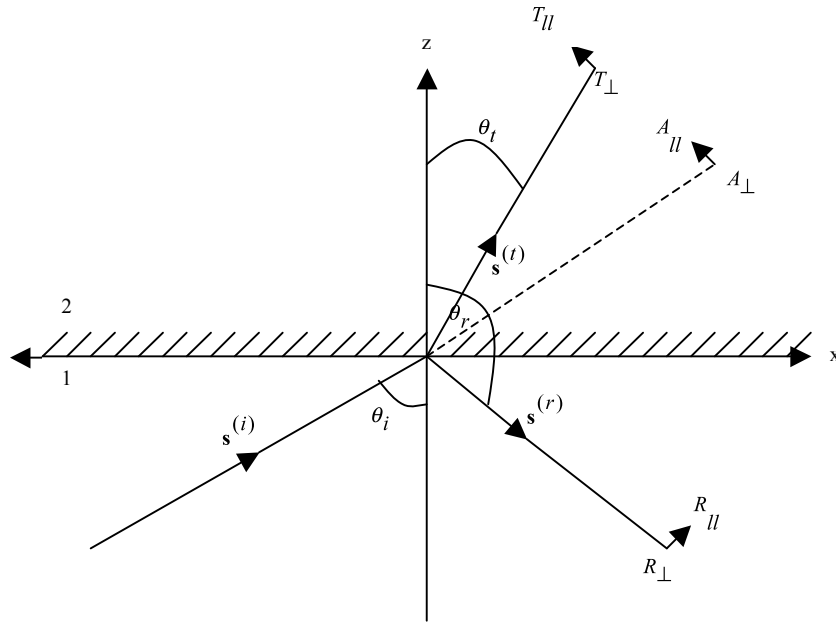
Figure 2.1. Refraction And Reflection Of A Plane Wave Plane Of Incidence

The first set in equation (2.3) gives within equation (2.4)

$$\frac{\sin\theta_i}{v_1} = \frac{\sin\theta_r}{v_1} = \frac{\sin\theta_t}{v_2} \tag{2.6}$$

Hence, $\sin\theta_r = \sin\theta_i$, and we find, also using equation (2.5), that $\cos\theta_r = -\cos\theta_i$, so that

$$\theta_r = \pi - \theta_i \tag{2.7}$$

This relation, together with the statement that the reflected wave normal $s^{(r)}$ is in the plane of incidence, constitutes the **law of reflection.**

Also from equation (2.6), using Maxwell relation known as $n = \sqrt{\varepsilon\mu}$, where μ is nonmagnetic substance, n is absolute refractive index and ε is static dielectric constant, we can define

$$n_{12} = \frac{n_2}{n_1} = \frac{v_1}{v_2}, \qquad \frac{\sin\theta_i}{\sin\theta_t} = \frac{v_1}{v_2} = \sqrt{\frac{\varepsilon_2}{\mu_2}} = \frac{n_2}{n_1} = n_{12} \tag{2.8}$$

known as **Snell's law.**

2.2. Fresnel Formulae

Assume two homogeneous and isotropic media are both of zero conductivity and consequently perfectly transparent; their magnetic permeabilities will then in fact differ from unity by negligible amounts, and accordingly we take $\mu_1 = \mu_2 = 1$.

Let A be the amplitude of the electric vector of the incident field. We take A to be complex, with its phase equal to the constant part of the argument of the wave function; the variable part is

$$\tau_i = \omega\left(t - \frac{\mathbf{r} \bullet \mathbf{s}^{(i)}}{v_1}\right) = \omega\left(t - \frac{x \sin\theta_i + z \cos\theta_i}{v_1}\right) \tag{2.9}$$

We resolve each vector into components parallel (denoted by subscript ll) and perpendicular (subscript $\perp$) to the plane of incidence. The choice of the perpendicular components must be visualized at right angles to the plane of the figure.

The components of the electric vector of the incident field then are

$$\left.\begin{aligned}
E_x^{(i)} &= -A_{ll}\cos\theta_i e^{-i\tau_i} \\
E_y^{(i)} &= A_{\perp} e^{-i\tau_i} \\
E_z^{(i)} &= -A_{ll}\sin\theta_i e^{-i\tau_i}
\end{aligned}\right\} \tag{2.10}$$

The components of the magnetic vector are immediately obtained by using Maxwell relations; $\quad \mathbf{H} = \sqrt{\varepsilon}\mathbf{s} \times \mathbf{E}$

$$H_x^{(i)} = -A_{\perp}\cos\theta_i\sqrt{\varepsilon_1}e^{-i\tau_i}, H_y^{(i)} = -A_{ll}\sqrt{\varepsilon_1}e^{-i\tau_i}, H_z^{(i)} = A_{\perp}\sin\theta_i\sqrt{\varepsilon_1}e^{-i\tau_i} \tag{2.11}$$

Being R and T are the complex amplitude of the reflected and transmitted waves, the corresponding components of the electric and magnetic vectors are:

Reflected wave

$$E_x^{(r)} = -R_{ll} \cos\theta_r e^{-i\tau_r}, \qquad E_y^{(r)} = R_\perp e^{-i\tau_r}, \qquad E_z^{(r)} = -R_{ll} \sin\theta_r e^{-i\tau_r}$$
$$H_x^{(r)} = -R_\perp \cos\theta_r \sqrt{\varepsilon_1} e^{-i\tau_r}, \quad H_y^{(r)} = -R_{ll}\sqrt{\varepsilon_1} e^{-i\tau_r}, \quad H_z^{(r)} = R_\perp \sin\theta_r \sqrt{\varepsilon_1} e^{-i\tau_r} \quad \right\} \quad (2.12)$$

With the phase of

$$\tau_r = \omega\left(t - \frac{\mathbf{r}\bullet\mathbf{s}^{(r)}}{v_1}\right) = \omega\left(t - \frac{x\sin\theta_r + z\cos\theta_r}{v_1}\right) \tag{2.13}$$

Transmitted wave

$$E_x^{(t)} = -T_{ll} \cos\theta_t e^{-i\tau_t}, \qquad E_y^{(t)} = T_\perp e^{-i\tau_t}, \; E_z^{(t)} = -T_{ll} \sin\theta_t e^{-i\tau_t}$$
$$H_x^{(t)} = -T_\perp \cos\theta_t \sqrt{\varepsilon_2} e^{-i\tau_t}, \quad H_y^{(t)} = -T_{ll}\sqrt{\varepsilon_2} e^{-i\tau_t}, \quad H_z^{(t)} = T_\perp \sin\theta_t \sqrt{\varepsilon_2} e^{-i\tau_t} \quad \right\} \quad (2.14)$$

With the phase of

$$\tau_r = \omega\left(t - \frac{\mathbf{r}\bullet\mathbf{s}^{(t)}}{v_2}\right) = \omega\left(t - \frac{x\sin\theta_t + z\cos\theta_t}{v_2}\right) \tag{2.15}$$

As we know that the tangential components of E and H should be continuous across the surface and we have;

$$E_x^{(i)} + E_x^{(r)} = E_x^{(t)}, \qquad\qquad E_y^{(i)} + E_y^{(r)} = E_y^{(t)}$$
$$H_x^{(i)} + H_x^{(r)} = H_x^{(t)}, \qquad\qquad H_y^{(i)} + H_y^{(r)} = H_y^{(t)} \quad \right\} \quad (2.16)$$

By substituting the electric and magnetic field vectors and using the fact that $\cos\theta_r = \cos(\pi - \theta_i) = -\cos\theta_i$ we have;

$$\left. \begin{aligned} - A_{ll} \cos\theta_i e^{-i\tau_i} + - R_{ll} \cos\theta_r e^{-i\tau_r} = -T_{ll} \cos\theta_t e^{-i\tau_t} \\ A_\perp e^{-i\tau_i} + R_\perp e^{-i\tau_r} = T_\perp e^{-i\tau_t} \\ - A_\perp \cos\theta_i \sqrt{\varepsilon_1} e^{-i\tau_i} + - R_\perp \cos\theta_r \sqrt{\varepsilon_1} e^{-i\tau_r} = -T_\perp \cos\theta_t \sqrt{\varepsilon_2} e^{-i\tau_t} \\ - A_{ll} \sqrt{\varepsilon_1} e^{-i\tau_i} + - R_{ll} \sqrt{\varepsilon_1} e^{-i\tau_r} = -T_{ll} \sqrt{\varepsilon_2} e^{-i\tau_t} \end{aligned} \right\} \quad (2.17)$$

Within boundary conditions we can say that we have four relations representing two groups, one of which contains only the components parallel to the plane of incidence, while the other contains only those which are perpendicular to the plane of incidence. These two kinds of waves are, therefore, independent of one another.

$$\left. \begin{aligned} \cos\theta_i (A_{ll} - R_{ll}) = \cos\theta_t T_{ll} \\ \sqrt{\varepsilon_1} \cos\theta_i (A_\perp - R_\perp) = \sqrt{\varepsilon_2} \cos\theta_t T_\perp \\ A_\perp + R_{ll} = T_\perp \\ \sqrt{\varepsilon_1} (A_{ll} + R_{ll}) = \sqrt{\varepsilon_2} T_{ll} \end{aligned} \right\} \quad (2.18)$$

We can solve equation (2.18) for the components of the reflected and transmitted terms of those of the incident wave, using $n = \sqrt{\varepsilon}$ from Maxwell relations;

$$\left. \begin{aligned} T_{ll} = \frac{2n_1 \cos\theta_i}{n_2 \cos\theta_i + n_1 \cos\theta_t} A_{ll} \\ T_\perp = \frac{2n_1 \cos\theta_i}{n_1 \cos\theta_i + n_2 \cos\theta_t} A_\perp \end{aligned} \right\} \quad (2.19)$$

$$\left. \begin{aligned} R_{ll} = \frac{n_2 \cos\theta_i - n_1 \cos\theta_t}{n_2 \cos\theta_i + n_1 \cos\theta_t} A_{ll} \\ R_\perp = \frac{n_1 \cos\theta_i - n_2 \cos\theta_t}{n_1 \cos\theta_i + n_2 \cos\theta_t} A_\perp \end{aligned} \right\} \quad (2.20)$$

Are called **Fresnel Formulae**, we can write these in alternative form using Snell's law and trigonometric functions;

$$T_{//} = \frac{2\cos\theta_i \sin\theta_t}{\cos(\theta_i - \theta_t) + \sin(\theta_i + \theta_t)} A_{//}$$

$$T_{\perp} = \frac{2\cos\theta_i \sin\theta_t}{\sin(\theta_i + \theta_t)} A_{\perp}$$

(2.21)

$$R_{//} = \frac{\tan(\theta_i - \theta_t)}{\tan(\theta_i + \theta_t)} A_{//}$$

$$R_{\perp} = -\frac{\sin(\theta_i - \theta_t)}{\sin(\theta_i + \theta_t)} A_{\perp}$$

(2.22)

Since θ_i and θ_t are real[1] because of total internal reflection, the trigonometric factors on the right hand sides of equation (2.21) and equation (2.22) will also be real and one can say that the phase of each component of the reflected or transmitted wave is either equal to the phase of the corresponding component of the incident wave or differs from it by π. Since $R_{//}$ and $R_{\perp}$ have the opposite signs, the phase will depend on the relative magnitudes of θ_i and θ_t. For if the second medium is optically denser then the first medium (our usual case), then $\theta_t < \theta_i$. According to equation (2.22), the signs of $A_{\perp}$ and $R_{\perp}$ are different and the phases therefore differ by π. Under the same circumstances we expect $A_{//}$ and $R_{//}$ have the same phase differences[2] and if we look closer by the help of Figure 2.1 we can see that $\tan(\theta_i + \theta_t)$ becomes negative for $\theta_i + \theta_t > \pi/2$ whereas $\tan(\theta_i - \theta_t)$ is positive.

---

[1] When $n_2 > n_1$, the second medium is optically denser than the first medium, there is a real angle θ_t of refraction for every angle of incidence.

$$\sin\theta_t = \frac{1}{n_{12}} \sin\theta_i < \sin\theta_i$$

[2] From equation (2.10) and (2.12) we conclude that in the plane z=0, the phase of $E_y^{(r)}$ and $E_y^{(i)}$ differ by π, whereas the phases of $E_x^{(r)}$ and $E_x^{(i)}$ are equal to each other. This difference in the behaviour of phases of the y and x components are formal according to the definition of reflected angle from the Figure (2.1)

$$\frac{E_y^{(r)}}{E_y^{(i)}} = \frac{R_{\perp}}{A_{\perp}}, \qquad\qquad \frac{E_x^{(r)}}{E_x^{(i)}} = -\frac{R_{//}}{A_{//}}$$

For normal incidence (our usual case), $\theta_i = 0$ and consequently $\theta_t = 0$ and the reflection formulas reduce to

$$
\left.
\begin{aligned}
R_{//} &= \frac{n_{12} - 1}{n_{12} + 1} A_{//} \\[2ex]
R_{\perp} &= \frac{n_{12} - 1}{n_{12} + 1} A_{\perp}
\end{aligned}
\right\}
\qquad (2.23)
$$

2.3. Wave Propagation in a Stratified Medium
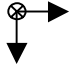
A medium whose properties are constant throughout each plane perpendicular to a fixed direction is called a stratified medium. If the z-axis of a Cartesian reference system is taken along this special direction, then $\varepsilon = \varepsilon(z)$, $\mu = \mu(z)$.

We shall consider the propagation of a plane, time harmonic electromagnetic wave through such a medium; this is a natural generalization of the simple case treated in the previous section.

The theory of stratified media is of considerable importance in connection with multilayer parallel thin films. Such films have many useful applications, as can be employed as antireflection films. On the other hand such films can be designed to enhance the reflection of electromagnetic waves. In order to use dielectric stratified films to prevent from being detected, we need to understand the stratified medium.

2.3.1. Wave Propagation

When a plane, time harmonic electromagnetic wave propagated through stratified medium is linearly polarized with its electric vector perpendicular to the plane of incidence we shall speak of a transverse electric wave (TE); when it is linearly polarized with its magnetic vector perpendicular to the plane of incidence we shall speak of a transverse magnetic wave (TM). So, the arbitrary polarized wave is resolved in two ways. These two waves either be independent of each other or mutually independent. And moreover, Maxwell's equations remain when **E** and **H** and simultaneously ε and μ are interchanged. Thus any theorem relating to TM waves

may immediately be deduced from the corresponding result for TE waves by making this change. ⊗→ It is sufficient to study only on TE waves.

We take the plane of incidence y, z-plane (different from previous section), z being the direction of stratification. For a TE wave, $E_y = E_z = 0$ and Maxwell's equations reduce to the following six scalar equations (time dependence $\exp(-i\omega t)$ being assumed)

$$\frac{\partial H_z}{\partial y} - \frac{\partial H_y}{\partial z} + \frac{i\varepsilon\omega}{c} E_x = 0 \qquad (2.24)$$

$$\frac{i\omega\mu}{c} H_x = 0 \qquad (2.27)$$

$$\frac{\partial H_x}{\partial z} - \frac{\partial H_z}{\partial x} = 0 \qquad (2.25)$$

$$\frac{\partial E_x}{\partial z} - \frac{i\omega\mu}{c} H_y = 0 \qquad (2.28)$$

$$\frac{\partial H_y}{\partial x} - \frac{\partial H_x}{\partial y} = 0 \qquad (2.26)$$

$$\frac{\partial E_x}{\partial y} + \frac{i\omega\mu}{c} H_z = 0 \qquad (2.29)$$

These equations show that H_y, H_z and E_x are functions of y and z only. Eliminating H_y and H_z between equations (2.24), (2.28) and (2.29);

$$\frac{\partial^2 E_x}{\partial y^2} + \frac{\partial^2 E_x}{\partial z^2} + n^2 k_0^{\ 2} E_x = \frac{d(\ln \mu)}{dz} \frac{\partial E_x}{\partial z} \qquad (2.30)$$

Where

$$n^2 = \varepsilon\mu, \qquad k_0 = \frac{\omega}{c} = \frac{2\pi}{\lambda_0} \qquad (2.31)$$

To solve equation (2.30) we take, as a trial solution, a product of two functions, one involving y only and the other involving z only:

$$E_x(y, z) = Y(y)U(z) \qquad (2.32)$$

And equation (2.30) becomes

14

$$\frac{\partial^2 (Y(y)U(z))}{\partial y^2} = -\frac{\partial^2 (Y(y)U(z))}{\partial z^2} - n^2 k_0^2 Y(y)U(z) + \frac{d(\ln \mu)}{dz} \frac{\partial (Y(y)U(z))}{\partial z}$$

$$\frac{1}{Y} \frac{d^2 Y}{dy^2} = -\frac{1}{U} \frac{d^2 U}{dz^2} - n^2 k_0^2 + \frac{d(\ln \mu)}{dz} \frac{1}{U} \frac{dU}{dz} \qquad (2.33)$$

Now the term on the left belongs to y while the term on the right belongs to z. This holds only when both sides are equal to $-K^2$.

$$\frac{1}{Y} \frac{d^2 Y}{dy^2} = -K^2 \qquad (2.34)$$

$$-\frac{1}{U} \frac{d^2 U}{dz^2} - n^2 k_0^2 + \frac{d(\ln \mu)}{dz} \frac{1}{U} \frac{dU}{dz} = -K^2 \qquad (2.35)$$

When we set (convenience) $K^2 = k_0^2 \alpha^2$,

$$Y = e^{ik_0 \alpha y} \qquad (2.36)$$

So from equation (2.30),

$$E_x = U(z)e^{i(k_0 \alpha y - \omega t)} \qquad (2.37)$$

From equations (2.26) and (2.27), H_y and H_z are given by expressions of the same form:

$$H_y = V(z)e^{i(k_0 \alpha y - \omega t)} \qquad (2.38)$$

$$H_z = W(z)e^{i(k_0 \alpha y - \omega t)} \qquad (2.39)$$

On the account of equations (2.24), (2.28) and (2.29), the amplitude functions U, V and W are related by the following equations:

$$V' = ik_0(\alpha W + \varepsilon U) \qquad (2.40)$$

$$U' = ik_0 \mu V \qquad (2.41)$$

$$\alpha U + \mu W = 0 \qquad (2.42)$$

The prime denotes the differentiation with respect to z. Substituting for W from equation (2.42) into equation (2.40) we have, together with equation (2.41), a pair of simultaneous first order differential equations for U and V:

$$
\left.
\begin{array}{l}
U' = ik_0 \mu V \\[2ex]
V' = ik_0 \left(\varepsilon - \dfrac{\alpha^2}{\mu} \right) U
\end{array}
\right\} \qquad (2.43)
$$

Elimination between there equations finally give the following second-order linear differential equations for U and V:

$$\frac{d^2 U}{dz^2} + k_0^{\;2}(n^2 - \alpha^2)U - \frac{d(\ln \mu)}{dz}\frac{dU}{dz} = 0 \qquad (2.44)$$

$$\frac{d^2 V}{dz^2} + k_0^{\;2}(n^2 - \alpha^2)V - \frac{d\left(\ln\left(\varepsilon - \dfrac{\alpha^2}{\mu} \right) \right)}{dz}\frac{dV}{dz} = 0 \qquad (2.45)$$

U, V and W are in general complex functions of z. The surfaces of constant amplitude of E_x are given by $|U(z)| = \text{constant}$, while the surfaces of constant phase have the equation ; $\phi(z) + k_0 \alpha y = \text{constant}$,

Where $\phi(z)$ is the phase of U. The two sets of surface do not in general coincide so that E_x is an homogeneous wave. For a small displacement (dy,dz) along a cophasal surface, $\phi'(z)dz + k_0 \alpha y = 0$; hence if θ denotes the angle which the normal to the co-phasal surface makes with OZ, then

$$\tan \theta = -\frac{dz}{dy} = \frac{k_0 \alpha}{\phi'(z)}$$

When the wave is an homogenous plane wave,

$$\phi(z) = k_0 nz \cos\theta, \qquad \alpha = n \sin\theta \qquad (2.46)$$

2.3.2. The Characteristic Matrix of a Stratified Medium

In need of usage properties of matrices, we need to determine the definitions and properties of matrices that are only ones necessary for our purposes [12-13]. The solutions we reached can most conveniently be expressed in terms of matrices. By a matrix one can understands a system of real or complex numbers, arranged in a rectangular or a square array:

$$\begin{bmatrix} a_{11} & a_{12} & ... & a_{1n} \\ . & . & . & a_{2n} \\ . & . & . & . \\ a_{m1} & . & . & a_{mn} \end{bmatrix} \qquad a_{ij} \text{ denoting the element in the ith row and the jth column}$$

since it contains m rows and n columns. The matrix is denoted symbolically by $\mathbf{A}$ or $\lfloor a_{ij} \rfloor$, and is said to be an m by n matrix since it contains m rows and n columns. In the special case when m=n, $\mathbf{A}$ is said to be a square matrix of order m. If $\mathbf{A}$ is a square matrix, the determinant whose elements are the same, and are in the same positions as the elements of A, is said to be the determinant of the matrix $\mathbf{A}$; it is denoted by $|\mathbf{A}|$ or $\lfloor a_{ij} \rfloor$. If $|\mathbf{A}| = 1$, $\mathbf{A}$ is said to be unimodular [5].

By definition two matrices are equal only if they have the same number of rows(m) and the same number of columns (n) and if their corresponding elements are equal. If $\mathbf{A} = \lfloor a_{ij} \rfloor$ and $\mathbf{B} = \lfloor b_{ij} \rfloor$ are two matrices with the same number of rows and the same number of columns, then their sum $\mathbf{A+B}$ is defined as the matrix $\mathbf{C}$ with elements $c_{ij} = a_{ij} + b_{ij}$. Similarly their difference $\mathbf{A-B}$ is defined as the matrix $\mathbf{D}$ with elements $d_{ij} = a_{ij} - b_{ij}$.

A matrix is having every element zero is called a null matrix. The square matrix with elements $a_{ij} = 0$ when $i \neq j$ and $a_{ij} = 1$ for every value of i is called unit matrix and will be denoted by $\mathbf{I}$.

The product of a matrix $\mathbf{A}$ and a number λ (real or complex) is defined as the matrix $\mathbf{B}$ with elements $b_{ij} = \lambda a_{ij}$.

The product of **AB** of two matrices is defined only when the number of columns in **A** is equal to the number of two rows in **B**. If **A** is an $m \times p$ matrix and **B** is a $p \times n$ matrix the product is then by definition the $m \times n$ matrix with elements.

$$c_{ij} = \sum_{k=1}^{p} a_{ik} b_{kj} \qquad (2.47)$$

The process of multiplication of two matrices is thus analogous to the row-by-column rule for multiplication of determinants of equal orders. In general $\mathbf{AB} \neq \mathbf{BA}$. In the special case when **AB=BA,** the matrices A and B are said to commute.

Since the functions U(z) and V(z) each satisfy a second-order linear differential equation (2.44) and (2.45), it follows that U and V may each be expressed as a linear combination of two particular solutions, say U_1, U_2 and V_1, V_2. These particular solutions cannot be arbitrary; they must be coupled by the first order differential equations (2.43):

$$\left. \begin{array}{l} U_1' = ik_0 \mu V_1 \\[2mm] V_1' = ik_0 \left(\varepsilon - \dfrac{\alpha^2}{\mu} \right) U_1 \end{array} \right\} \qquad\qquad \left. \begin{array}{l} U_2' = ik_0 \mu V_2 \\[2mm] V_2' = ik_0 \left(\varepsilon - \dfrac{\alpha^2}{\mu} \right) U_2 \end{array} \right\} \qquad (2.48)$$

From these relations;

$$V_1 U_2' - U_1' V_2 = 0 \qquad\qquad U_1 V_2' - V_1' U_2 = 0 \qquad (2.49)$$

So that
$$\frac{d}{dz}(U_1 V_2 - U_2 V_1) = 0$$

This implies that the determinant associated with two arbitrary solutions of equation (2.43) is constant.

$$D = \begin{vmatrix} U_1 & V_1 \\ U_2 & V_2 \end{vmatrix} \qquad (2.50)$$

For our solution the most convenient choice of the particular solution is

$$U_1 = f(z) \qquad\qquad U_2 = F(z)$$
$$V_1 = g(z) \qquad\qquad V_2 = G(z) \qquad\qquad\qquad (2.51)$$

Such that $\qquad$ f(0)=G(0)=0 $\qquad$ and $\qquad$ F(0)=g(0)=1 $\qquad\qquad$ (2.52)

Then with the solutions, $U(0) = U_0$ and $V(0) = V_0$, it can be expressed that;

$$U = FU_0 + fV_0$$
$$V = GU_0 + gV_0 \qquad\qquad\qquad (2.53)$$

Or in matrix solution,

$$\mathbf{Q} = \mathbf{N}\mathbf{Q_0} \qquad\qquad\qquad (2.54)$$

$$\mathbf{Q} = \begin{bmatrix} U(z) \\ V(z) \end{bmatrix}, \qquad \mathbf{Q_0} = \begin{bmatrix} U_0 \\ V_0 \end{bmatrix}, \qquad \mathbf{N} = \begin{bmatrix} F(z) & f(z) \\ G(z) & g(z) \end{bmatrix} \qquad (2.55)$$

On the account of relation D=constant, the determinant of the square matrix N is a constant. The value of this constant may immediately be found by taking z=0, giving $|\mathbf{N}| = fg - fG = 1$, it is usually more convenient to express U_0 and V_0 as functions of U(z) and V(z). Solving for U_0 and V_0 we obtain

$$\mathbf{Q_0} = \mathbf{M}\mathbf{Q} \qquad\qquad\qquad (2.56)$$

Where; $\qquad\qquad\qquad \mathbf{M} = \begin{bmatrix} g(z) & -f(z) \\ -G(z) & F(z) \end{bmatrix} \qquad\qquad (2.57)$

This matrix is also unimodular, $\qquad\qquad\qquad |\mathbf{M}| = 1$

The significance of **M** is clear: it relates the x- and y-components of the electric vectors in the plane z=0 to the components in an arbitrary plane z=constant. These information given is sufficient for the complete specification of the field. Hence for the purposes of determining the propagation of a plane monochromatic wave through a stratified medium, the medium only need be specified by an appropriate two by unimodular matrix **M.** For this reason we shall call M the characteristic matrix of the stratified medium. The constancy of the determinant $|\mathbf{M}|$ may be shown to imply the conservation of energy.

2.3.3. Homogeneous Dielectric Film

In this case ε, μ and $n = \sqrt{\varepsilon\mu}$ are constants. If θ denotes the angle which the normal to the wave makes with the z-axis, we have $\alpha = n\sin\theta$. For TE wave, we have according to equations (2.44) and (2.45),

$$\left.\begin{aligned}\frac{d^2U}{dz^2} + \left(k_0 n^2 \cos^2\theta\right)U = 0 \\[2mm] \frac{d^2V}{dz^2} + \left(k_0 n^2 \cos^2\theta\right)V = 0\end{aligned}\right\} \qquad (2.58)$$

The solution of these equations, subject to the relations, equation (2.43) can be noticed as;

$$\left.\begin{aligned}U(z) = A\cos(k_0 nz\cos\theta) + B\sin(k_0 nz\cos\theta) \\[2mm] V(z) = \frac{1}{i}\sqrt{\frac{\varepsilon}{\mu}}\cos\theta\left[B\cos(k_0 nz\cos\theta) - A\sin(k_0 nz\cos\theta)\right]\end{aligned}\right\} \qquad (2.59)$$

Hence the particular solutions equation (2.51) which satisfy the boundary conditions equation (2.52) are

$$U_1 = f(z) = \frac{i}{\cos\theta}\sqrt{\frac{\mu}{\varepsilon}}\sin(k_0 nz \cos\theta),$$

$$V_1 = g(z) = \cos(k_0 nz \cos\theta),$$

$$U_2 = F(z) = \cos(k_0 nz \cos\theta),$$

(2.60)

$$V_2 = G(z) = i\sqrt{\frac{\varepsilon}{\mu}}\cos\theta \sin(k_0 nz \cos\theta).$$

If we set

$$p = \sqrt{\frac{\varepsilon}{\mu}}\cos\theta \qquad (2.61)$$

Then the characteristic matrix of a TE wave can be seen as;

$$M(z) = \begin{bmatrix} \cos(k_0 nz \cos\theta) & -\dfrac{i}{p}\sin(k_0 nz \cos\theta) \\ -ip\sin(k_0 nz \cos\theta) & \cos(k_0 nz \cos\theta) \end{bmatrix} \qquad (2.62)$$

And the characteristic matrix of a TM wave is replaces p by $q = \sqrt{\dfrac{\varepsilon}{\mu}}\cos\theta$.

As it can be seen that the characteristic matrix of a stratified matrix is in the form of;

$$M = \begin{bmatrix} a & ib \\ ic & d \end{bmatrix} \qquad \text{where a, b, c and d are real.} \qquad (2.63)$$

If we are talking about more than one dielectric films, say first one extends from $z = 0$ to $z = z_1$ and second one extends from $z = z_1$ to $z = z_2$, electromagnetic definition of these combined dielectric films can be described by matrix method.

If $\mathbf{M}_1(z)$ and $\mathbf{M}_2(z)$ are the characteristic matrices of two stratified medium, overall matrix of these two adjacent mediums can be represented as;

$$\mathbf{M}(z_2) = \mathbf{M}_1(z_1)\mathbf{M}_2(z_2 - z_1) \qquad (2.64)$$

If we generalize these formulae by using more than one matrices adjacent to each other;

$$\mathbf{M}(z_N) = \mathbf{M}_1(z_1)\mathbf{M}_2(z_2 - z_1)\dots\mathbf{M}_N(z_N - z_{N-1}) \tag{2.65}$$

2.3.4. Representation of Reflection Coefficient

As we have studied so far, we found out the Fresnel Formulae and matrix definition of the characteristic matrix of a TE wave in which we will derive the reflection matrix.

Let A, R and T represent the amplitudes of electric vectors of the incident, reflected and transmitted waves; θ_1 and θ_l be the angles which the normal to the incident and the transmitted waves make with the z axis.

According to the boundary conditions, the tangential components of $\mathbf{E}$ and $\mathbf{H}$ must be continuous across each of the two boundaries of the stratified medium. So as we know,

$$\mathbf{E} = -\sqrt{\frac{\mu}{\varepsilon}}\mathbf{s}\times\mathbf{H} \qquad , \qquad \mathbf{H} = \sqrt{\frac{\varepsilon}{\mu}}\mathbf{s}\times\mathbf{E} \tag{2.66}$$

Thus for a TE wave the Fresnel coefficients of wave components can be expressed as;

$$\left. \begin{aligned} U_0 &= A + R & U(z_1) &= T \\ V_0 &= p_1(A - R) & V(z_1) &= p_l T \end{aligned} \right\} \tag{2.67}$$

$$p_1 = \sqrt{\frac{\varepsilon_1}{\mu_1}}\cos\theta_1 \qquad\qquad p_l = \sqrt{\frac{\varepsilon_l}{\mu_l}}\cos\theta_l \tag{2.68}$$

By evaluating equations (2.55) and (2.67) we can define these coefficients in matrix formation;

$$\begin{bmatrix} U_0 \\ V_0 \end{bmatrix} = \begin{bmatrix} m_{11} & m_{12} \\ m_{21} & m_{22} \end{bmatrix} \begin{bmatrix} U(z_1) \\ V(z_1) \end{bmatrix} \tag{2.69}$$

$$\left. \begin{aligned} A + R &= (m_{11} + m_{12}p_l)T \\ p_1(A - R) &= (m_{21} + m_{22}p_l)T \end{aligned} \right\} \tag{2.70}$$

If we derive these formulas we can discriminate reflection and transmission coefficients each other. Thus we reach our reflection coefficient as;

$$r = \frac{R}{A} = \frac{(m_{11} + m_{12}p_l)p_1 - (m_{21} + m_{22}p_l)}{(m_{11} + m_{12}p_l)p_1 + (m_{21} + m_{22}p_l)} \tag{2.71}$$

$$\mathbf{R} = |r|^2 \tag{2.72}$$

We can evaluate reflectivity (R) for TM wave by replacing p_1 and p_l with

$$q_1 = \sqrt{\frac{\mu_1}{\varepsilon_1}} \cos\theta_1 \qquad\qquad q_l = \sqrt{\frac{\mu_l}{\varepsilon_l}} \cos\theta_l \tag{2.73}$$

As we derived the reflection coefficient, approving our definitions exactly, we can now start representing what in fact we really deal with and find ways to diminish the amplitude of reflecting waves. It is apparent that reflection from a dielectric slab depends on the electric and magnetic permeabilities, incident angle (we will assume the beam come nearly with zero angle), index and thickness of the slab and wavelength. The reflection coefficient in which some books call it reflectance is derived for plane waves. Our laser is in Gaussian shape and we need to analyze which effects it exposes to.

CHAPTER 3

REFLECTION OF A GAUSSIAN BEAM FROM A DIELECTRIC SLAB

Optical communication systems have been a part of daily communication systems because of its speedy applications and its ever lasting applicable designs [14]. Above these in lightwave communication by the help of precisely detectable systems, differences that are not mere to be seen can be observed more accurately.

Light is an electromagnetic wave phenomenon described by the same theoretical principles that govern all forms of electromagnetic radiation [15-17]. Electromagnetic radiation propagates in the form of two mutually coupled vector waves, an electric field wave and a magnetic field wave.

Although the wave nature of light precludes the existence of being confined and transported in free space without angular spread idealization, light can take the form of beams that come as close as possible to spatially localized and non diverging waves.

In most laser applications it is necessary to focus, modify, or shape the laser beam by using lenses and other optical elements. In general, laser-beam propagation can be approximated by assuming that the laser beam has an ideal Gaussian intensity profile, which corresponds to the theoretical TEM_{00} mode. In order to select the best optics for a particular laser application, it is important to understand the basic properties of Gaussian beams.

3.1. Gaussian Beam Propagation

Unfortunately, the output from real-life lasers is not truly Gaussian (although helium neon lasers and argon-ion lasers are a very close approximation). To accommodate this variance, a quality factor, M^2 (called the "M-squared" factor), has been defined to describe the deviation of the laser beam from a theoretical Gaussian. For a theoretical Gaussian, $M^2 = 1$. Collimated TEM_{00} diode laser beams usually have an M^2 ranging from 1.1 to 1.7. For high-energy multimode lasers, the M^2 factor can be

as high as 25 or 30. In all cases, the M^2 factor affects the characteristics of a laser beam and cannot be neglected in optical designs. The beam waist is magnified by M, the beam depth of focus is magnified by M^2, and the angular divergence is minified by the factor M.

Although in some respects component design and tolerancing for lasers is more critical than for conventional optical components, the designs often tend to be simpler since many of the constraints associated with imaging systems are not present. For instance, laser beams are nearly always used on axis, which eliminates the need to correct asymmetric aberration.

Because laser light is generated coherently, it is not subject to some of the limitations normally associated with incoherent sources. All parts of the wavefront act as if they originate from the same point; consequently, the emergent wavefront can be precisely defined. Starting out with a well-defined wavefront permits more precise focusing and control of the beam than otherwise would be possible.

For virtually all laser cavities, the propagation of an electromagnetic field, E(0), through one round trip in an optical resonator can be described mathematically by a propagation integral, which has the general form

$$E^{(1)}(x,y) = e^{-jkp} \iint\limits_{InputPlane} K(x,y,x_0,y_0) E^{(0)}(x_0,y_0) dx_0 dy_0 \qquad (3.1)$$

where K is the propagation constant at the carrier frequency of the optical signal, p is the length of one period or round trip, and the integral is over the transverse coordinates at the reference or input plane. The function K is commonly called the propagation kernel since the field $E^{(1)}(x,y)$ after one propagation step, can be obtained from the initial field $E^{(0)}(x_0,y_0)$ through the operation of the linear kernel or "propagator" $K(x,y,x_0,y_0)$.

By setting the condition that the field, after one period, will have exactly the same transverse form, both in phase and profile (amplitude variation across the field), we get the equation

$$\gamma_{nm} E_{nm}(x,y) = \iint\limits_{InputPlane} K(x,y,x_0,y_0) E_{nm}(x_0,y_0) dx_0 dy_0 \qquad (3.2)$$

where E_{nm} represents a set of mathematical eigenmodes, and γ_{nm} a corresponding set of eigenvalues. The eigenmodes are referred to as transverse cavity modes, and, for stable resonators, are closely approximated by Hermite-Gaussian functions, denoted by TEM_{nm}.

The lowest order, or "fundamental" transverse mode, TEM_{00} has a Gaussian intensity profile, shown in Figure 3.1, which has the form

$$I(x, y) \propto e^{-k(x^2 + y^2)} \tag{3.3}$$

3.1.1. Beam Waist And Divergence

In order to gain an appreciation of the principles and limitations of Gaussian beam optics, it is necessary to understand the nature of the laser output beam. In TEM_{00} mode, the beam emitted from a laser begins as a perfect plane wave with a Gaussian transverse intensity profile as shown in Figure 3.1. The Gaussian shape is truncated at some diameter either by the internal dimensions of the laser or by some limiting aperture in the optical train.
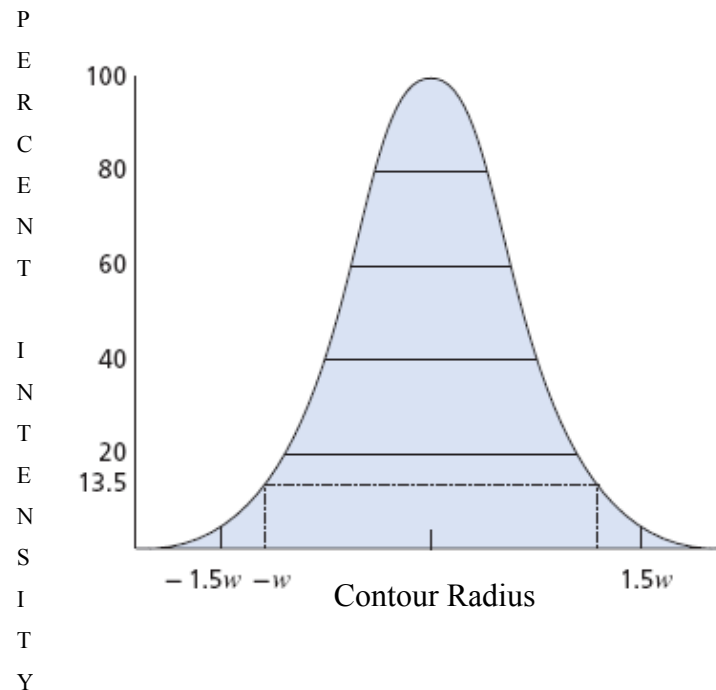
Figure 3.1. Intensity Profile Of A Gaussian TEM_{00} Mode
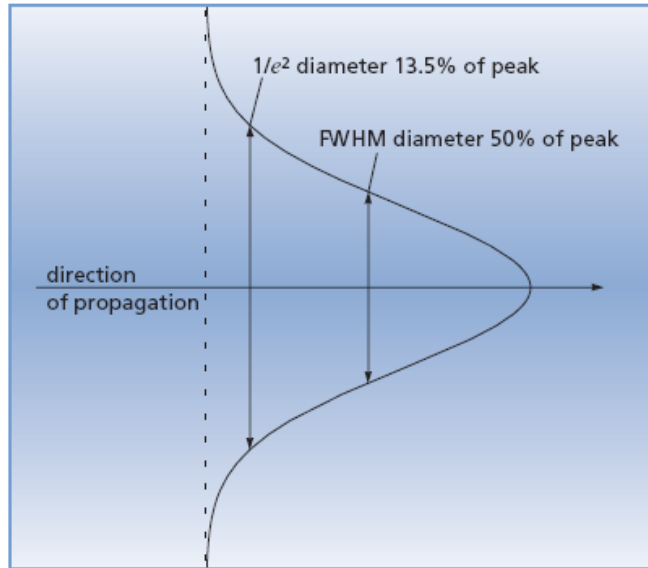
Figure 3.2. Diameter Of A Gaussian Beam

The diameter at which the beam irradiance (intensity) has fallen to $1/e^2$ (13.5 percent) of its peak, or axial value and the other is the diameter at which the beam irradiance (intensity) has fallen to 50 percent of its peak, or axial value, as shown in Figure 3.2. This second definition is also referred to as FWHM, or full width at half maximum. General usage is the $1/e^2$ definition as described and compared above.

Diffraction causes light waves to spread transversely as they propagate, and it is therefore impossible to have a perfectly collimated beam. The spreading of a laser beam is in precise accord with the predictions of pure diffraction theory; aberration is totally insignificant in the present context. Under quite ordinary circumstances, the beam spreading can be so small that it can go unnoticed. The accurately describe beam spreading, making it easy to see the capabilities and limitations of laser beams are described above.

Even if a Gaussian TEM_{00} laser-beam wavefront were made perfectly flat at some plane, it would quickly acquire curvature and begin spreading in accordance with

$$R(z) = z \left[1 + \left(\frac{\pi . w_0^{\,2}}{\lambda . z} \right)^2 \right]$$

(3.4)

$$w(z) = w_0 \left[1 + \left(\frac{\lambda.z}{\pi.w_0^{\,2}} \right)^2 \right]^{1/2} \tag{3.5}$$

where z is the distance propagated from the plane where the wavefront is flat, λ is the wavelength of light, w_0 is the radius of the $1/e^2$ irradiance contour at the plane where the wavefront is flat, w(z) is the radius of the $1/e^2$ contour after the wave has propagated a distance z, and R(z) is the wavefront radius of curvature after propagating a distance z. R(z) is infinite at z = 0, passes through a minimum at some finite z, and rises again toward infinity as z is further increased, asymptotically approaching the value of z itself. The plane z=0 marks the location of a Gaussian waist, or a place where the wavefront is flat, and w_0 is called the beam waist radius.

The intensity distribution of the Gaussian TEM_{00} beam, namely,

$$I(r) = I_0.e^{-2r^2/w^2} = \frac{2.P}{\pi.w^2} e^{-2r^2/w^2} \tag{3.6}$$

where w=w(z) and P is the total power in the beam, is the same at all cross sections of the beam.

The invariance of the form of the distribution is a special consequence of the presumed Gaussian distribution at z = 0. If a uniform irradiance distribution had been presumed at z = 0.

Simultaneously, as R(z) asymptotically approaches z for large z, w(z) asymptotically approaches the value

$$w(z) = \frac{\lambda.z}{\pi.w_0} \tag{3.7}$$

where z is presumed to be much larger than $\pi.w_0/\lambda$ so that the $1/e^2$ irradiance contours asymptotically approach a cone of angular radius

$$\theta = \frac{w(z)}{z} = \frac{\lambda}{\pi.w_0} \tag{3.8}$$

This value is the far-field angular radius (half-angle divergence) of the Gaussian TEM_{00} beam. The vertex of the cone lies at the center of the waist, as shown in Figure 3.3.

It is important to note that, for a given value of λ, variations of beam diameter and divergence with distance z are functions of a single parameter, w_0, the beam waist radius.
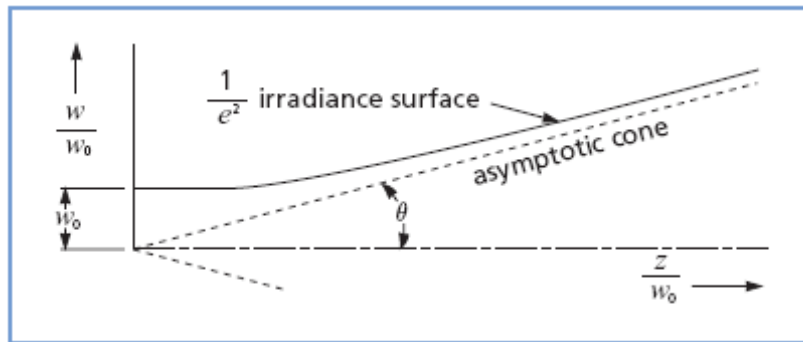
Figure 3.3. Growth In $1/e^2$ Radius With Propagated Away From Gaussian Waist

3.1.2. Near-Field vs Far-Field Divergence

Unlike conventional light beams, Gaussian beams do not diverge linearly. Near the beam waist, which is typically close to the output of the laser, the divergence angle is extremely small; far from the waist, the divergence angle approaches the asymptotic limit described above. The Raleigh range (z_R), defined as the distance over which the beam radius spreads by a factor of $\sqrt{2}$, is given by

$$z_R = \frac{\pi . w_0^{\,2}}{\lambda} \tag{3.9}$$

At the beam waist (z = 0), the wavefront is planar $[R(0) = \infty]$ Likewise, at z=∞, the wavefront is planar $[R(\infty) = \infty]$. As the beam propagates from the waist, the wavefront curvature, therefore, must increase to a maximum and then begin to decrease, as shown in figure 3.4. The Raleigh range, considered to be the dividing line between

near-field divergence and midrange divergence, is the distance from the waist at which the wavefront curvature is a maximum. Far-field divergence (the number quoted in laser specifications) must be measured at a distance much greater than z_R (usually $> 10 \times z_R$ will suffice). This is a very important distinction because calculations for spot size and other parameters in an optical train will be inaccurate if near- or mid-field divergence values are used. For a tightly focused beam, the distance from the waist (the focal point) to the far field can be a few millimeters or less. For beams coming directly from the laser, the far-field distance can be measured in meters.
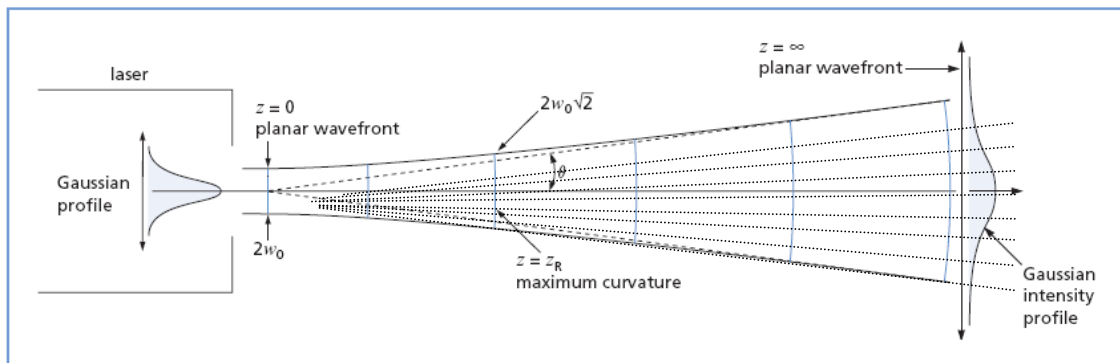
Figure 3.4. Changes In Wavefront Radius With Propagation Distance

Typically, one has a fixed value for w_0 and uses the expression

$$w(z) = w_0 \left[1 + \left(\frac{\lambda . z}{\pi . w_0^{\,2}} \right)^2 \right]^{1/2} \tag{3.10}$$

to calculate w(z) for an input value of z. However, one can also utilize this equation to see how final beam radius varies with starting beam radius at a fixed distance, z.

The beam radius at 100m reaches a value for a starting beam waist of about 0.1 mm ($\lambda = 1000nm$). Therefore, if we want to achieve the best combination of beam diameter and spread (or best collimation) over a distance of 100m, $w(z)$ is approximately calculated as 3 cm.

We can find the general expression for the optimum starting beam radius for a given distance, z. Doing so yields

$$w_0(optimum) = \left(\frac{\lambda.z}{\pi} \right)^{1/2} \qquad\qquad (3.11)$$

As can be seen, Gaussian beam diverges as it propagates. Defining the Gaussian beam in these parameters will help us to understand how a laser propagates, diverges and which distribution it has. Now Gaussian beam shape laser in plane wave decomposition will be described according to our situation in terms of representing laser beam.

3.2. Description of Gaussian Beam Propagation In Terms Of Plane Wave Decomposition

We can say that when a Gaussian beam comes to a dielectric slab, the beam changes according to the propagation and reflection to the slab. The reflected wave with the shape of a Gaussian beam does not properly protect its own structure. By the way until the beam comes to a dielectric slab, the beam profile changes and broadens along the x-axis [7]. While the beam reflects from the dielectric slab, the amplitude and phase changes and the beam profile alters.

The reflected beam profiles of electromagnetic radiation have different effects from reflected plane waves [18-21]. Gaussian beams which reflect from a dielectric slab have a shifting maximum point in one direction. Lateral shift, focal shift and angular shift represent this shifting and the distortion of the beam profile. The Gaussian beam propagates in the z direction and broadens in x direction in two dimension and is composed of plane wave components [7].

Above consideration the results indicate that the path followed by the reflected maximum does not evolve a lateral shift, but consists of an angular deviation to one side only of the geometric path.

The reflected beam profile must be evaluated according to the incident angle, the thickness, reflective indices of the slab and wavelength of the Gaussian beam. Although the beam first propagates, then reflects and then propagates again, we will reflect the beam and combine the propagating distance before and after reflection then take into account.

The electric field distribution along the x axis is described with $\mathrm{E}_z(x)$ and the Fourier transform of it is $\mathrm{E}_z(f)$ where f is the spatial frequency and λ is the wavelength. We need to decompose it in Fourier series and after analyzing the reflection effects I will compose it and the transverse plane will help us to see the results.

$$\mathrm{E}_z(x) = \int_{-\infty}^{\infty} \breve{\mathrm{E}}_z(f) \exp(i2\pi f x) df \qquad \text{as} \qquad f = \frac{\sin\alpha}{\lambda} \qquad (3.12)$$

$\mathrm{E}_z(x)$ is described and can be thought as a plane wave traveling along z direction and making an angle α. The radiation field of a beam propagating at z direction has a spatial spectrum $\breve{\mathrm{E}}_z(f)$ that can be appreciable when $f \gg \dfrac{1}{\lambda}$. Then paraxial approximation can also be used. The launched beam at z=0 is in the form of

$$\mathrm{E}_0(x) = A \exp\left[-\left(\frac{x^2}{2\sigma^2}\right)\right] \qquad (3.13)$$

Where A is the amplitude, σ is the width of the beam which is being assumed in one dimension. Thus the corresponding spatial spectrum of the beam is called antenna function.

$$\breve{\mathrm{E}}_0(f) = A\sqrt{\pi} \exp\left(-\frac{(2\pi\sigma)^2 f^2}{2}\right) \qquad (3.14)$$

3.2.1 Propagation Effects

The beam changes its profile in x axis as it propagates in z direction. We mean the width of the beam enlarges according to the wavelength, spatial frequency and the propagation distance. We can take into account the after and before reflection effects and combine them and can think about just like the beam is reflected at z=0 and propagated the total distance.

Under paraxial approximation the transfer function of the propagating beam is described as

$$P(f) = \exp\left[-i\left(\pi z \lambda f^2\right)\right]$$ (3.15)

The beam propagating along z axis broadens in the x axis and this can be seen when multiplying the transfer function and antenna function and then taking the Fourier transform of the product as described in equation (3.12) that will take us to a Gaussian field with a broadened profile and a phase curvature both being the function of the propagating distance.

3.2.2 Reflection Effects

As I define; before reflection is taken into account, the beam never propagated before. The beam reflects from a dielectric slab at an angle close to the incident angle θ_i. As described in second chapter, the reflection is taken into account with film structure assuming all the media to be non-magnetic $(\mu = 1)$ and as we know $n = \sqrt{\varepsilon\mu}$

So, equation (2.59) becomes as $\qquad p_i = n_i \cos\theta_i \qquad$ (i=1,2,3..)

The subscriptions n_1, n_2, n_3 are the indices of the materials and D is the thickness of the slab is denoted. We take $n_3 = n_1$ because we decide to use one material and want to measure just the reflecting part for only Gaussian beam for one material. θ_1 is the angle between the normal of the slab and the Gaussian beam waist point.

In accordance, we can show the situation in schematic form.
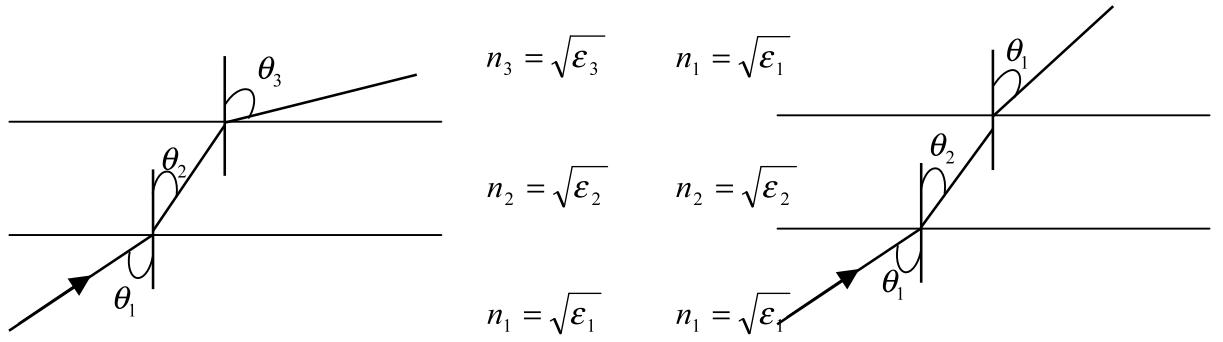
Figure 3.5. One Slab Configuration

From Chapter 2 we know that reflectivity can be represented as matrix form and when we take

$$\beta_x = \frac{2\pi}{\lambda_0} n_x D \cos(\theta_x) \qquad\qquad (x=1,2,3\ldots) \qquad (3.16)$$

The reflection coefficient becomes as;

$$
\left.
\begin{aligned}
m_{11} &= \cos(\beta) & m_{11} &= m_{22} \\
m_{12} &= -\frac{i}{p_2}\sin(\beta) & m_{21} &= -ip_2\sin(\beta)
\end{aligned}
\right\} \qquad (3.17)
$$

Given in the Chapter 2, the reflection coefficient is described by

$$r = \frac{R}{A} = \frac{\left(m_{11}+m_{12}p_l\right)p_1 - \left(m_{21}+m_{22}p_l\right)}{\left(m_{11}+m_{12}p_l\right)p_1 + \left(m_{21}+m_{22}p_l\right)} \qquad (3.18)$$

With $l = 3$, according to equation (2.19);

$$r_{12\perp} = \frac{n_1\cos(\theta_1)-n_2\cos(\theta_2)}{n_1\cos(\theta_1)+n_2\cos(\theta_2)} = \frac{p_1-p_2}{p_1+p_2} \qquad (3.19)$$

$$r_{23\perp} = \frac{n_2\cos(\theta_2)-n_3\cos(\theta_3)}{n_2\cos(\theta_2)+n_3\cos(\theta_3)} = \frac{p_2-p_3}{p_2+p_3} \qquad (3.20)$$

According to the definitions given above we can evaluate the reflection coefficient from a dielectric slab.

$$r_\perp = \frac{\left(\cos(\beta) - \dfrac{i}{p_2}\sin(\beta)p_3\right)p_1 - (\cos(\beta)p_3 - ip_2\sin(\beta))}{\left(\cos(\beta) - \dfrac{i}{p_2}\sin(\beta)p_3\right)p_1 + (\cos(\beta)p_3 - ip_2\sin(\beta))} \tag{3.21}$$

And becomes in the form of:

$$r_\perp = \frac{(p_1 p_2 \cos(\beta)) - (ip_1 p_3 \sin(\beta)) - (p_2 p_3 \cos(\beta)) + i(p_2)^2 \sin(\beta)}{(p_1 p_2 \cos(\beta)) - (ip_1 p_3 \sin(\beta)) + (p_2 p_3 \cos(\beta)) + i(p_2)^2 \sin(\beta)} \tag{3.22}$$

Taking the parenthesis of cos and sin functions,

$$r_\perp = \frac{[(p_1 p_2 - p_2 p_3)\cos(\beta)] - i\sin(\beta)[p_1 p_3 - (p_2)^2]}{[(p_1 p_2 + p_2 p_3)\cos(\beta)] - i\sin(\beta)[p_1 p_3 + (p_2)^2]} \tag{3.23}$$

$$r_\perp = \frac{p_1 p_2 - p_2 p_3 - i\dfrac{\sin(\beta)}{\cos(\beta)}[p_1 p_3 - (p_1)^2]}{p_1 p_2 + p_2 p_3 - i\dfrac{\sin(\beta)}{\cos(\beta)}[p_1 p_3 + (p_1)^2]} \tag{3.24}$$

As we know,

$$e^{i\beta} = \cos(\beta) - i\sin(\beta), \qquad -i\frac{\sin(\beta)}{\cos(\beta)} = \frac{1 - e^{i2\beta}}{1 + e^{i2\beta}} \tag{3.25}$$

Then we substitute the parts

$$r_\perp = \frac{p_1 p_2 - p_2 p_3 + \dfrac{\left(1 - e^{i2\beta}\right)}{\left(1 + e^{i2\beta}\right)}[p_1 p_3 - (p_2)^2]}{p_1 p_2 + p_2 p_3 + \dfrac{\left(1 - e^{i2\beta}\right)}{\left(1 + e^{i2\beta}\right)}[p_1 p_3 + (p_2)^2]} \tag{3.26}$$

$$r_\perp = \frac{p_1 p_2\left(1 + e^{i2\beta}\right) - p_2 p_3\left(1 + e^{i2\beta}\right) + p_1 p_3\left(1 - e^{i2\beta}\right) - p_2{}^2\left(1 - e^{i2\beta}\right)}{p_1 p_2\left(1 + e^{i2\beta}\right) + p_2 p_3\left(1 + e^{i2\beta}\right) + p_1 p_3\left(1 - e^{i2\beta}\right) + p_2{}^2\left(1 - e^{i2\beta}\right)} \tag{3.27}$$

$$r_\perp = \frac{[p_1 p_2 + (p_2 p_3 e^{i2\beta})] + [-(p_2 p_3) - p_2 p_3 e^{i2\beta}] + [p_1 p_3 - (p_1 p_3 e^{i2\beta})] - (p_2)^2 + (p_2)^2 e^{i2\beta}]}{[p_1 p_2 + (p_2 p_3 e^{i2\beta})] + [(p_2 p_3) + p_2 p_3 e^{i2\beta}] + [p_1 p_3 - (p_1 p_3 e^{i2\beta})] - (p_2)^2 - (p_2)^2 e^{i2\beta}]}$$

$$r_\perp = \frac{p_1 p_2 - p_2 p_3 - (p_2)^2 + p_1 p_3 + [p_1 p_2 - p_2 p_3 + (p_2)^2 - p_1 p_3] e^{i2\beta}}{p_1 p_2 - p_2 p_3 + (p_2)^2 - p_1 p_3 + [p_1 p_2 + p_2 p_3 - (p_2)^2 - p_1 p_3] e^{i2\beta}} \qquad (3.28)$$

$$r_\perp = \frac{(p_1 - p_2)(p_2 + p_3) + (p_1 + p_2)(p_2 - p_3) e^{i2\beta}}{(p_1 + p_2)(p_2 + p_3) + (p_1 - p_2)(p_2 - p_3) e^{i2\beta}} \qquad (3.29)$$

$$r_\perp = \frac{(p_1 - p_2)(p_2 + p_3) + (p_1 + p_2)(p_2 - p_3) e^{i2\beta}}{\left[(p_2 + p_3)(p_1 + p_2)\right]\left[1 + \left(\dfrac{p_1 - p_2}{p_1 + p_2}\right)\left(\dfrac{p_2 - p_3}{p_2 + p_3}\right)\right] e^{i2\beta}} \qquad (3.30)$$

$$r_\perp = \frac{\dfrac{p_1 - p_2}{p_1 + p_2} + \dfrac{p_2 - p_3}{p_2 + p_3} e^{i2\beta}}{1 + r_{12} r_{23} e^{i2\beta}} \qquad , \qquad r_\perp = \frac{r_{12} + r_{23} e^{i2\beta}}{1 + r_{12} r_{23} e^{i2\beta}} \qquad (3.31)$$

$$r_{23\perp} = \frac{n_2 \cos(\theta_2) - n_3 \cos(\theta_3)}{n_2 \cos(\theta_2) + n_3 \cos(\theta_3)} \qquad \text{where} \qquad n_3 = n_1, \ \theta_3 = \theta_1 \qquad (3.32)$$

For only one dielectric slab

$$r_{23\perp} = \frac{n_2 \cos(\theta_2) - n_1 \cos(\theta_1)}{n_2 \cos(\theta_2) + n_1 \cos(\theta_1)} \qquad , \qquad r_{23\perp} = -r_{12\perp} \qquad (3.33)$$

$$r_\perp = \frac{r_{12\perp} - r_{12\perp} e^{i2\beta}}{1 + r_{12\perp}(-r_{12\perp}) e^{i2\beta}} \qquad (3.34)$$

$$r_\perp = r_{12\perp} \frac{1 - e^{i2\beta}}{1 - r_{12\perp} e^{i2\beta}} \qquad (3.35)$$

$$n_1 \sin(\theta_1) = n_2 \sin(\theta_2) \qquad \text{(Snell's Law)} \qquad (3.36)$$

$$\sin(\theta_2) = \frac{F}{N} \qquad\qquad N = \frac{n_2}{n_1} \qquad , \qquad F = \sin(\theta_1) \qquad (3.37)$$

$$(\cos(\theta_2))^2 = 1 - \left(\frac{F}{N}\right)^2 \qquad , \qquad N\cos(\theta_2) = \sqrt{N^2 - F^2} \qquad (3.38)$$

$$\beta_2 = \frac{2\pi D}{\lambda} N\cos(\theta_2) \qquad , \qquad \beta_2 = \frac{2\pi D\sqrt{N^2 - F^2}}{\lambda} \qquad (3.39)$$

$$n_1\sin(\theta_1) = n_2\sin(\theta_2) \qquad\longrightarrow\qquad 1 - (\cos(\theta_1))^2 = N\sin(\theta_2) \qquad (3.40)$$

$$\cos(\theta_1) = \sqrt{1 - F^2} \qquad (3.41)$$

$$r_{12\perp} = \frac{\sqrt{1-F^2} - \sqrt{N^2-F^2}}{\sqrt{1-F^2} + \sqrt{N^2-F}^2} \qquad (3.42)$$

$$\sin(A+B) = \sin(A)\cos(B) + \cos(A)\sin(B)$$

In order to identify the Gaussian beam we define F above. In this equation we decompose the Gaussian beam using α components as the angle between decomposed beams which is shown in Figure 3.4 and denoted as θ.

$$F = \sin(\theta_i + \alpha) \qquad\longrightarrow\qquad F = \sin(\theta_i)\cos(\alpha) + \cos(\theta_i)\sin(\alpha) \qquad (3.43)$$

$$f = \frac{\sin(\alpha)}{\lambda} \qquad\longrightarrow\qquad \sin(\alpha) = \lambda f \qquad (3.44)$$

$$\cos(\alpha) = \sqrt{1 - (\lambda f)^2} \qquad (3.45)$$

$$F = \sqrt{1 - \lambda^2 f^2}\,\sin(\theta_i) + \lambda f\cos(\theta_i) \qquad (3.46)$$

We can say that the Gaussian beam which comes from the source reflects from one dielectric slab with the angle θ_i. And the divergence of the beam is defined and used in the identification of the beam with α. So if we just focus on the reflection we can say that the beam reflects according to the wavelength λ, index parameter N, incident angle θ_i and α that shows the divergence of the beam representing the angle of the k vector in beam. Above you will see some figures calculated and drawn for the given parameters clarified.

3.2.2.1. Figures Related to the Reflection Coefficient

$$N = 1.5 \qquad D = \frac{10.9}{1.5} \qquad \lambda = 1 \qquad \text{F changes from 0 to 1 increasing by 0.001}$$

$$\beta(F) = \left(\frac{2\pi D}{\lambda}\right)\sqrt{N^2 - F^2}$$
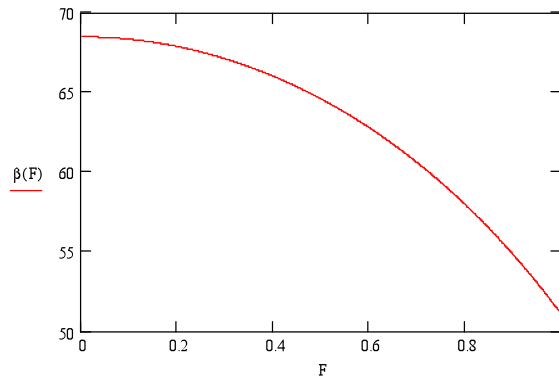
Figure 3.6. $\beta(F)$ Derived From Boundary Conditions

$$r_{12\perp}(F) = \frac{\sqrt{1-F^2} - \sqrt{N^2-F^2}}{\sqrt{1-F^2} + \sqrt{N^2-F^2}}$$

$r_{12\perp}(F) =$

-0.2
-0.2
-0.2
-0.2

Figure 3.7. $r_{12}(F)$ (Reflection From One Boundary Of One Dielectric Slab)

$$r_\perp(F) = r_{12\perp}(F)\frac{1-e^{i2\beta(F)}}{1-[A(F)]^2 e^{i2\beta(F)}}$$

$r(F) =$

-0.147-0.187
-0.147-0.187
-0.147-0.187
-0.147-0.187
-0.147-0.187
-0.147-0.187
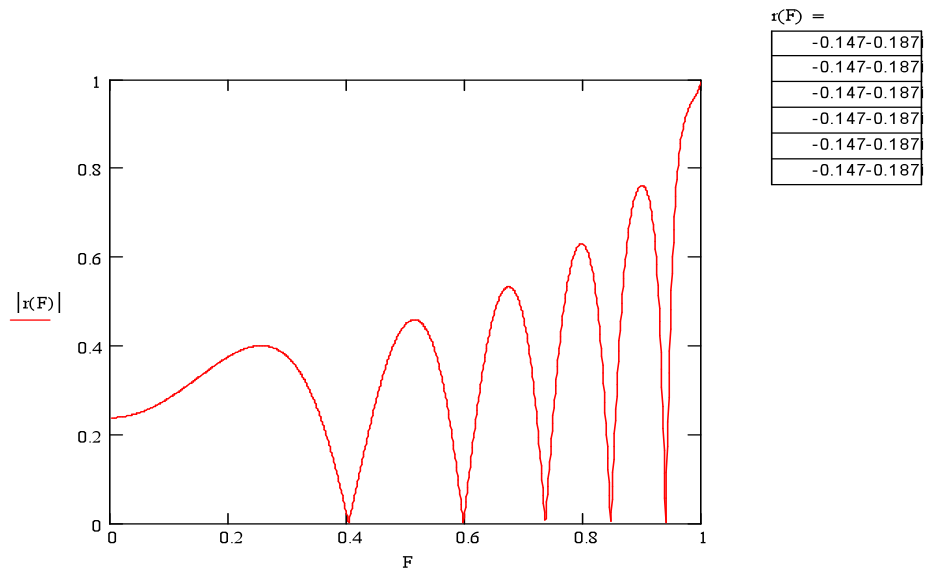
Figure 3.8. $r(F)$ (Reflection From One Dielectric Slab)

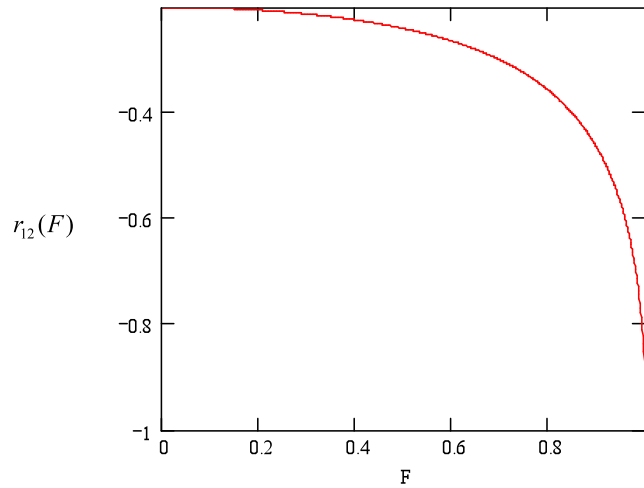$$N = 1.5 \qquad D = \frac{2.7}{1.5} \qquad \lambda = 1 \qquad \beta(F) = \frac{2D\pi}{\lambda\sqrt{N^2 - F^2}}$$

F changes from 0 to 1 increasing 0.001 step by step.

$$r_{12\perp}(F) = \frac{\sqrt{1-F^2} - \sqrt{N^2-F^2}}{\sqrt{1-F^2} + \sqrt{N^2-F^2}} \qquad\qquad r_\perp(F) = r_{12\perp}(F)\frac{1 - e^{i2\beta(F)}}{1 - (r_{12\perp})^2 e^{i2\beta(F)}}$$

β(F) =

16.965
16.965
16.965
16.965
16.965
16.964

$r_{12}(F) =$

-0.2
-0.2
-0.2
-0.2
-0.2
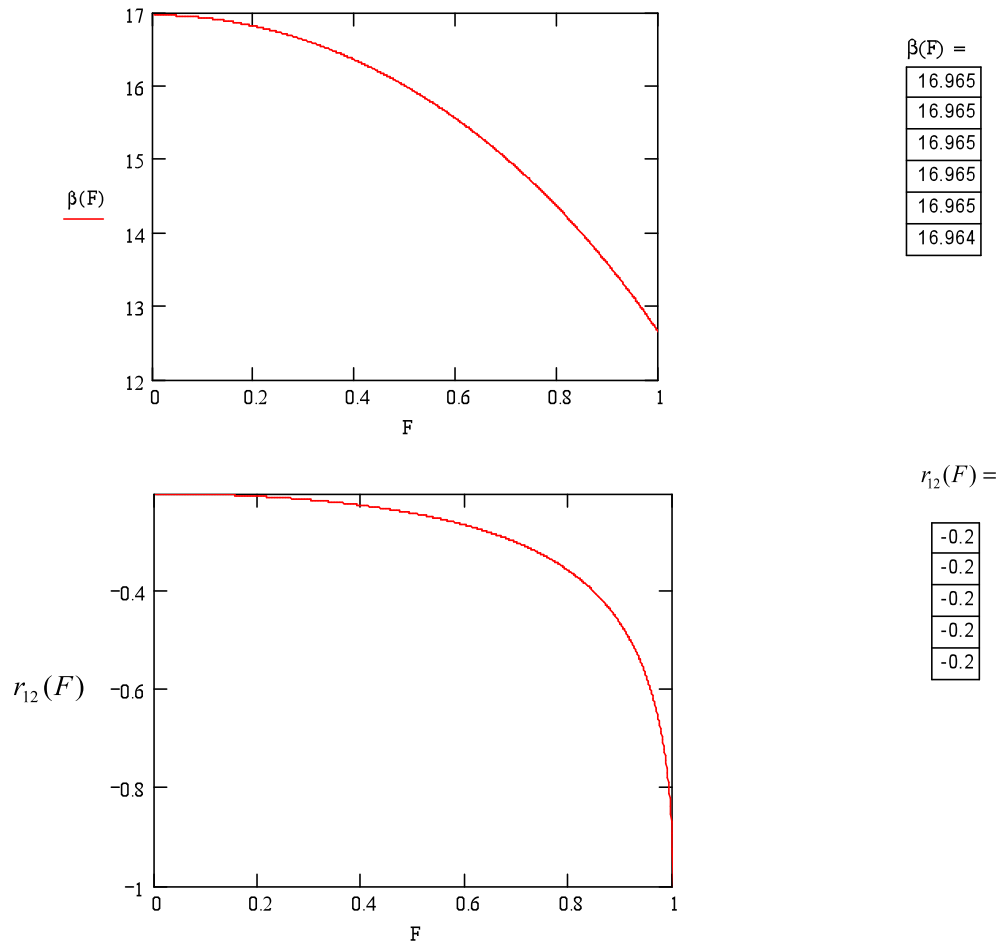
Figure 3.9. $r_{12}(F)$ And $\beta(F)$ Representation For Various Thicknesses

r(F) =
-0.353+0.106i
-0.353+0.106i
-0.353+0.106i
-0.353+0.106i
-0.353+0.106i
-0.353+0.106i
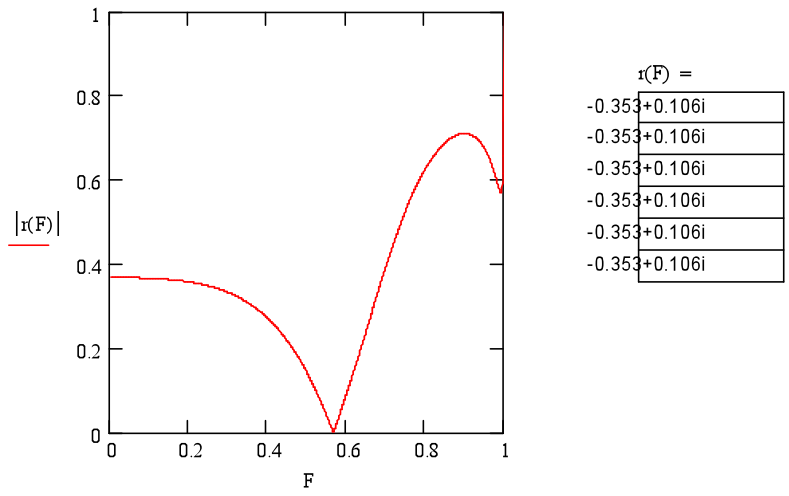
Figure 3.10. $r(F)$ Representation For Various Thicknesses

3.2.2.2. Phase Effects of Reflection
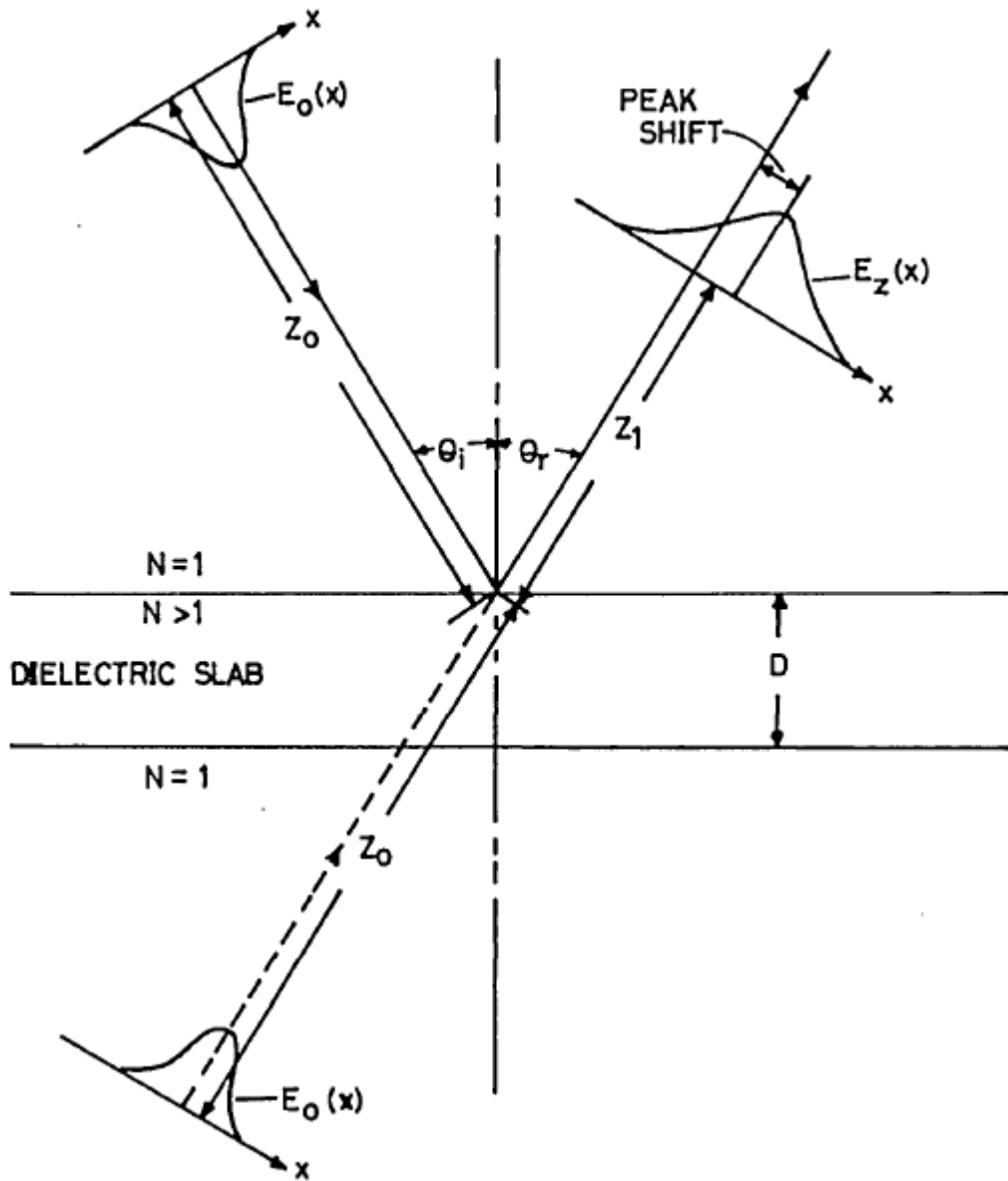
Figure 3.11. The Beam Profile Before And After Reflection Related To The Reflection
Effects

Before talking about our total beam shape we need to look at how reflection
coefficient effects on the beam;

$$r(f) = r(f)e^{i\delta(f)} \longrightarrow \text{is the complex reflection transfer function}$$

and let's look at how the phase of the reflection coefficient changes with reflection.

$$\delta(f) = \delta(0) + \left(\frac{d}{df}\delta(0)\right)f + \frac{1}{2!}\frac{d^2}{df^2}\delta(0)f^2 + ... \longrightarrow \text{Taylor Series of phase term}$$

$$\underbrace{}_{\text{dc-term}} \underbrace{}_{\text{linear}} \underbrace{}_{\text{quadratic}} \tag{3.47}$$

First term is independent of f and will not affect the beam profile:

$$\exp(\frac{-t^2}{2a^2}) \xrightarrow{FT} \sqrt{2}[\pi|a|)^2]\exp\left[\frac{-1}{2}\omega^2(|a|)^2\right] \xrightarrow{FT^{-1}} \exp\left[\frac{-1}{2}\frac{t^2}{(|a|)^2}\right] \tag{3.48}$$

The second term is the linear term and will affect the profile most. Any phase shift in the Fourier space will shift the plane beam in the transverse plane:

$$\exp(-i\omega b)\left[\sqrt{2\pi}(|a|)^2\exp\left[\frac{-1}{2}\omega^2(|a|)^2\right]\right] \xrightarrow{FT^{-1}} \exp\left[b\frac{t}{(|a|)^2}\right]\exp\left[\frac{-1}{2}\frac{(b^2+t^2)}{(|a|)^2}\right] \xrightarrow{FT} \exp\left[\frac{-1}{2}\frac{(b-t)^2}{(|a|)^2}\right]$$

$$\tag{3.49}$$

As we can see $\sigma_x = |a| \Rightarrow$ rms is the width of the Gaussian beam in transverse plane propagating in z direction.

$$\text{Lateral shift in} - x = 2\pi b, \quad 2\pi b = -\delta'(0) \Rightarrow b = -\frac{\delta'(0)}{2\pi} \tag{3.50}$$

$$L = b = -\frac{\delta'(0)}{2\pi} \tag{3.51}$$

In quadratic term, the propagating beam diverges just like it has been while propagating in free space and a focal shift occurs;

$$\exp(i\omega^2 b)\left[\sqrt{2\pi}(|a|)^2\exp\left[\frac{-1}{2}\omega^2(|a|)^2\right]\right] \xrightarrow{FT^{-1}} |a|\frac{\exp\left[\frac{-1}{2}\frac{t^2}{[(|a|)^2+2|b|]}\right]}{\sqrt{(|a|)^2+2|b|}} \tag{3.52}$$

In free space propagation;

$$-j\omega^2 b = -j\pi\lambda z f^2 = -j\pi\lambda D_f f^2 \qquad \Rightarrow \qquad b = \frac{\pi\lambda D_f}{(2\pi)^2} = \frac{\lambda}{4\pi} D_f \qquad (3.53)$$

In quadric term occurs with reflection;

$$-j\omega^2 b = \frac{j}{2!}\delta''(0)f^2 \qquad \Rightarrow \qquad -\omega^2 b = \frac{\delta''(0)f^2}{2} \qquad (3.54)$$

$$\Rightarrow -(2\pi f)^2 \frac{\lambda}{4\pi} D_f = \delta''(0)f^2 \qquad \Rightarrow \qquad D_f = \frac{-\delta''(0)}{2\pi\lambda} \qquad (3.55)$$

$$\text{Where } \omega = 2\pi f \qquad (3.56)$$

Thus it can be noticed that reflection has two effects. One is lateral shift which shifts the beam profile in the transverse plane by an amount L, the other is focal shift (D_f) which focally shifts the propagating beam profile as we can see in Figure 3.11. And we can say that the shift after reflection (lateral and focal shift) depends on the wavelength of the beam, the index of the slab and the incident angle [22].

3.2.2.3. Amplitude Effects of Reflection

The amplitude of the beam which is reflecting from a dielectric slab also changes with respect to the optical thickness of the slab, wavelength and the angle of incidence. The reflected beam profile composes of the launched spectrum and reflection function. So if we define the maximum amplitude of the reflected beam profile:

$$\frac{d}{df}\left[r(f)E_0(f)\right]_{fm} = 0 \qquad (3.57)$$

$$\frac{d}{df}\left[r(f)A\sqrt{\pi}\exp\left(\frac{-(2\pi\sigma)^2}{2}f^2\right)\right] = 0 \qquad (3.58)$$

$$A\sqrt{\pi}\left[r'(f)\exp\left(\frac{-(2\pi\sigma)^2 f^2}{2}\right) - (2\pi\sigma)^2 f^2 r(f)\exp\left(\frac{-(2\pi\sigma)^2 f^2}{2}\right)\right] = 0 \quad (3.59)$$

$$r'(f_m) - (2\pi\sigma)^2 f_m r(f_m) = 0 \qquad \Rightarrow \qquad f_m = \frac{(2\pi\sigma)^{-2}\frac{d}{df}r(f_m)}{r(f_m)} \quad (3.60)$$

if fm is not far from the f=0;

$$f_m = (2\pi\sigma)^{-2}\frac{r'(0)}{r(0)} \quad (3.61)$$

F changes the direction of the peak of the profile which propagates in the far zone. According to the plane-wave component having largest amplitude being in the direction f we define $\Delta\alpha$;

Angular Shift: $\qquad \Delta\alpha = \dfrac{1}{\sin(\lambda f_m)} \qquad \Delta\alpha = \lambda f_m \qquad (3.62)$

$$\Delta\alpha = \lambda(2\pi\sigma)^{-2}\frac{r'(0)}{r(0)} \quad (3.63)$$

Angular shift is inversely proportional to the square of the beam width and directly proportional to the rate of change of r with f. By the way wave components are unnoticeably changes with the reflection. And this is smaller in narrow beams [23,24].

3.2.3. Phase, Amplitude and Propagation Effects of Reflection

Total propagation distance $z = z_0 + z_1$ from waist will be gained by taking the Fourier transform of the launched beam.

$$E_z(x) = \int_{-\infty}^{\infty} \widetilde{E}_0(f)r(f)\exp[i\Psi(f)]df \quad (3.70)$$

And according to the method of stationary phase, phase term can be defined by

$$\Psi(t) = \delta(f) - \pi\lambda z f^2 + 2\pi f x \qquad (3.71)$$

so the phase term consists of three term, first of which comes from the reflection factor and depends on the properties of the slab, the wavelength and the angle of incidence. Second term comes from beam propagation effects and the third term represents the Fourier transform.

When we discuss the propagated and reflected beam equation (3.70) profile we can easily see that reflection from a dielectric slab have some effects on the beam. The beam profile does not stay still and does not behave the way it is first designed. These are the effects we want in order not to be detected by. And this equation for one slab can be graphed as;

$z = 0$
$\sigma = 0.02$
$n_2 = 1.5$
$D = 0.018m$
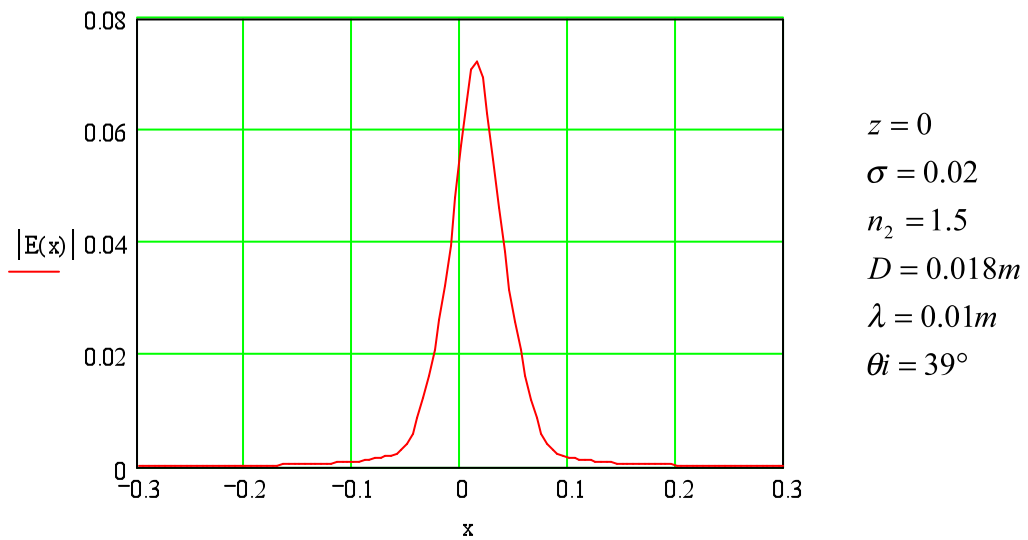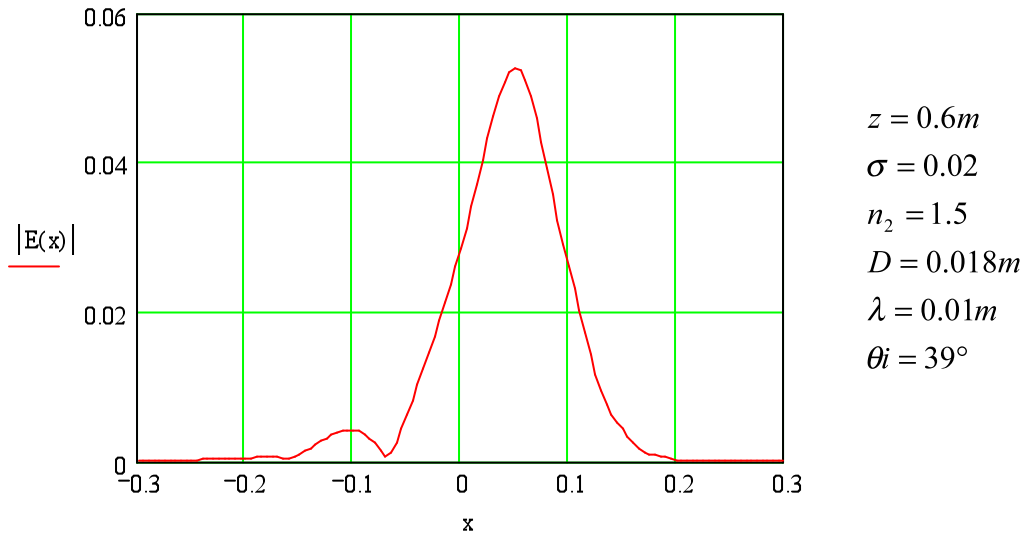$\lambda = 0.01m$
$\theta i = 39°$

Figure 3.12. Electromagnetic Field Representation Of A Gaussian Beam Without Propagation

Figure 3.13. Electromagnetic Field Representation Of A Gaussian Beam After Propagation (60cm)

$z = 0.6m$
$\sigma = 0.02$
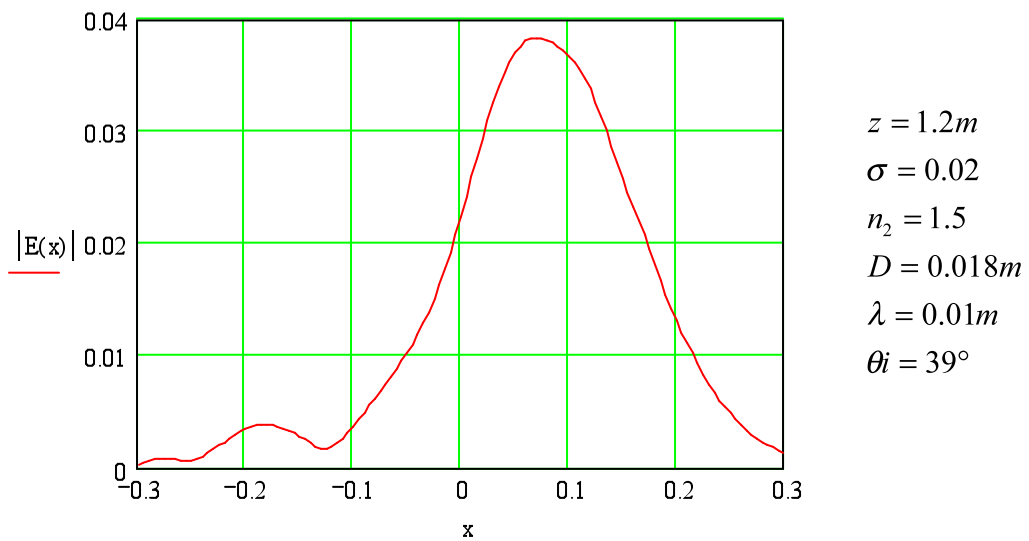$n_2 = 1.5$
$D = 0.018m$
$\lambda = 0.01m$
$\theta i = 39°$

Figure 3.14. Electromagnetic Field Representation Of A Gaussian Beam After Propagation (120cm)

$z = 1.2m$
$\sigma = 0.02$
$n_2 = 1.5$
$D = 0.018m$
$\lambda = 0.01m$
$\theta i = 39°$

$z = 0$

$\sigma = 0.02$

$n_2 = 1.5$

$D = 0.018m$

$\lambda = 0.01m$

$\theta i = 30°$
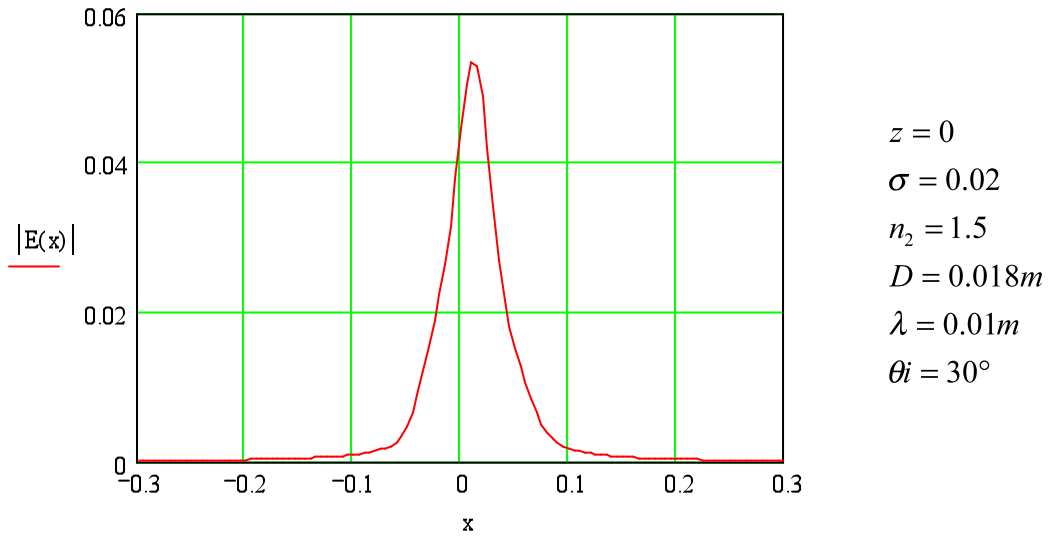
Figure 3.15. Electromagnetic Field Representation Of A Gaussian Beam Without Propagation

$z = 0.6$

$\sigma = 0.02$

$n_2 = 1.5$

$D = 0.018m$

$\lambda = 0.01m$

$\theta i = 30°$
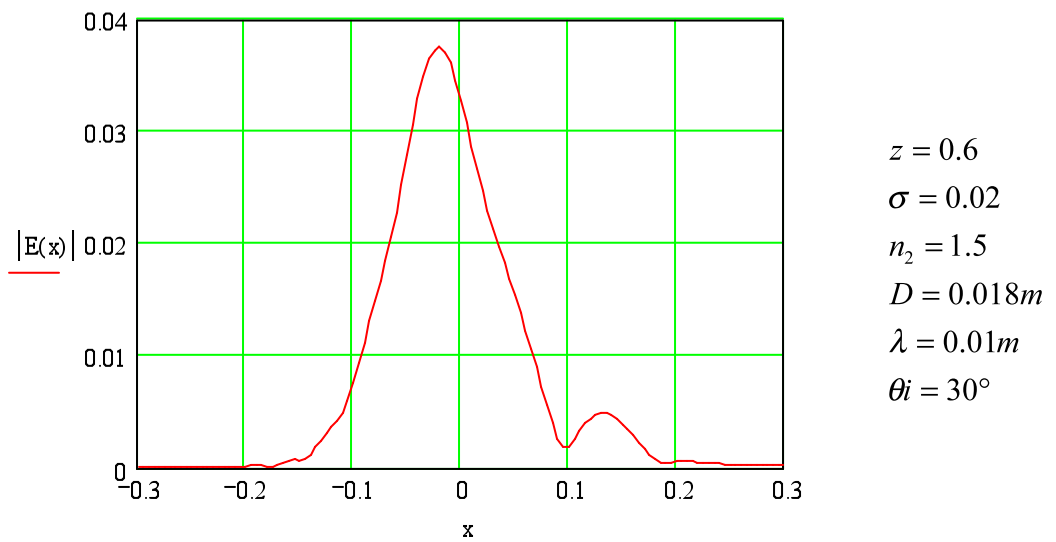
Figure 3.16. Electromagnetic Field Representation Of A Gaussian Beam After Propagation (60cm)

$z = 1.2$

$\sigma = 0.02$

$n_2 = 1.5$

$D = 0.018m$

$\lambda = 0.01m$

$\theta i = 30°$

Figure 3.17. Electromagnetic Field Representation Of A Gaussian Beam After Propagation (120cm)

CHAPTER 4

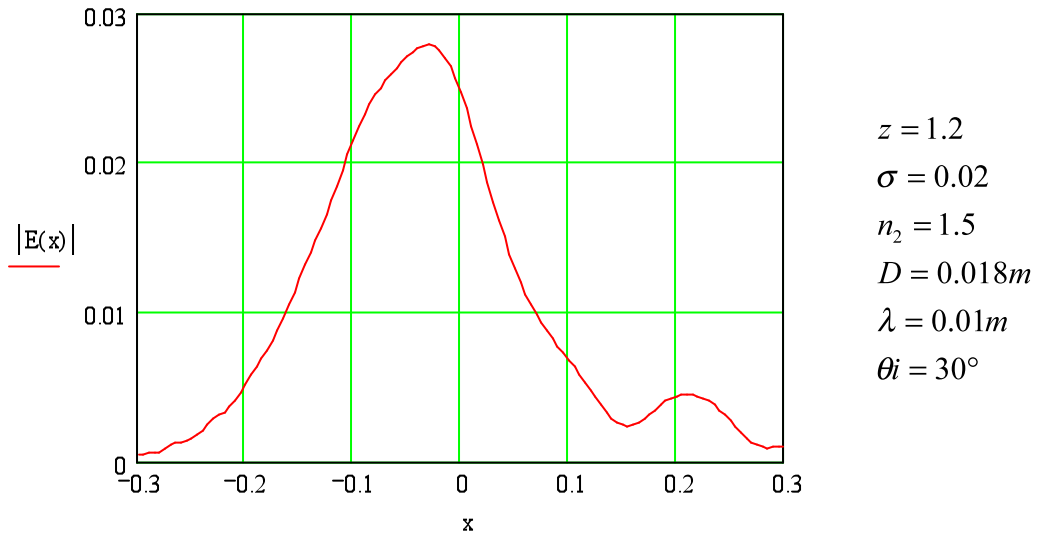# REFLECTION FROM MULTILAYER DIELECTRIC SLABS USING MATRIX REPRESENTATION

In the previous chapters, the reflection of a Gaussian shape laser beam from a dielectric slab is discussed entirely. Within analysis, the beam faces off with various effects that can be expressed mathematically. In this chapter we will investigate these reflection and propagation effects numerically by using diagrams, define minimum reflection from multilayer dielectric films which is the aim of our proposal using paraxial approximation [25-28].
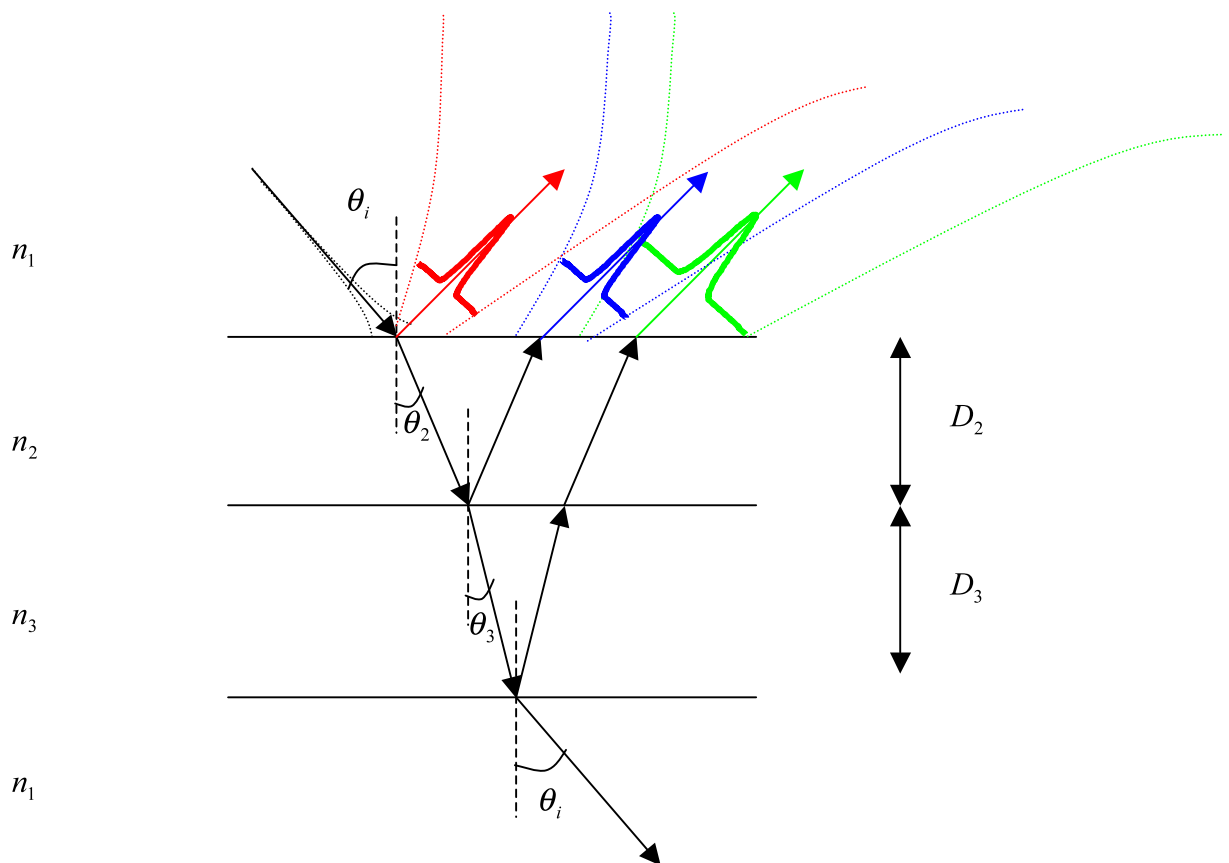

Figure 4.1. Schematic Representation Of Multilayer Reflection

In order to reduce the reflection and diverge it to undetectable regions, we need to investigate the reflection coefficient using graphical analysis and need to compute the

minimum reflection parts. Now that the reflection of a Gaussian shape laser beam is computable and the differences in variables makes it understandable, redefining the reflection coefficient would help us to prove our suggestion.

4.1. Derivation of Reflectivity for Multilayer Dielectric Slabs

We got the reflection of a Gaussian beam and how it treats by using equation (3.70) as far as we found out in the previous chapter. We have to redefine this expression for multilayer structure.

From this equation the components represent propagation and reflection of a Gaussian beam are described. As one can guess multilayer structures will not affect the propagation factor [29-31]. We need to redefine the reflection coefficient.

For multilayer structure, the representation of matrix changes as described in section 2.3.2. In order to compute the reflection coefficient for two adjacent layers, we need to define the matrix as;

$$M(z) = M_1(z)M_2(z) \tag{4.1}$$

$$\left. \begin{array}{l} M_1(z) = \begin{bmatrix} \cos(\beta_2) & -\dfrac{i}{p_2}\sin(\beta_2) \\ -ip_2\sin(\beta_2) & \cos(\beta_2) \end{bmatrix} \\[3em] M_2(z) = \begin{bmatrix} \cos(\beta_3) & -\dfrac{i}{p_3}\sin(\beta_3) \\ -ip_3\sin(\beta_3) & \cos(\beta_3) \end{bmatrix} \end{array} \right\} \tag{4.2}$$

Where p_2, p_3 are represented in section 3.2.2 and;

$$\beta_2 = \left(\frac{2\pi D_2}{\lambda}\right)\sqrt{\left(\frac{n_2}{n_1}\right)^2 - F_1^2} \qquad \beta_3 = \left(\frac{2\pi D_3}{\lambda}\right)\sqrt{\left(\frac{n_3}{n_2}\right)^2 - F_2^2} \tag{4.3}$$

Both related to equation (3.39). We can define D_2 as the thickness of first, n_2 as the index of first and n_3 as the index of second slab which our light faces off. After

evaluating θ_2 using Snell's law, F_1 and F_2 can be redefined from equation (3.46) and described as;

$$
\left.\begin{aligned}
F_1 &= \sqrt{1 - \lambda^2 f^2}\,\sin(\theta_1) + \lambda f \cos(\theta_1) \\
F_2 &= \sqrt{1 - \lambda^2 f^2}\,\sin(\theta_2) + \lambda f \cos(\theta_2)
\end{aligned}\right\} \tag{4.4}
$$

Where f is defined in equation (3.44) in order to use the Gaussian plane wave decomposition. When we expand equation (4.2) we get the reflection matrix for two layered dielectric film structure:

$$
M(z) = \begin{bmatrix}
\cos(\beta_2)\cos(\beta_3) - \dfrac{p_3}{p_2}\sin(\beta_2)\sin(\beta_3) & -\dfrac{i}{p_3}\cos(\beta_2)\sin(\beta_3) - \dfrac{i}{p_2}\sin(\beta_2)\cos(\beta_3) \\
-ip_2\sin(\beta_2)\cos(\beta_3) - ip_3\cos(\beta_2)\sin(\beta_3) & \cos(\beta_2)\cos(\beta_3) - \dfrac{p_2}{p_3}\sin(\beta_2)\sin(\beta_3)
\end{bmatrix}
$$

$$\tag{4.5}$$

4.1.1. Figures Related to Reflectivity for Two Dielectric Slabs

Using the $m_{11}, m_{12}, m_{21}, m_{22}$ components which are derived in equation (4.5) and putting them in equation (2.69) we get the reflection coefficient. When we get the square of reflection coefficient, we could easily get the reflectivity equation (2.72) which will affect our beam profile profoundly.

In order to minimize the reflectivity, the whole graph needs to be defined and the minimum points need to be analyzed. Various fields of graphs can give us precise solution and it is better for testing whether the definition is correct.
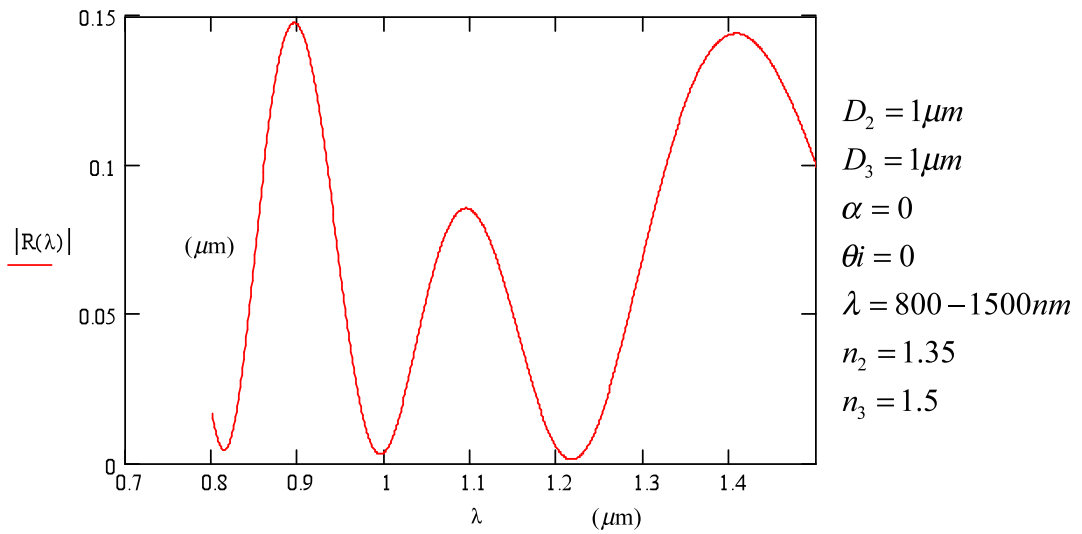
4.1.1.1. Reflectivity upon Wavelength

Figure 4.2. Reflection Representation For Various Wavelengths

It is shown in the figure that reflection is dependent upon the thickness and indices of the slabs, incident angle and divergence angle of Gaussian beam and the wavelength. We can notice that reflectivity does not usually get above 0.15; and more, in some wavelengths, depending on other numerous inputs, becomes close zero which is the case we are looking for.

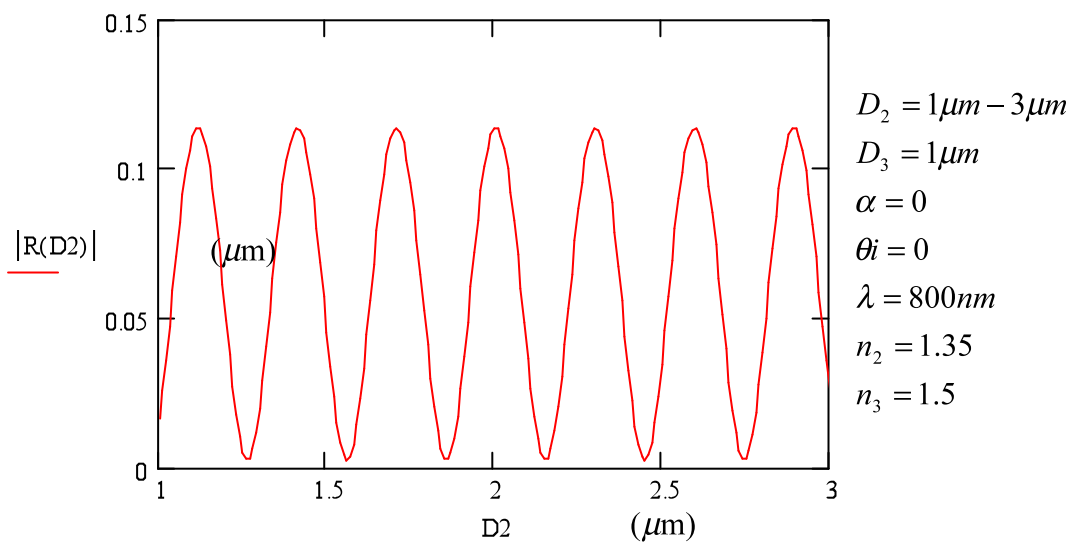## 4.1.1.2. Reflectivity upon Thicknesses of the First Slab

Figure 4.3. Change Of Reflectivity For Various Thicknesses Of First Slab

In this graph we hold each variable stable and make differences only on the first thickness of the slab. As we can observe from the graph, when we hold each variable stable, and make difference only using the thickness of the first, we could notice that reflectivity changes periodically and in this periodicity reflectivity either increases or decreases. According to this periodical structure thickness affects reflectivity limitedly and we can decrease reflectivity using the thickness of the slab.

4.1.1.3. Reflectivity upon the Index of the First Slab

$$D_2 = 1\mu m$$
$$D_3 = 1\mu m$$
$$\alpha = 0$$
$$\theta i = 0$$
$$\lambda = 800nm$$
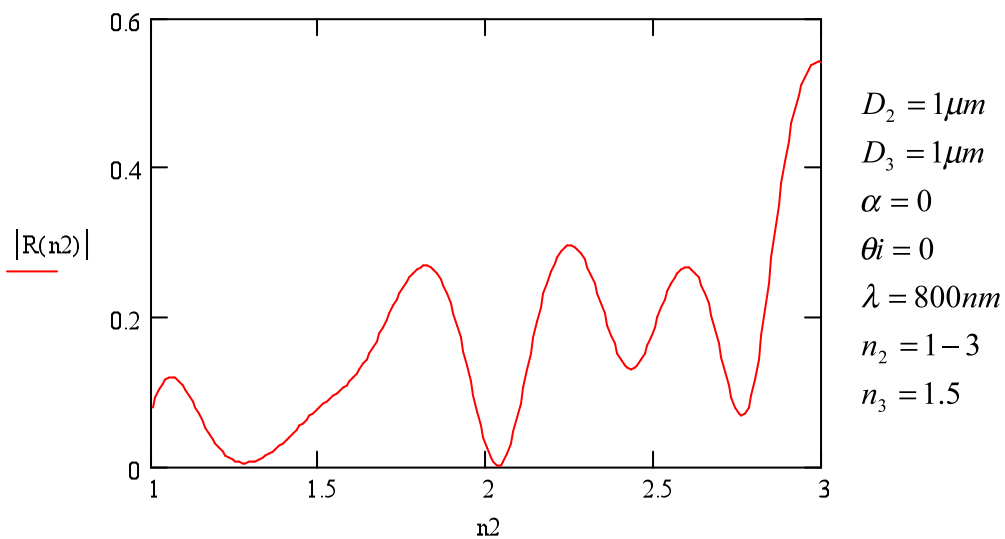$$n_2 = 1-3$$
$$n_3 = 1.5$$

Figure 4.4. Change Of Reflectivity For Various Indices Of First Slab

Here it can be noticed that as index increases reflection increases and it is better for us not to choose greater indices and we can see that reflectivity becomes zero or becomes closer to zero. Because these kind of dielectric film structures indices are usually between 1 and 2, the index has to be chosen between these values. We need to analyze the places where reflectivity is zero and choose closer variables to these points.

Although it can be seen that when index is chosen in the vicinity of 1.35, reflectivity is close to zero, it is true only for given parameters. But it can be understood that we need to choose small index of first slab.

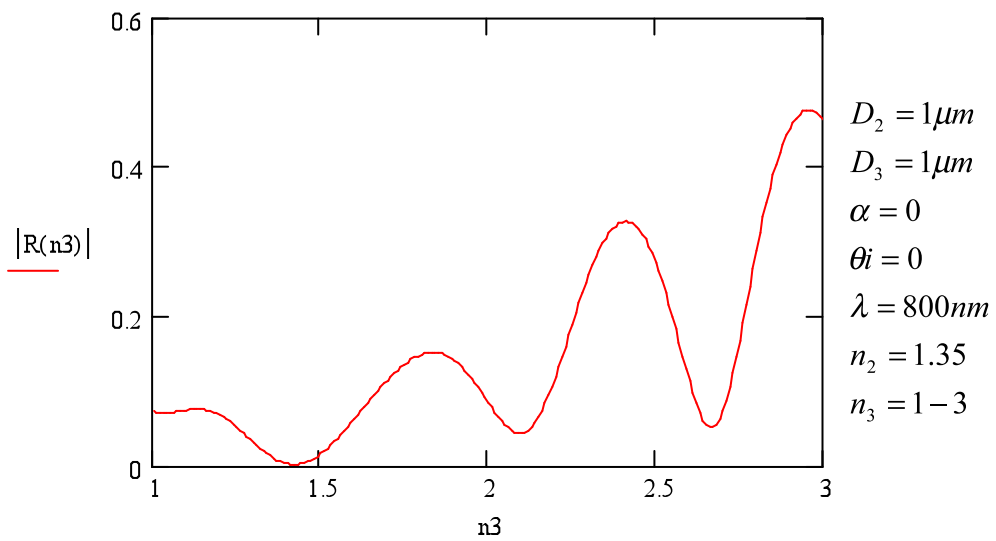## 4.1.1.4 Reflectivity upon the Index of the Second Slab

Figure 4.5. Change Of Reflectivity For Various Indices Of Second Slab

In case of any increase in wavelength causes an increase in reflectivity. Although in some cases reflectivity becomes close to zero, there we can see that this depends on too many variables. But it is clear that we can decrease the reflectivity. It would be good to choose the indices close to 1.

4.1.2. Figures for Two Dielectric Slabs Within Two Variables

4.1.2.1. Reflectivity upon the Change on Indices of Both Two Media

$$D_2 = 1\mu m$$
$$D_3 = 1\mu m$$
$$\alpha = 0$$
$$\theta i = 0$$
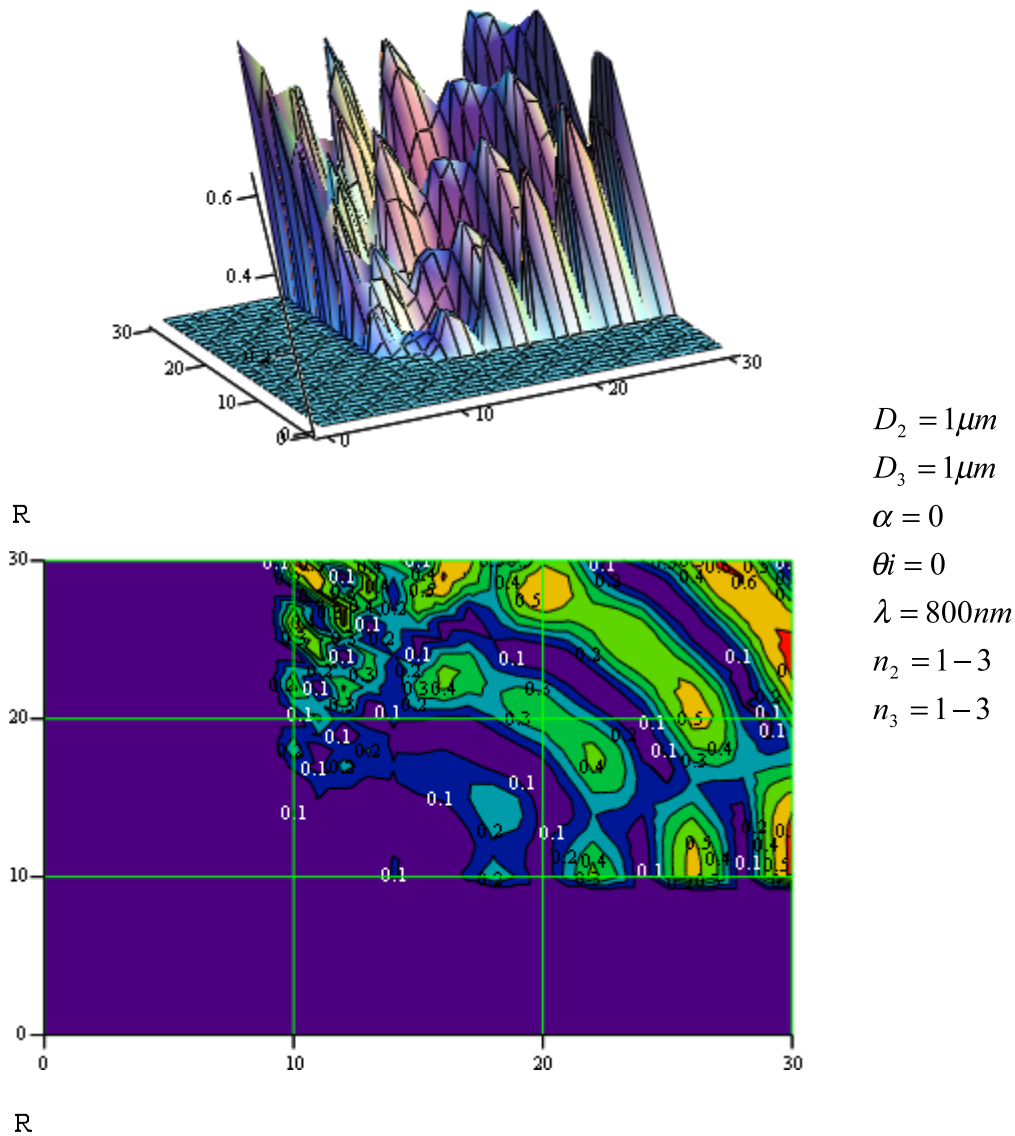$$\lambda = 800nm$$
$$n_2 = 1-3$$
$$n_3 = 1-3$$

Figure 4.6. Reflection Value For Various Indices Of Both Medias

In these graphs x axis represents the index of first slab, and y axis represents the index of the second slab, and z axis represents the reflectivity. Although it seems that indexes changes from 10 to 30, in fact this corresponds to 1-3 in my formula. There are two graphs one of which is drawn in 3-D and the other is the counter plotted of the other. The change in indices causes reflectivity to change. As can be understood from

the graph, it would be better for us not to choose the indices more than 2 although in some regions there is a decrease in reflectivity.

4.1.2.2. Reflectivity upon the Change on Thicknesses of Medias

R

$$D_2 = 1 - 9\mu m$$

$$D_3 = 1 - 10\mu m$$

$$\alpha = 0$$

$$\theta i = 0$$

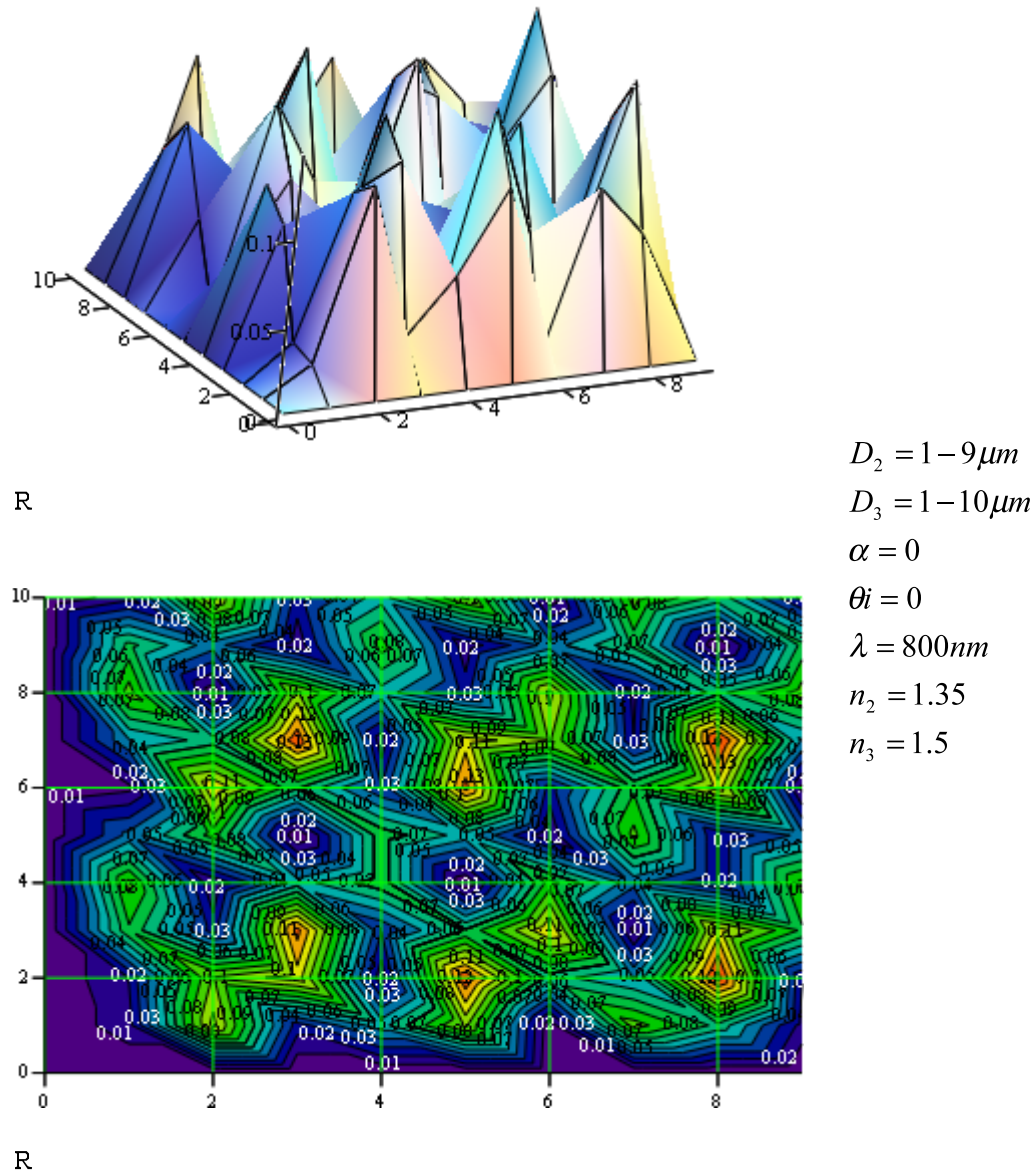$$\lambda = 800nm$$

$$n_2 = 1.35$$

$$n_3 = 1.5$$

R

Figure 4.7. Change Of Reflectivity For Various Thicknesses Of Both Medias

4.1.2.3. Reflectivity upon the Change on Incident Angle and the Index of the First Slab

R

$D_2 = 1\mu m$

$D_3 = 1\mu m$

$\alpha = 0$

$\theta i = 0° - 20°$

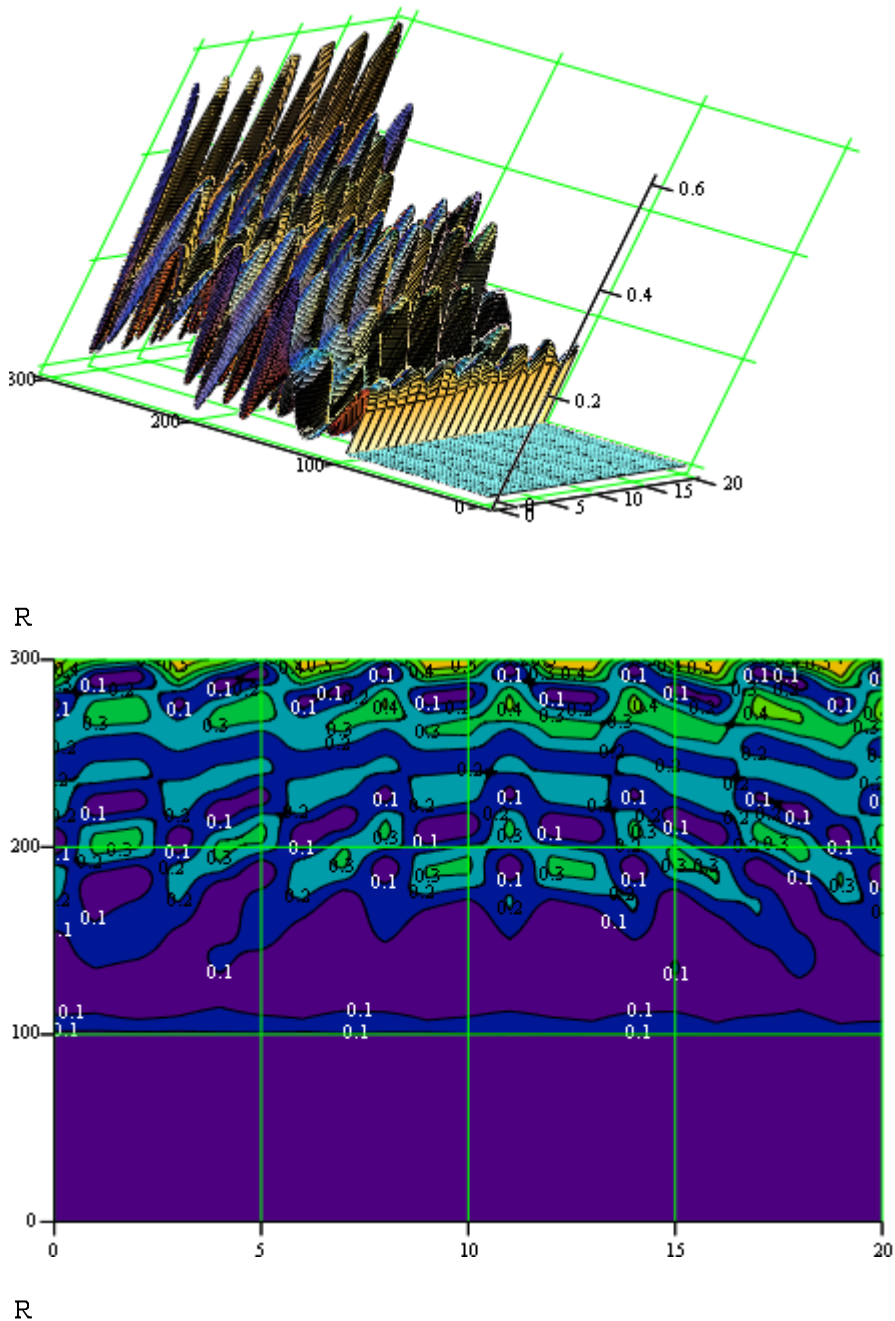$\lambda = 800 nm$

$n_2 = 1 - 3$

$n_3 = 1.5$

R

Figure 4.8. Change Of Reflectivity According To The Incident Angle And The Index Of The First Slab

In this figure, x axis represents the incident angle and y axis represents the index of the first slab. Although it seems to be changing from 100-300, in fact it changes from

1-3. Here we can see that as index increases reflection increases and incident angle affects reflection slightly.

4.2. Calculating the Minimum Reflectivity

As we have observed from the figures, we can minimize the reflectivity. We need to analyze and decide what changes can be made. Reflectivity depends on the matrix representation of the two adjacent slabs which is discussed in equation (4.5).

In order to minimize the reflectivity we need to analyze the equation (4.5). Taking;

$$D_2 = \frac{\lambda n_1}{2n_2} \quad \text{and} \quad D_3 = \frac{\lambda n_2}{2n_3} \tag{4.6}$$

And equation (4.3) becomes as;

$$\beta_2 = \frac{\pi n_1}{n_2}\sqrt{\left(\frac{n_2}{n_1}\right)^2 - F_1^{\,2}} \quad \text{and} \quad \beta_3 = \frac{\pi n_2}{n_3}\sqrt{\left(\frac{n_3}{n_2}\right)^2 - F_2^{\,2}} \tag{4.7}$$

Assuming incident angle is 0° and a plane wave with $\alpha = 0$ angle $F_{1,2} = 0$.
So equation (4.7) becomes as

$$\beta_2 = \beta_3 = \pi \tag{4.8}$$

And equation (4.5) becomes as ;

$$M(z) = \begin{bmatrix} 1 & 0 \\ 0 & 1 \end{bmatrix} \tag{4.9}$$

Thus we can write reflection coefficient from (2.69) as;

$$r = \frac{R}{A} = \frac{p_1 - p_l}{p_1 + p_l} \qquad \text{,where;} \tag{4.10}$$

$$p_1 = n_1 \cos(\theta i), \qquad p_1 = -n_1$$

$$p_2 = n_2 \cos(\theta_2), \qquad p_2 = -n_2$$

$$p_3 = n_3 \cos(\theta_3), \qquad p_3 = -n_3 \qquad (4.11)$$

$$p_4 = n_4 \cos(\theta_4), \qquad p_4 = -n_4$$

Assuming 2 dielectric adjacent film layers in the air $(p_l = p_1)$, reflection coefficient becomes zero. What we don't have to forget is that this is the case which incident angle is exactly zero for a plane wave. Incident angle is close to zero and we need to assume a Gaussian beam. But our case is close to this. Our Gaussian beam does not diverge and incident angle can not be more than a few angles.

4.2.1. Figures Related to Minimum Reflectivity for Two Dielectric Slabs

Finding out the minimum reflection positions, we need to find the minimum parts by using figures. $R1(\lambda)$ is used for calculated thickness instead of $R(\lambda)$ in all figures.
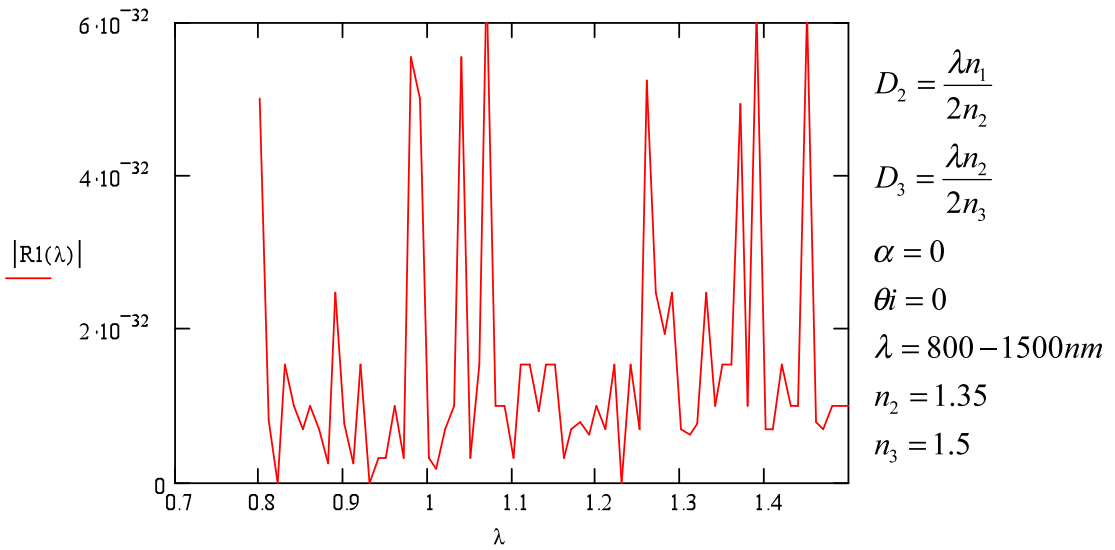
4.2.1.1. Reflectivity upon Wavelength

Figure 4.9. Change Of Minimum Reflectivity According To Change On Wavelength

Although in section 4.1.1.1 reflectivity does not becomes more than 0.15, here we can see that reflectivity is not more than 10^{-31}.
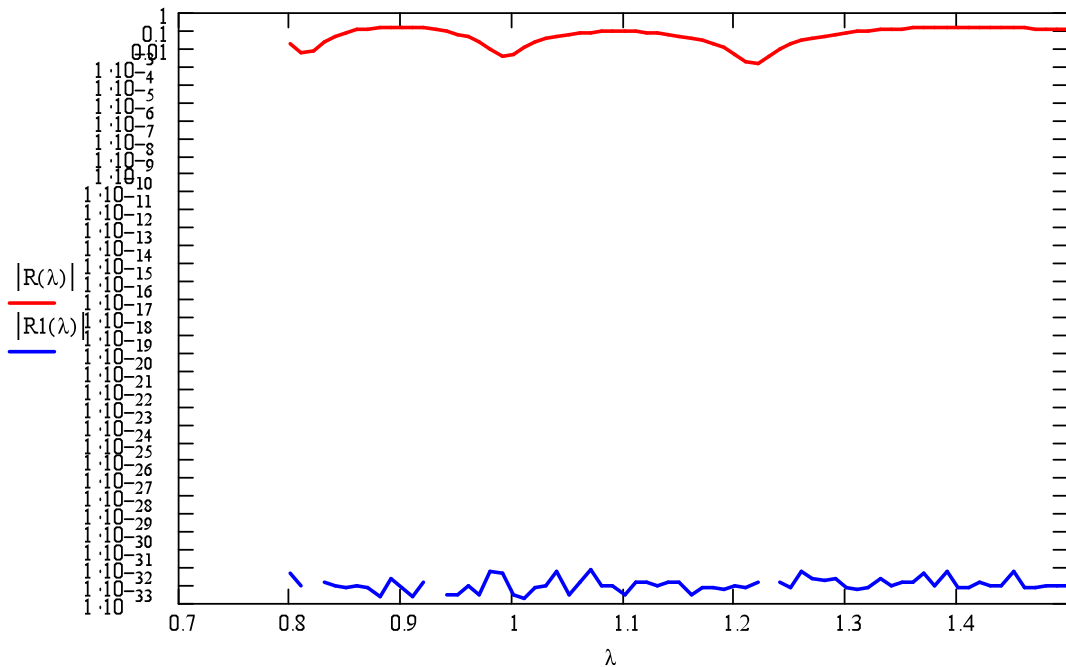

Figure 4.10. Calculated Change Of Minimum Reflectivity And Normal Reflectivity According To The Change On Wavelength In Log Scale.

In this figure $R(\lambda)$ is calculated with normal thickness and $R1(\lambda)$ is calculated with minimum thickness. Y-axis is presented as log scale in order to make observable the differences of between R's. It can be easily calculated that $10\log(10^{-33}) = -330$ where as $10\log(10^{0.1}) = -10$. The decrement is more than we expected. But while analyzing the figure we don't have to forget that as wavelength changes, the minimum thickness depending on the R changes. In order to minimize the reflectivity we have to know in which frequency the device works.

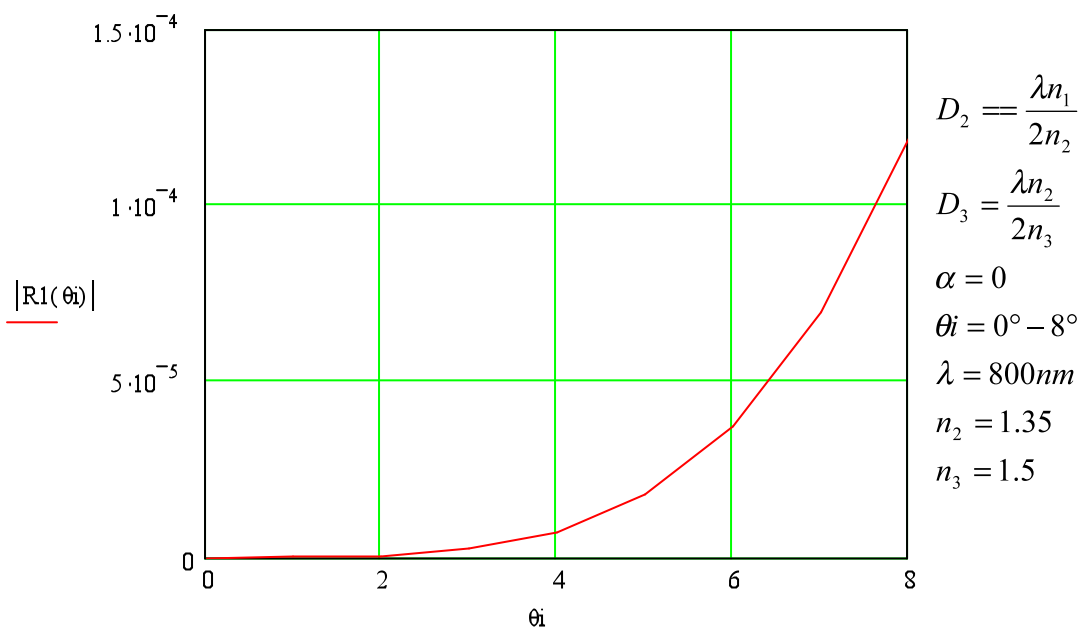## 4.2.1.2. Reflectivity upon Incident Angle

Figure 4.11. Calculated Change Of Minimum Reflectivity Upon Change On Incident Angle

While defining minimum reflection, we assumed the Gaussian beam comes to an angle close to zero. Thus as incident angle increases, reflectivity also increases. Our case validates itself in small incident angles.
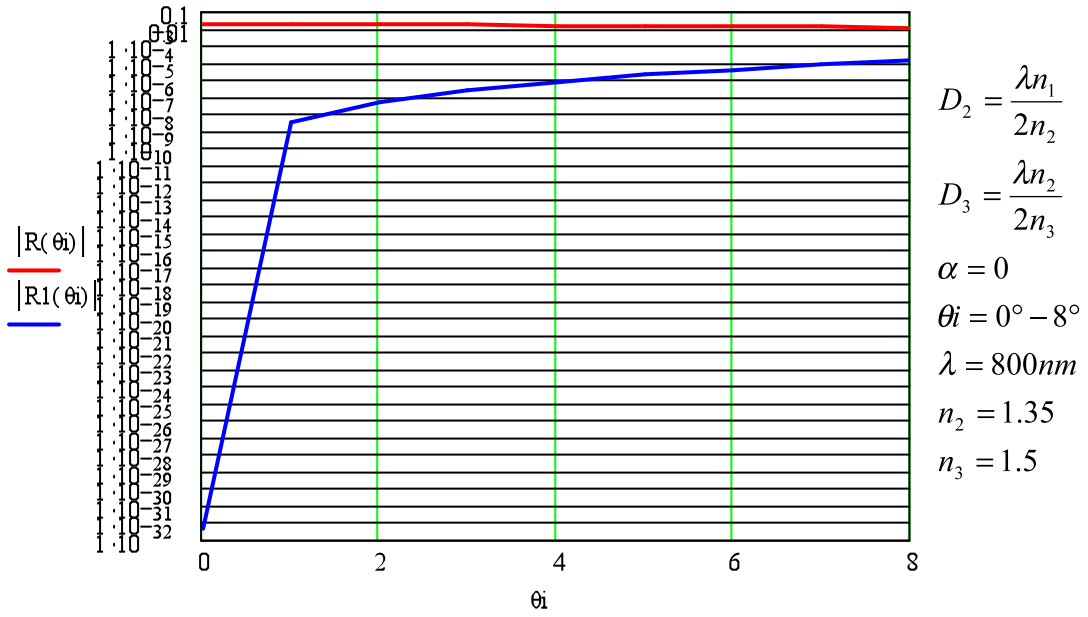
Figure 4.12. Calculated Change Of Minimum Reflectivity And Normal Reflectivity According To The Change On Incident Angle In Log Scale

Also it can be easily seen that when the incident angle is zero our reflectivity decreases with 300 db. In this case reflectivity without defining minimum thickness is 0.1 by choosing thickness as $1\mu m$. It is absolute that as incident angle increases reflectivity increases. In a few angles it increases sharply. The most important observable part is that when incident angle is zero, our gain is more than 300db and no matter how much incident angle increases calculated minimum reflectivity is below the normal calculated reflectivity.

4.2.1.3. Reflectivity upon the Index of the First Slab

$$D_2 = \frac{\lambda n_1}{2 n_2} nm$$

$$D_3 = \frac{\lambda n_2}{2 n_3} nm$$

$$\alpha = 0$$

$$\theta i = 0$$

$$\lambda = 800 - 1500 nm$$
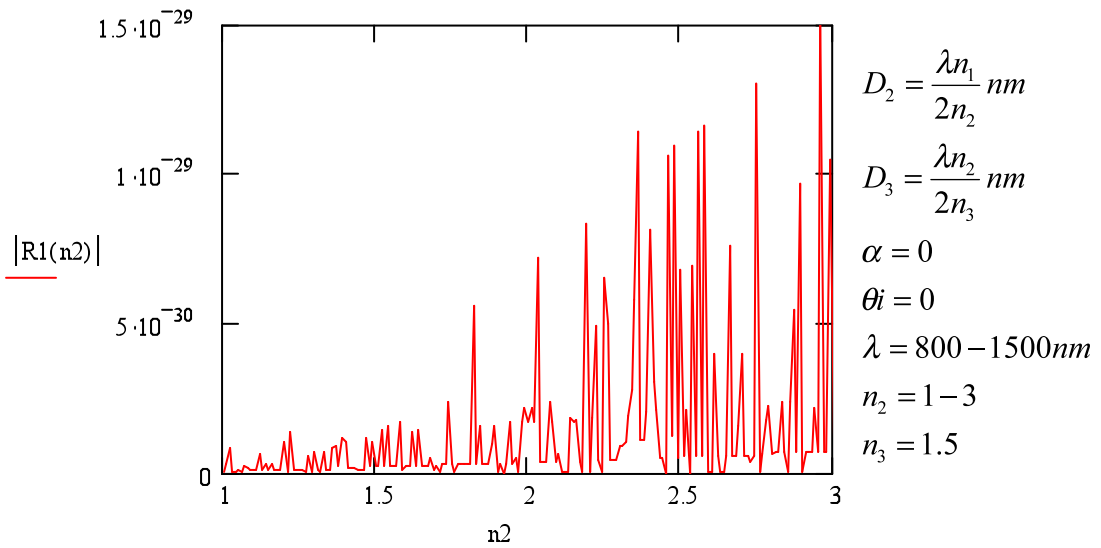
$$n_2 = 1 - 3$$

$$n_3 = 1.5$$

Figure 4.13. Calculated Change Of Minimum Reflectivity Upon Change On The Index Of The First Media
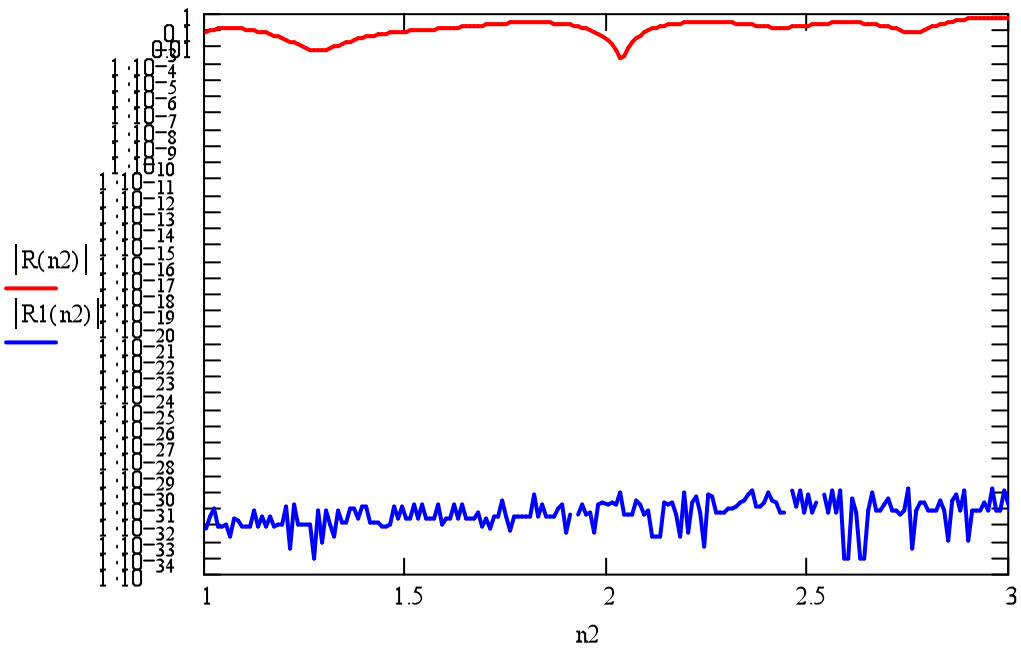

Figure 4.14. Calculated Change Of Minimum Reflectivity And Normal Reflectivity According To The Change On The Index Of The First Media In Log Scale

As it can be analyzed that because the minimum thickness depends on the index of the first slab and as slab index changes, thickness changes. Thus reflectivity is in decrease of 300 db like we expected.

4.2.1.4. Reflectivity upon the Index of the Second Slab

$$D_2 = \frac{\lambda n_1}{2n_2} nm$$

$$D_3 = \frac{\lambda n_2}{2n_3} nm$$

$$\alpha = 0$$

$$\theta i = 0$$

$$\lambda = 800 - 1500 nm$$
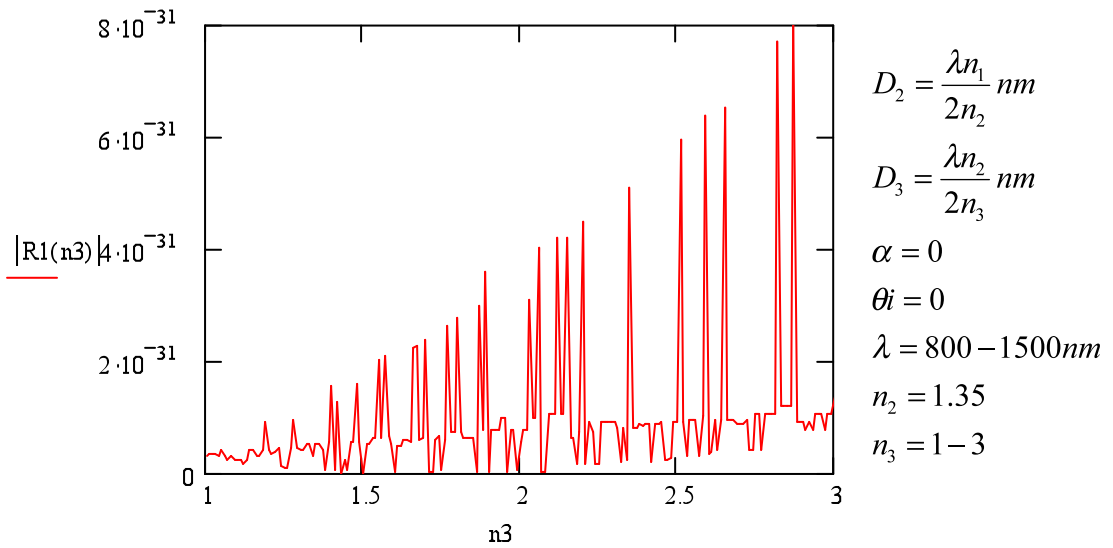
$$n_2 = 1.35$$

$$n_3 = 1 - 3$$

Figure 4.15. Calculated Change Of Minimum Reflectivity According To The Change On The Index Of The Second Media
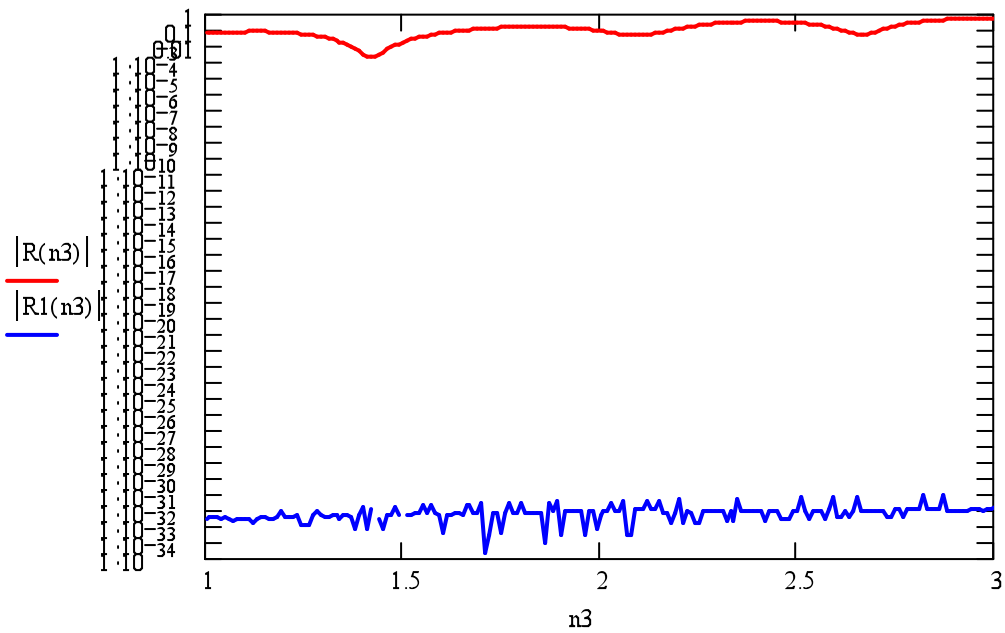

Figure 4.16. Calculated Change Of Minimum Reflectivity And Normal Reflectivity According To The Change On The Index Of The Second Media In Log Scale.

4.2.2. Figures Related to Minimum Reflectivity for Two Dielectric Slabs Depending on the Change in the Value of Two Variables

Section 4.1.2. can help us to see the whole situation but we need to be sure whether our solutions are true and applicable. Because of this we need to see three dimensions and analyze each of them related to each other. But until this point we noticed that after defining the thicknesses by calculation and reaching an exact point of minimum reflection reflectivity decreased by a factor of nearly 300db. This is an amazing result but when incident angle is 15°, the gain in reflectivity becomes 20 db.

4.2.2.1. Reflectivity upon the Change on Indices of Both Two Media

$$\alpha = 0$$
$$\theta i = 0$$
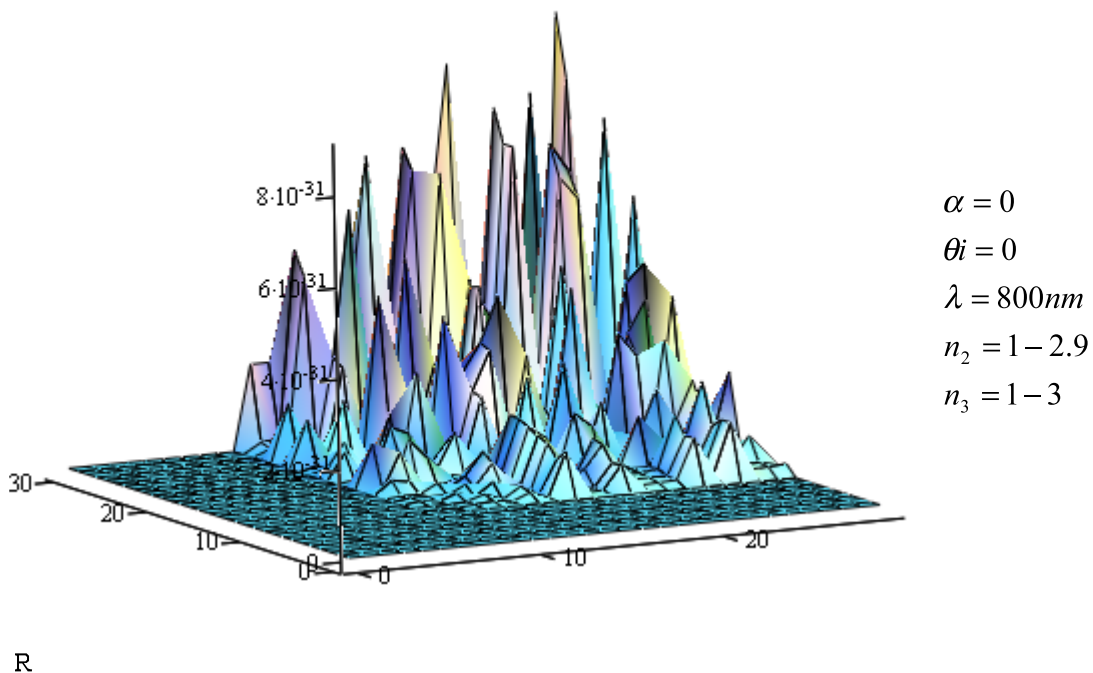$$\lambda = 800 nm$$
$$n_2 = 1 - 2.9$$
$$n_3 = 1 - 3$$

R

Figure 4.17. Calculated Change Of Minimum Reflectivity According To The Change On The Indices Of Both Medias
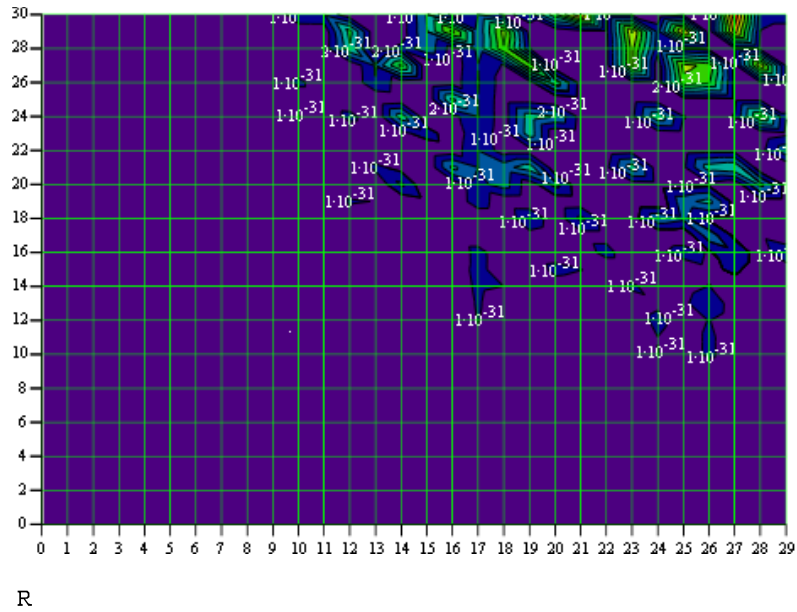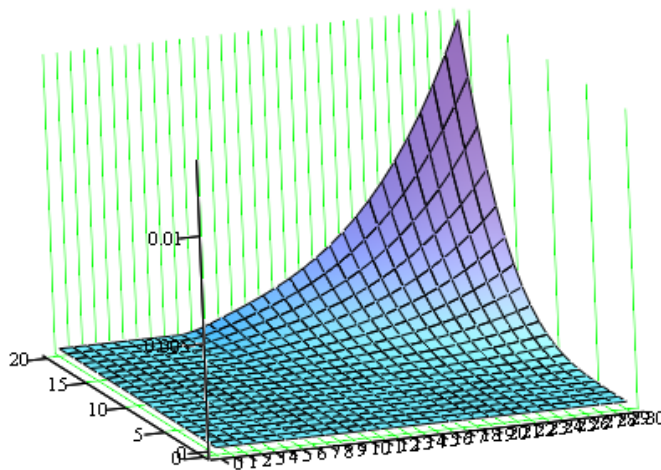
Figure 4.18. Calculated Change Of Minimum Reflectivity According To The Change
On The Indices Of Both Medias In Contour Plot

Expected results can be seen from the graph while index of the first slab changes from 1 to 2.9 and second changes from 1 to 3[3]

4.2.2.2. Reflectivity upon the Change on the Index of the First Media and Gaussian Beam

$$\alpha = 0° - 11,459°$$
$$\theta i = 0°$$
$$\lambda = 800nm$$
$$n_2 = 1 - 3$$
$$n_3 = 1.5$$

R

Figure 4.19. Calculated Minimum Reflectivity For A Gaussian Beam And Various
Indices Of First Media

---

[3] Scales are chosen for beter results from 0 to 29 and 0 to 30. They represent 0 to 2.9 and 0 to 3.
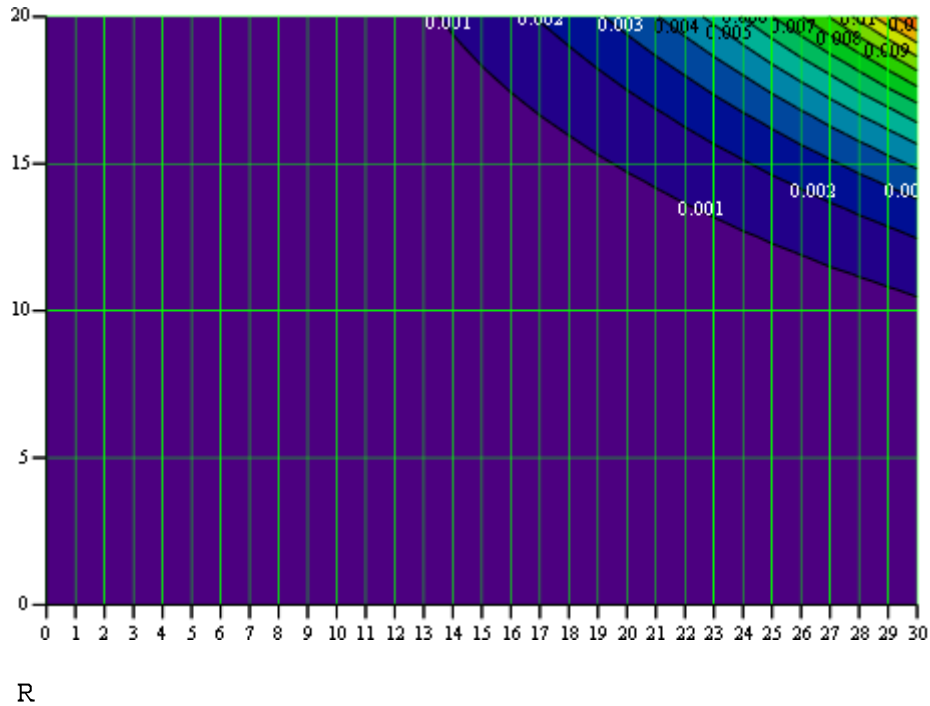
R

Figure 4.20. Minimum Reflectivity Representation In Contour Plot

Here, x-axis represents the index of the first media. For calculational disadvantages it is designed from 1 to 3 though it seems 0-30. And y-axis represents the divergence of Gaussian beam. For its obedience of being matrix, it is drawn with these parameters. 20 corresponds to $\frac{20 \times 180}{100 \times \pi} = 11{,}459°$. Thus, our represented Gaussian beam propagates with diverging from 0 º to 11,459º. This is also an extreme situation because our beam does not diverge more than a few degrees. So our reflectivity is nearly zero within defined values.

4.2.2.3. Reflectivity upon the Change of the Incident Angle and Gaussian Beam

$$\alpha = 0° - 11,459°$$
$$\theta i = 0° - 20°$$
$$\lambda = 800 nm$$
$$n_2 = 1.35$$
$$n_3 = 1.5$$
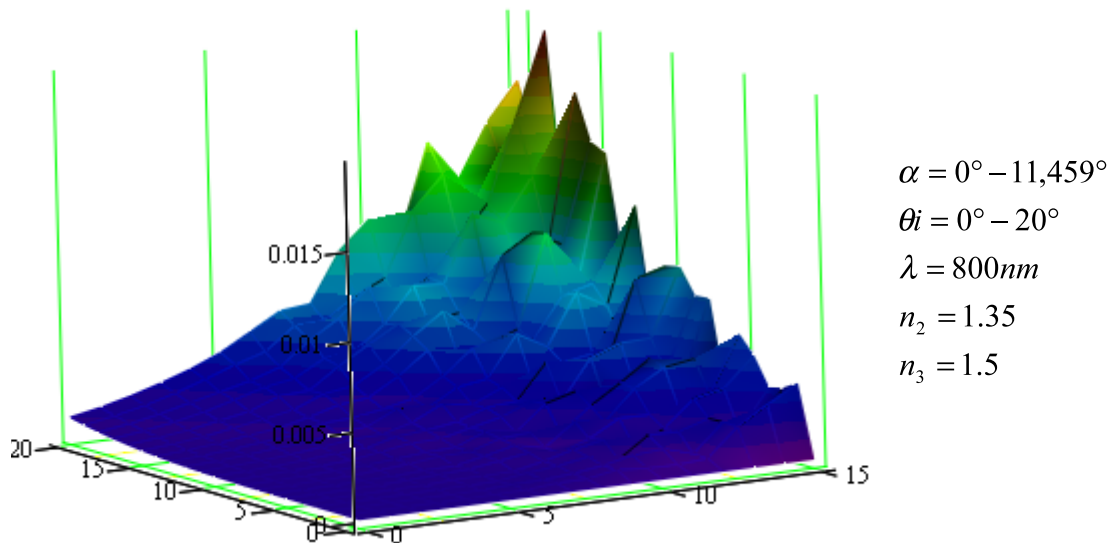
R

Figure 4.21. Minimum Reflectivity Representation Of A Gaussan Beam For Various Incident Angles
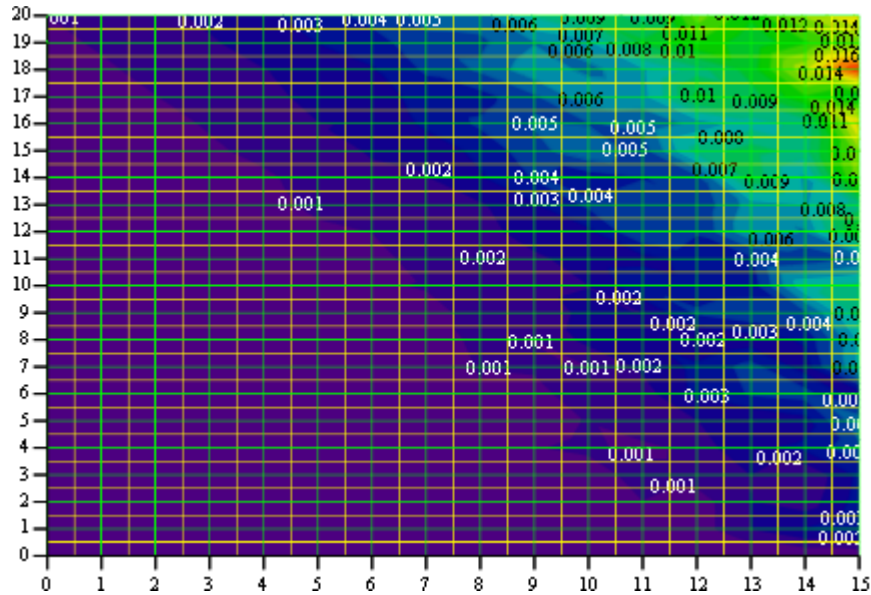
R

Figure 4.22. Minimum Reflectivity Representation In Contour Plot

Assuming a Gaussian beam not diverging more than 11.459° and an incident angle not more than 15°, the graph tells us every detail. We have to have a laser beam

which needs to diverge more than it is and an incident angle more than espionage can use.

4.2.2.4. Reflectivity upon the Change of the Incident Angle and Index of the First Slab

$$\alpha = 0°$$
$$\theta i = 0° - 15°$$
$$\lambda = 800nm$$
$$n_2 = 1 - 3$$
$$n_3 = 1.5$$
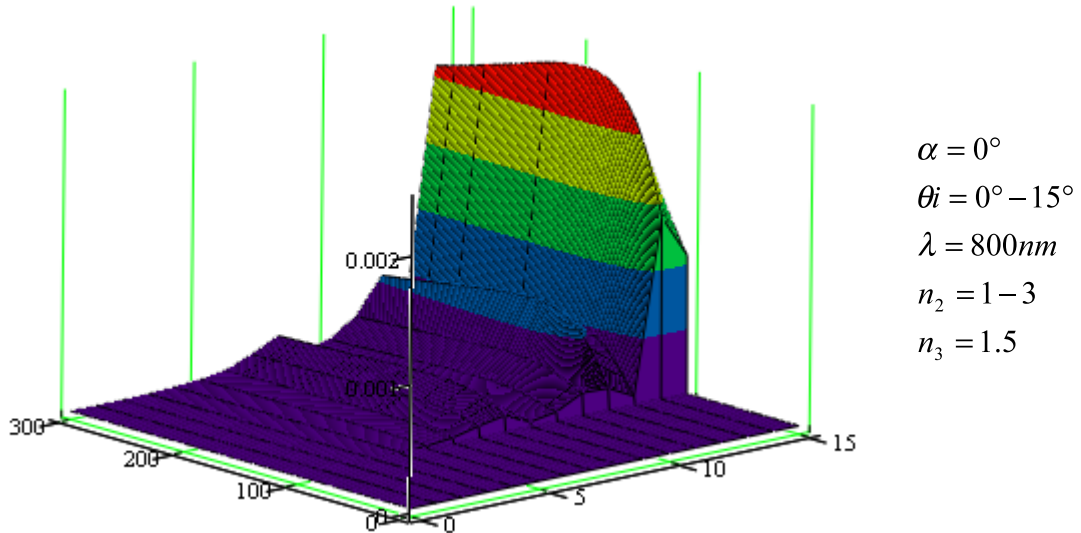
R

Figure 4.23. Minimum Reflectivity Representation For Various Incident Angle And Various Indices
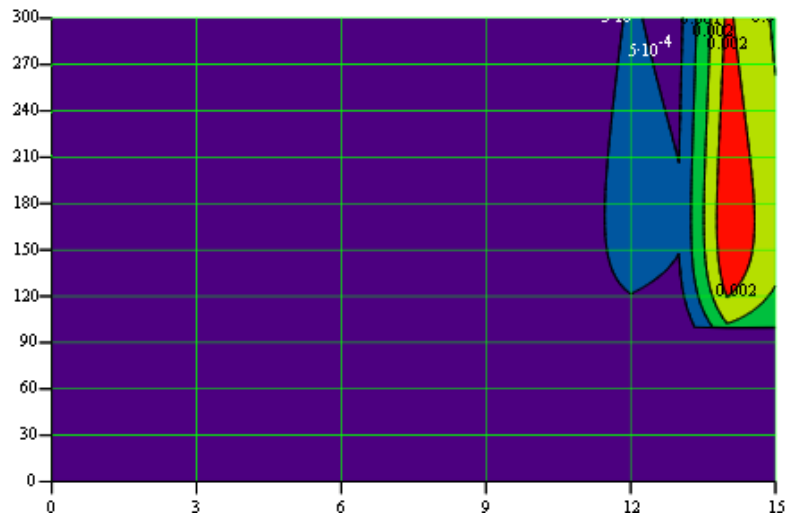
R

Figure 4.24. Minimum Reflectivity Representation In Contour Plot

4.2.2.5. Reflectivity upon the Change of the Wavelength and Index of the First Slab

$\alpha = 0°$

$\theta i = 0°$

$\lambda = 800 - 1500 nm$

$n_2 = 1 - 3$

$n_3 = 1.5$

Figure 4.25. Minimum Reflectivity Representation For Various Wavelengths And Various Indices

Figure 4.26. Minimum Reflectivity Representation In Contour Plot

In this graph x-axis represents the index of the first slab changing from 1 to 3 and y-axis represents the wavelength changing from 800nm to 1500nm (usually our case).
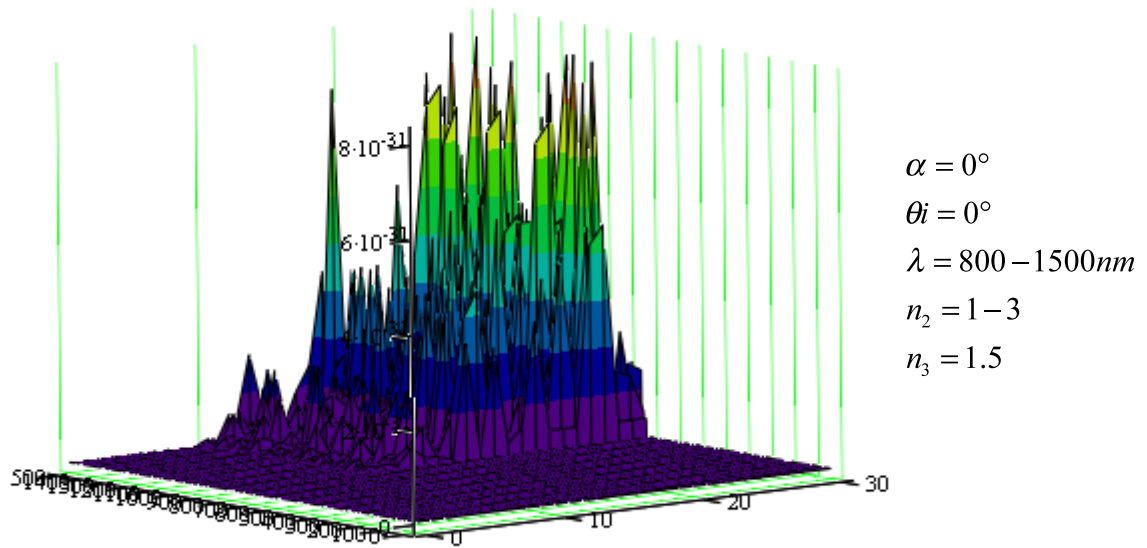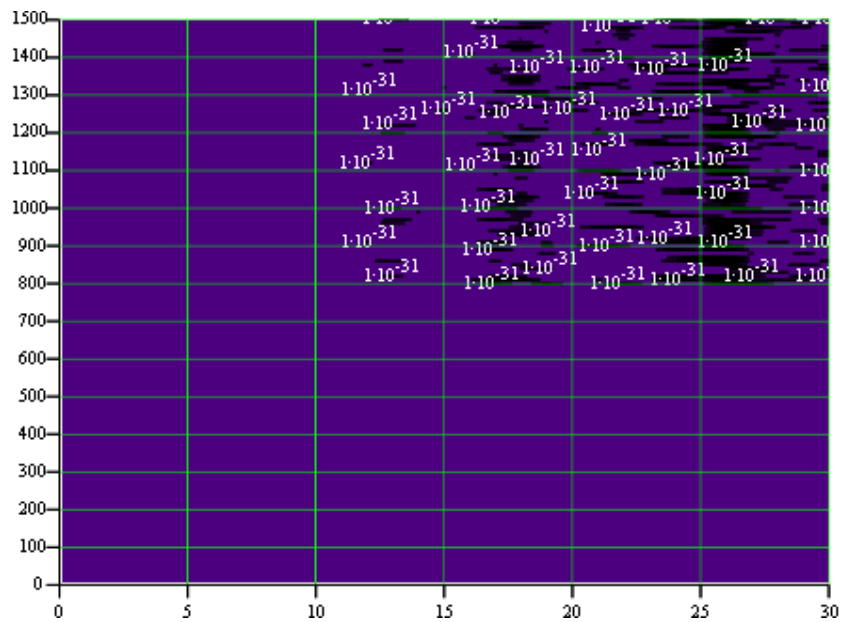
After analyzing the graphs we can say that reflectivity depends upon wavelength, indices of the media, incident angle, divergence angle of the Gaussian beam and the thicknesses of the slabs. If we focus on the minimum reflectivity case, we can easily notice that after minimizing reflectivity the most important factor for non-reflectance is the incident angle and divergence angle of the Gaussian beam. They need to be narrow angles and it seems that it is our natural case.

The next optimization parameter is a stable wavelength. We always assumed to know the wavelength of the laser because these kinds of weapons technical characteristics same. After knowing the wavelength not exactly but nearly, we can minimize the reflectivity in order not be detected by these kind of unauthorized weapons.

CHAPTER 5

RESULTS

The mathematical model developed in previous sections is applied for the problem of reflection of the Gaussian beam from two slabs configuration. The purpose of our project is to minimize light reflection from this two layer structure, therefore; the thickness of the slabs adjusted such that at the normal incident the reflectivity will be zero at the same time minimum for the oblique incidents. In the case of Gaussian beam, which decomposed into plane waves, consist of all sorts of plane waves at the same time and location.

It is not possible to make the Gaussian beam not reflected for all case because representing laser beam as plane wave decomposition, it comes to the target with $\theta_i + \alpha$ angles. Because plane waves come to the surface with θ_i angle, it is applicable to make non-reflectance by adjusting the thickness. Because reflection depends on the incident angles and Gaussian beam is composed of plane waves in different incident angles, non-reflection is not possible.

At the beginning of our project a 20 dB decrease is desired by reflection in order to diminish the reflected beam power. Using minimum reflectivity for multilayer structures it is believed to be done.

Although R represents the reflectivity which has its meaning in and when R is minimized the beam power is expected to be minimized, we need to look the whole table whether decreasing it decreases our laser beam shape or not. The Gaussian beam shape is defined in equation 3.70. All calculations and graphs above are made referring to this equation.

Calculating the beam profile after reflection, it can be analyzed that when the amplitude of the Gaussian beam is 1, the reflected Gaussian beam amplitude must be;

$$\frac{n_2 - n_1}{n_2 + n_1} = \frac{1.5 - 1}{1.5 + 1} = 0.2$$

In order to optimize the amplitude of the Gaussian beam profile, a normalization factor A is used. In Figure 5.1. the amplitude of the Gaussian beam is 0.2 as emphasized. It is graphed to compare with the Gaussian beam shape from only a surface of a dielectric film.

The parameter R parameter is changed for only one surface with the matrix $M = \begin{bmatrix} r_{12} & 0 \\ 0 & -r_{12}n_1 \cos(\theta_i) \end{bmatrix}$ because with one surface reflection, our reflection coefficient is redefined from Fresnel Formulas. In Figure 5.1. the reflected Gaussian beam doesn't change in response to the reflection from one surface because no reflection from the backwards of the film is taken into account.
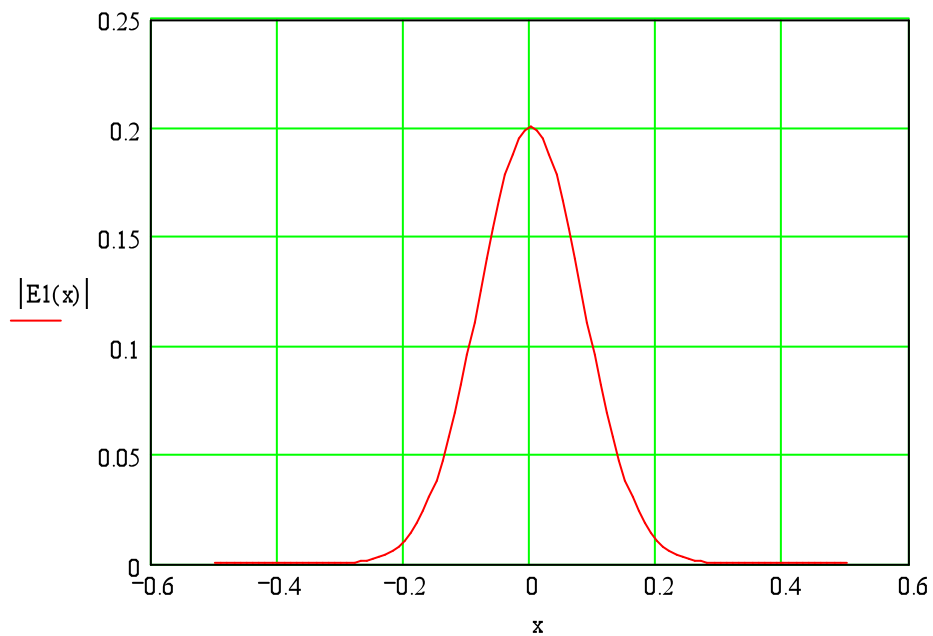

Figure 5.1. Minimum Reflected Gaussian Beam From Only One Surface Of A
      Dielectric Surface ($\theta_i = 0$)

Figure 5.2. Minimum Reflected Gaussian Beam From Single Film ($\theta_i = 0$)

Figure 5.3. Comparison Of Both Reflected Gaussian Beams ($\theta_i = 0$)

These graphs show that when the thickness of one dielectric film is adjusted and the laser beam is reflected from it, it gives us a total power reduction of 51.312 dB and a peak power gain of 54.734 dB when normal reflected Gaussian laser beam from only one surface is compared with it.

It can be noticed from figure 5.2 that when thickness is adjusted for minimum reflection, the center point goes nearly to zero. When incident angle is zero and when plane wave decomposition is made for the frontier light wave of this Gaussian beam, the frontier of the Gaussian beam is expected to be close to zero as graphed because from equation 3.70 a Gaussian beam is the representation of laser beam in plane wave components. And because the midpoint of the Gaussian beam having a zero incident angle is the integration of all the plane wave components of Gaussian laser beam, the TE components of the Gaussian beam's divergence waves hinder the midpoint being zero.
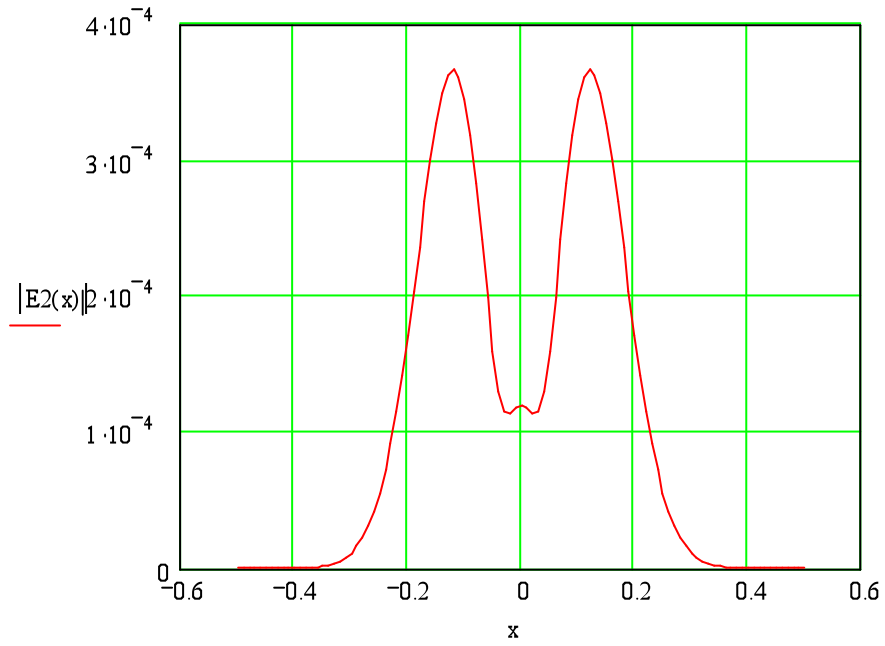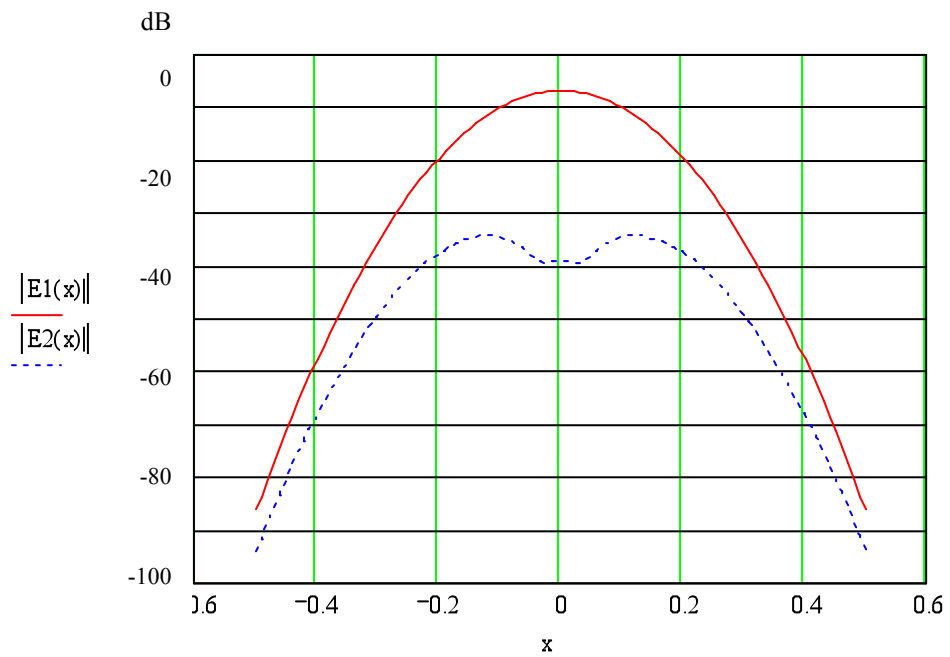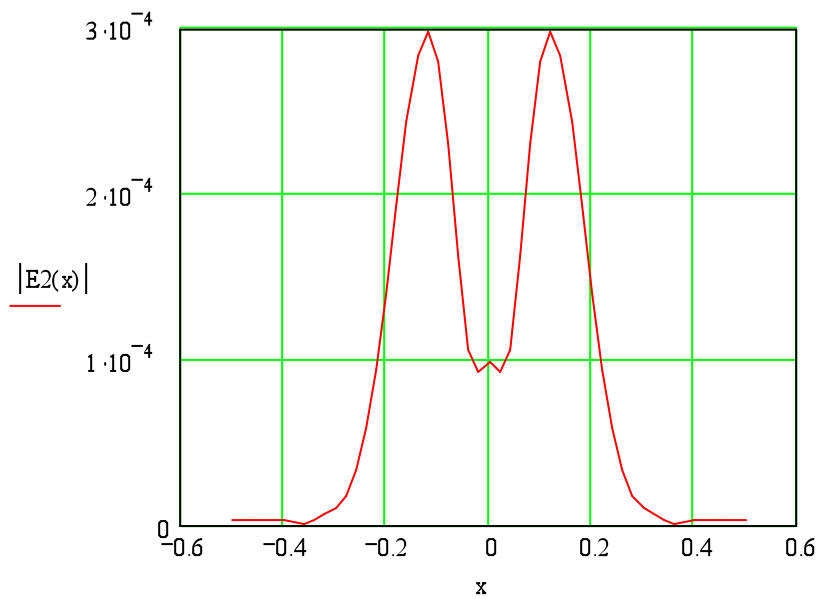

Figure 5.4. Minimum Reflected Gaussian Beam From Double Slabs ($\theta_i = 0$)
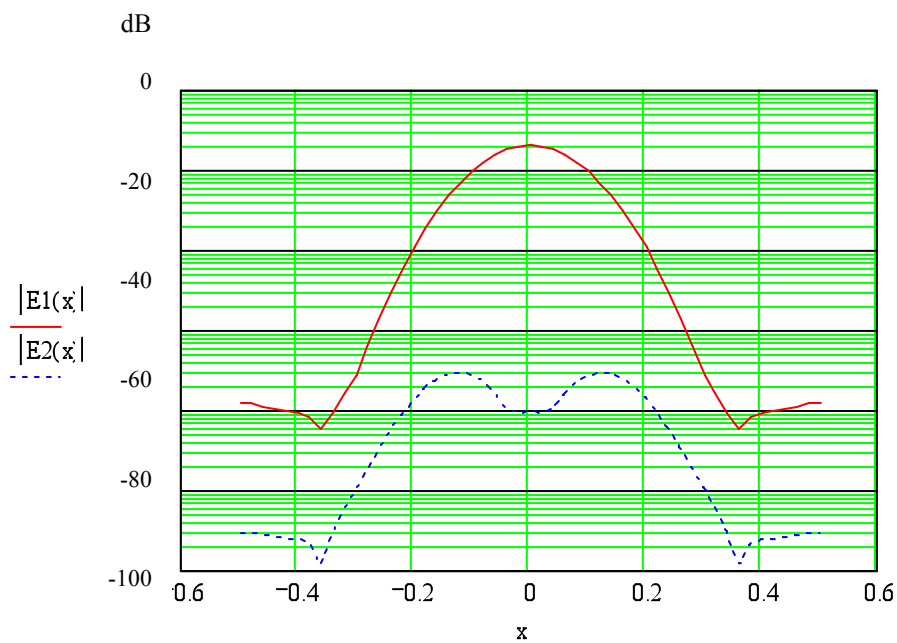
Figure 5.5. Comparison Of Both Reflected Gaussian Beams ($\theta_i = 0$)

It can be noticed that when we adjust both two dielectric slabs for their indices and wavelengths we can easily reduce the reflected Gaussian beam total power as 53.1 dB and peak power as 56.478 dB.
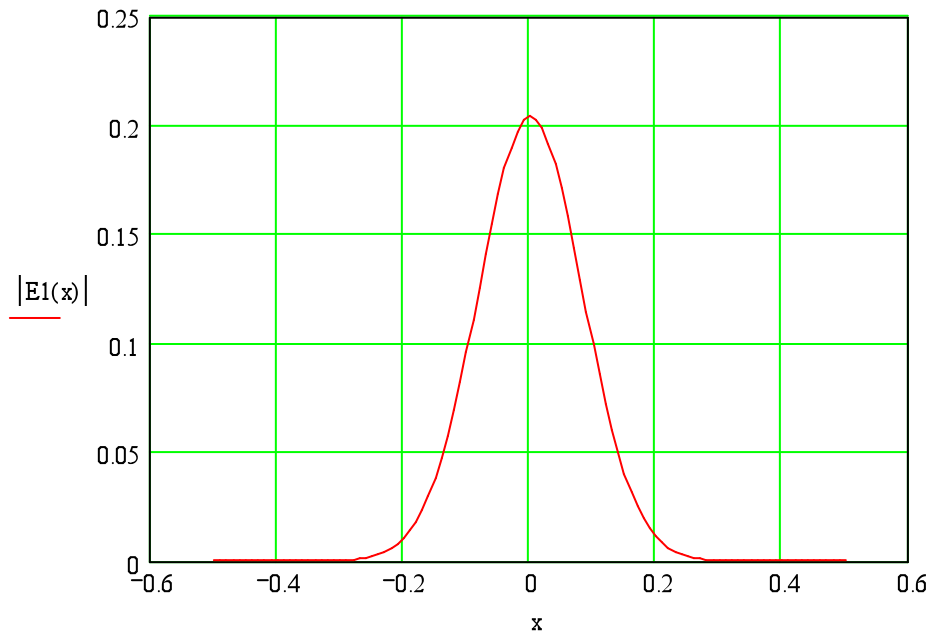
Figure 5.6. Minimum Reflected Gaussian Beam From Only One Surface Of A Dielectric Surface ($\theta_i = 10$)

What is expected when laser beam is reflected from only surface of a dielectric slab is of course shift a little (if we look closer, it can be seen) which is described in Chapter 3 and preserve its power except for a little change.
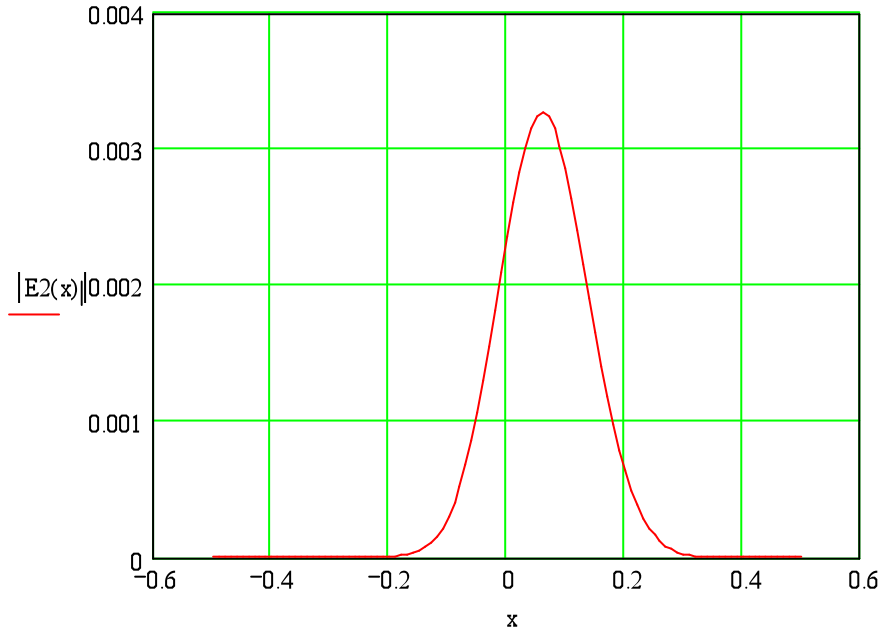
Figure 5.7. Minimum Reflected Gaussian Beam From One Slab($\theta_i = 10$)

It is noticed that when we increase the incident angle for 10 degrees minimum reflection which is counted when incident angle is zero increases. But there is still a decrement as expected. Also it can be seen that reflected Gaussian beam is exposed to lateral shift and focal shift after reflection.
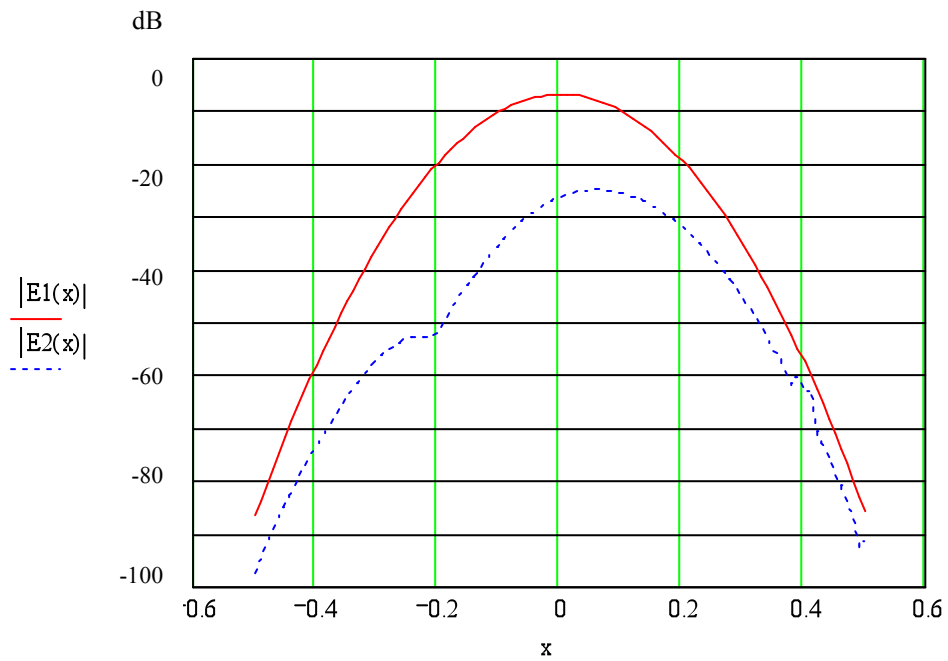
Figure 5.8. Comparison Of Both Reflected Gaussian Beams ($\theta_i = 10$)

From figure 5.8 it is clearly seen when incident angle is 10 degree, one of the plane wave decomposed components is in the temp of being zero. It is the case when we decomposed Gaussian beam for plane wave components, the interaction of plane wave which comes to the surface with -10 degree.

When we analyze figure 5.6, 5.7 and 5.8 using a Gaussian beam comes to one slab with 10 degree, we can notice that although we had set and calculated our minimum reflection for zero degree, there is still total power gain of 36.642 dB and peak power gain of 35.738 dB .
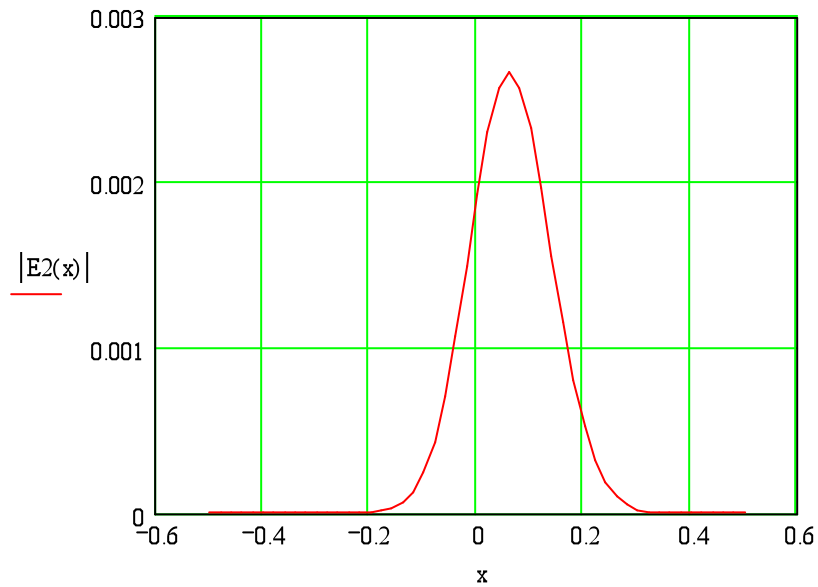

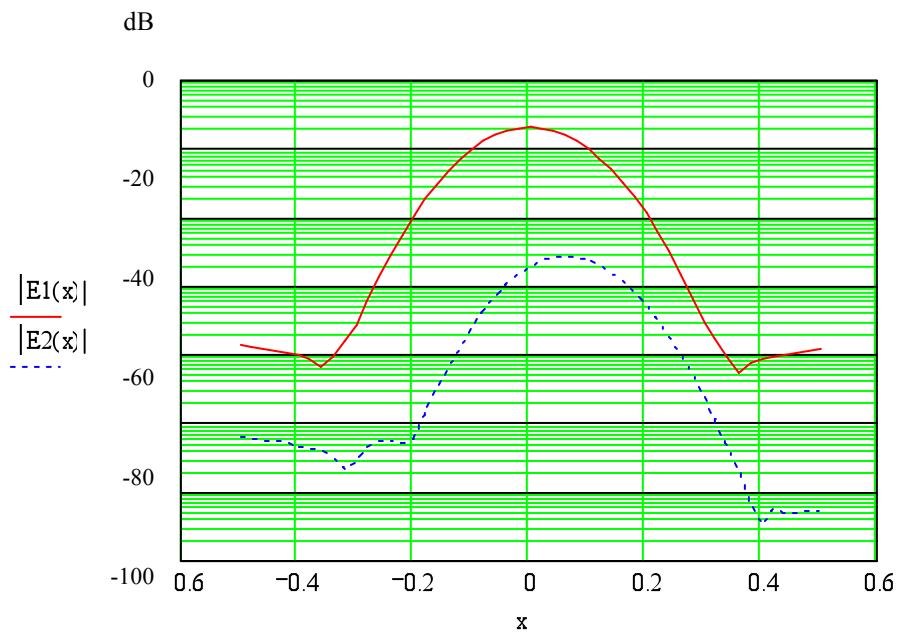Figure 5.9. Minimum Reflected Gaussian Beam From Double Slabs ($\theta_i = 10$)

Figure 5.10. Comparison Of Both Reflected Gaussian Beams ($\theta_i = 10$)

CHAPTER 6

CONCLUSION

These results show that when a Gaussian beam shape laser beam reflects from a dielectric slab, its maximum point shifts which is defined as lateral shift in equation (3.51) and broadens in transverse plane which is defined as focal shift in equation(3.55). Because of reflection Gaussian beam changes its propagation direction by an amount L which is represented by Lateral Shift. Also the Gaussian Beam exposes to a Focal shift which can be defined as extra broadening after reflection.

Although the reflectivity is adjusted for non reflectance, for a Gaussian laser beam non reflectance is not possible. Non reflectance of one point in Gaussian laser beam after reflection is not possible because Gaussian beam after reflection is the combination of the decomposed plane waves which propagate over different directions. Although it is minimized for one incident angle, decomposed plane waves comes to the surface with different angles. And Gaussian beam is represented by composing all the plane waves after reflection. Because all plane waves have TE components in different directions, their integration after reflection would never result a non reflectance. But the decrement of the power in one point can be seen. For example in Figure 5.2, the incident angle is zero and the film thickness is adjusted for minimum reflectance. The decrement in zero axis is observable.

Table 1. Comparison of Power and Advantages of Stratified Film Structures

	PEAK POWER		TOTAL POWER	
$\theta_{\acute{Y}}$	0°	10°	0°	10°
Normal Reflection	-13.979dB	-13.979dB	-27.535dB	-27.535Db
Single Slab Reflection(Minimum)	-68.714dB	-49.717dB	-78.847dB	-64.177dB
Double Slab Reflection(Minimum)	-70.458dB	-51.502dB	-80.635dB	-65.919dB

In Table 1., loss of normal reflection which can be thought as reflection from only one surface of a slab, loss of minimum reflection which can be thought as reflection from one slab that has a thickness, loss of reflection which can be thought as minimum reflection from double slabs that have various thicknesses are configured. Reflectivity may be minimized either for the total power or peak power, or may be both by selecting proper thicknesses for the slabs.

Using the solutions defined above it can be exactly said that when the window is covered with a proper dielectric slab/slabs structure none of the laser listening devices can detect the voice of the signals talking inside because of a decrement at least 50 dB.

Using double or more than two slabs can be a more precise solution in order to reduce the reflection but needs more slabs whose thicknesses are adjusted and designed properly. And these requirements make the structure cost more. So, two-layer slab structure is a conclusive solution in order not to be detected by these kind of devices.

APPENDIX A

METHOD OF STATIONARY PHASE

Let's consider the integrals of the form ;

$$I(x) = \int_a^b f(t) \exp(i\psi(t)) dt \qquad \text{as} \qquad x \to \infty \qquad (3.64)$$

Which we can call "generalized Fourier Integral". Riemann-Labergue Lemma says that If ψ is continuously differentiable on $[a,b]$ and not constant on any sub-integral of $[a,b]$, then

$$\lim_{x \to \infty} \int_a^b f(t) \exp(i\psi(t)x) dt = 0 \qquad (3.65)$$

Integration by parts of $I(x)$ given

$$I(x) = \frac{\int_a^b f(t)\psi'(t)\exp(i\psi(t)x)dt}{\psi'(t)} \qquad (3.66)$$

$$I(x) = \left(\frac{\exp[i\psi(t)x]}{xi\psi'(t)} f(t) \right)\Big|_a^b - \int_a^b \frac{\exp[i\psi\psi(t)]}{xi} \frac{d}{dt}\left(\frac{f(t)}{\frac{d}{dt}\psi(t)} \right) dt \qquad (3.67)$$

If $\quad \dfrac{d}{dt}\left[\dfrac{f(t)}{\psi'(t)} \right] \in L'([a,b])\quad$, then $\qquad \displaystyle\int_a^b \frac{\exp[i\psi(t)x]}{xi} \frac{d}{dt}\left(\frac{f(t)}{\psi'(t)} \right) \quad (3.68)$

And $\qquad I(x) = \dfrac{1}{x}\left(\dfrac{\exp[i\psi(t)x]}{i\psi'(t)} f(t) \right)\Big|_a^b \qquad (3.69)$

Provided that ψ' does not vanish at the end points.

REFERENCES

[1]   Yong Ma, Dan Tan, *"Characteristics of Lidar Returned Signals from Wavy Water Surface"*, Proc. of SPIE Vol. 4976

[2]   Kourosh Tatar, *"Machine tool vibrations and violin sound fields studied using laser vibrometry"*, Doktoral Thesis

[3]   A. Norman and D.P. Nyquist, *"Transient Scattering of a Beam from a Periodic Surface", 1996 IEEE*

[4]   *Justin* Peatross, Michael Ware *"Physics of Light and Optics"*, p.61

[5]   M. Born and E. Wolf, Principles of Optics, 4th ed. (Pergamon, Oxford, 1970), p. 40.

[6]   Gary D. Landry and Theresa A. *Maldonado*, *"Gaussian Beam Transmission And Reflection From A General Anisotropic Multilayer Structure"*, APPLIED OPTICS y Vol. 35, No. 30 y 20 October 1996

[7]   R. P. Riesz and R. Simon, *"Reflection Of A Gaussian Beam From A Dielectric Slab"*, Vol. 2, No. 11/November 1985/J. Opt. Soc. Am. A p.1809

[8]   Wojciech Nasalski, *"Modelling Of Beam Reflection At A Nonlinear–Linear Interface",* J. Opt. A: Pure Appl. Opt. 2 (2000) 433–441

[9]   Martin F. Schubert, Frank W. Mont, Sameer Chhajed, David J. Poxson, Jong Kyu Kim And E. Fred Schubert, *"Design Of Multilayer Antireflection Coatings Made From Co-Sputtered And Low-Refractive-Index Materials By Genetic Algorithm",* 2008 Optical Society of America

[10]   A. Padman And J A Murphy, *"A Scattering Matrix Formulation For Gaussian Beam-Mode Anlaysis",* 2009 IEEE

[11]   Hui Yu, Xiaoqing Jiang, Jianyi Yang, Wei Qi, and Minghua Wang." *Analytical Model For The Grazing Reflection Of A Narrow Beam"*, September 15, 2006 / Vol. 31, No. 18 / OPTICS LETTERS

[12]   Ingmar Renhorn, Christer Karlsson and Dietmar Letalick *"Coherent Laser Radar For Vibrometry: Robust Design And Adaptive Signal Processing"*

[13]   Naren ANAND, Jason HOLDEN, CJ Steuernagel, *"Remote Sound Detection Using A Laser"*

[14]   John P. Barton, *"Electromagnetic Field For A Tightly Focused Beam Incident Upon Ordinary And Layered Plane Surfaces"*, 10 April 2007 _ Vol. 46, No. 11 _ APPLIED OPTICS

[15]   M. Lehman , M. Garavaglia "*Beam Reflection From Multilayers With Periodic And Fractal Distributions*", Journal of Modern Optics,46:11,1579 – 1593

[16]   Miguel A. Porras, "*Nonspecular Reflection Of General Light Beams At A Dielectric Interface*", Optics Communications 135 (1997) 369-377

[17]   P. D. Kukharchik, V. M. Serdyuk, and I. A. Titovitski ," *Total internal reflection of a Gaussian light beam*", 1999 American Institute of Physics

[18]   Dimrity N. Goryushko, and Alexander A. Shmat'ko "*Reflection Of A Laser Beam From A Gyromagnetic Layer With A Magneto-Dielectric Substrate*", Kharkov, Ukraine, VIII-th International Conference on Mathematical Methods in Electromagnetic Theory

[19]   J. C. Valiere, P. Herzog, V. Valeau and G. Tournois "*Acoustic Velocity Measurements In The Air By Means Of Laser Doppler Velocimetry: Dynamic And Frequency Range Limitations And Signal Processing Improvements*", Journal of Sound and Vibration (2000) 229(3), 607-626

[20]   Chen-Chia Wang, Sudhir Trivedi, Feng Jin, V. Swaminathan, Ponciano Rodriguez, And Narasimha S. Prasad, "*High Sensitivity Pulsed Laser Vibrometer And Its Application As A Laser Microphone*", Applied Physics Letters 94, 051112 (2009)

[21]   M. A. Al-Habash, L. C. Andrews, R. L. Philips, "*Scintillation Of A Gaussian Beam Reflected By A Point Target*", Proceedings of SPIE Vol. 4035 (2000)

[22]   J. Fan, L.J. Wang, "*Reflection Of A Gaussian Laser Pulse By An Active Medium*", Optics Communications 259 (2006) 149–153

[23]   A. V. Sokolov, D. D. Yavuz, D. R. Walker, G. Y. Yin, and S. E. Harris, "*Light Modulation At Molecular Frequencies*", Physical Review A, Volume 63, 051801(R)

[24]   Ne´stor Bonomo and Ricardo A. Depine, "*Nonspecular Reflection Of Ordinary And Extraordinary Beams In Uniaxial Media*", J. Opt. Soc. Am. A/ Vol. 14, No. 12/December 1997

[25]   Zhigang Zhu, Weihong Li and George Wolberg, "*Integrating LDV Audio and IR Video for Remote Multimodal Surveillance*", Proceedings of the 2005 IEEE Computer Society Conference on Computer Vision and Pattern Recognition (CVPR'05)

[26]   Shekhar Guha, "*Nonlinear Beam Propagation*", ISPIE Vol. 2853

[27]   J. W. RA, H. L. Bertoni And L. B. Felsen, "*Reflection And Transmission Of Beams At A Dielectric Interface*", Appl. Math, Vol. 24, No. 3, May 1973

[28]   Chen-Chia Wang, Sudhir B. Trivedi, Feng Jin, Serguei Stepanov, Zhongyang Chen, Jacob Khurgin, Ponciano Rodriguez, and Narasimha S. Prasad, "*Human Life Signs Detection Using High-Sensitivity Pulsed Laser Vibrometer*", IEEE Sensors Journal, Vol. 7, No. 9, September 2007

[29]   Li-Gang Wang, Hong Chen, Nian-Hua Liu, and Shi-Yao Zhu, "*Negative And Positive Lateral Shift Of A Light Beam Reflected From A Grounded Slab*", OPTICS LETTERS / Vol. 31, No. 8 / April 15, 2006

[30]   Nosov V.V., "*Reflectance Of Small-Sıze Optıcs*", Proc. of SPIE Vol. 6160, 61601O, (2006)

[31]   N. A. Halliwell, A. Hocknell And S. J. Rothberg "*On The Measurement Of Angular Vibration Displacements: A Laser Tiltmeter*", Journal of Sound and Vibration (1997) 208(3), 497-50